ASSESSING THE EFFECT OF DIGITAL CONTACT TRACING, TESTING, AND SYMPTOM-BASED ISOLATION DURING DISEASE OUTBREAKS

TAIYE ESTWICK

A THESIS SUBMITTED TO THE FACULTY OF GRADUATE STUDIES
IN PARTIAL FULFILMENT OF THE REQUIREMENTS
FOR THE DEGREE OF
MASTER OF SCIENCE

GRADUATE PROGRAM IN DEPARTMENT OF MATHEMATICS AND STATISTICS
YORK UNIVERSITY
TORONTO, ONTARIO

JUNE 2026

© TAIYE ESTWICK, 2026

Abstract

Digital contact tracing (DCT) is a promising tool against infectious disease transmission, using wireless communication to rapidly identify and notify close contacts of confirmed cases. Despite its theoretical advantages over manual contact tracing, its development is limited, largely due to inadequate adoption and compliance. This thesis uses agent-based modelling to evaluate the effectiveness of DCT by simulating the progression of a hypothetical outbreak over 365 days. Two strategies were examined: DCT alone and when integrated with symptom-based isolation. Independently, increasing adoption consistently reduces transmission but the addition of symptomatic isolation weakens this relationship. Mandatory isolation significantly reduces incidence, thereby diminishing the marginal benefit of DCT. This indicates that while DCT can contribute to outbreak control, its effectiveness depends on participation, and its additional impact is limited when used alongside highly effective measures. Optimizing the integration of these strategies is essential for effective mitigation and minimizing the socioeconomic impact of disease.

To the extended McCollin family...

Acknowledgements

Firstly, I would like to thank my supervisor, Professor Seyed Moghadas, for his invaluable guidance and education throughout my Master of Science degree.

A special expression of gratitude and appreciation to Dr. Thomas Vilches for his consistent assistance and support during this project.

Thank you to my colleagues in the Agent-Based Modelling Laboratory and the members of my thesis supervisory committee for their time and feedback, which enhanced the quality of this submission.

I would be remiss if I did not acknowledge the efforts of my family and friends, both in Barbados and abroad, constantly offering words of encouragement and counsel wherever possible.

Finally, thank you to my mother, Liza, who has been beside me every step of this journey, as a source of unwavering support and advice.

The completion of this thesis could not have been possible without any of the aforementioned support.

Contents

Abstract ii

Acknowledgements iv

Table of Contents v

List of Tables viii

List of Figures ix

1 Introduction 1

1.1 Contact Tracing 2

1.2 Digital Contact Tracing (DCT) 3

1.3 Thesis Overview 4

2 Literature Review 7

2.1 Asymptomatic Testing 8

2.2 Applications of Mobile Technology During Outbreaks 10

2.3 Previous Models 13

3 Methodology 16

3.1 Study Design 16

3.2 Assumptions 17

3.3 Model Structure 18

3.4 Intervention Strategies 22
3.4.1 Strategy I: Use of DCT Only 22
3.4.2 Strategy II: DCT and Symptom-Based Isolation 23
3.5 Model Parameters 23
3.5.1 Disease and Framework Parameters 23
3.5.2 Testing and Contact Tracing Parameters 26
3.5.3 Contact Matrix 26
3.6 Computational Implementation 27

4 Digital Contact Tracing with Self-Testing 29
4.1 Outline of Policy Scenarios 29
4.2 Baseline Scenario 31
4.3 Assessment of Scenarios 33
4.3.1 Time Series 33
4.3.2 Attack Rates 34
4.3.3 Relative Reductions in Attack Rates 39
4.4 Statistical Analysis 44
4.4.1 Shapiro-Wilk Test 44
4.4.2 Fligner-Killeen Test 45
4.4.3 Welch's t-test 46

5 Digital Contact Tracing with Self-Testing and Symptom-Based Isolation 51
5.1 Baseline Scenario 52
5.2 Assessment of Scenarios 52
5.2.1 Time Series 52
5.2.2 Attack Rates 55
5.2.3 Relative Reductions in Attack Rates 61
5.3 Statistical Analysis 64
5.3.1 Shapiro-Wilk Test 64

5.3.2 Fligner-Killeen Test 65
5.3.3 One-Way ANOVA Test 66
5.3.4 Tukey's HSD Test 66
5.3.5 Welch's t-test 67

6 Discussion and Conclusion **73**

6.1 Age-Dependent Summary 76
6.2 Limitations 77
6.3 Future Work 78

Bibliography **81**

List of Tables

3.1 Description of the model variables. 19

3.2 Age-independent disease-related parameters. 24

3.3 Variations of the probabilities with which individuals transition out of the latent class with respect to age. 25

3.4 Variations of the probabilities with which individuals transition into the deceased class with respect to age. 25

3.5 Parameters related to testing and contact tracing. 26

4.1 P-values for the Shapiro-Wilk test (all age groups). 44

4.2 P-values for the Shapiro-Wilk test (individuals under 18 years of age). . . 44

4.3 P-values for the Shapiro-Wilk test (individuals 18–65 years of age). . . . 45

4.4 P-values for the Shapiro-Wilk test (individuals aged 66 years or older). . . 45

4.5 P-values for the Fligner-Killeen test. 45

5.1 P-values for the Shapiro-Wilk test (all age groups). 64

5.2 P-values for the Shapiro-Wilk test (individuals under 18 years of age). . . 65

5.3 P-values for the Shapiro-Wilk test (individuals aged 18–65 years). 65

5.4 P-values for the Shapiro-Wilk test (individuals aged 66 years or older). . . 65

5.5 P-values for the Fligner-Killeen test. 65

5.6 P-values for the One-Way ANOVA test. 66

List of Figures

1.1 Flow diagram of an SIR model with constant transmission and recovery rates, β and γ, respectively. 5

3.1 Flow diagram displaying the dynamics of the disease outbreak. 18

4.1 Daily incidence in the baseline scenario for the total population (red) and age-specific subpopulations: under 18 years (green), 18–65 years (blue), and over 65 years (purple). 32

4.2 Cumulative incidence in the baseline scenario for the total population (red) and age-specific subpopulations, expressed as proportions of the corresponding population sizes: under 18 years (green), 18–65 years (blue), and over 65 years (purple). 32

4.3 Incidence of infection under varying levels of application coverage, assuming one test per notification. Panels on the left correspond to a 1-day delay between notification and testing, while panels on the right correspond to a 2-day delay. Subplots (A) and (B) represent the total population, (C) and (D) correspond to individuals under 18 years of age, (E) and (F) represent individuals aged 18–65, and (G) and (H) correspond to individuals aged 66 years or older. 34

4.4 Incidence of infection under varying levels of application coverage, assuming up to two tests per notification. Panels on the left correspond to a 1-day delay between notification and testing, while panels on the right correspond to a 2-day delay. Subplots (A) and (B) represent the total population, (C) and (D) correspond to individuals under 18 years of age, (E) and (F) represent individuals aged 18–65, and (G) and (H) correspond to individuals aged 66 years or older. 35

4.5 Cumulative incidence of infection under varying levels of application coverage, expressed as totals of the corresponding populations, assuming one test per notification. Panels on the left correspond to a 1-day delay between notification and testing, while panels on the right correspond to a 2-day delay. Subplots (A) and (B) represent the total population, (C) and (D) correspond to individuals under 18 years of age, (E) and (F) represent individuals aged 18–65, and (G) and (H) correspond to individuals aged 66 years or older. 36

4.6 Cumulative incidence of infection under varying levels of application coverage, presented as totals of the corresponding populations, assuming up to two tests per notification. Panels on the left correspond to a 1-day delay between notification and testing, while panels on the right correspond to a 2-day delay. Subplots (A) and (B) represent the total population, (C) and (D) correspond to individuals under 18 years of age, (E) and (F) represent individuals aged 18–65, and (G) and (H) correspond to individuals aged 66 years or older. 37

4.7 Box plots of attack rates under different scenarios at the population level. Subplots (A) and (C) compare the effects of testing delay (1-day vs 2-day) for scenarios with a maximum of one test and up to two tests per notification, respectively. Subplots (B) and (D) compare the effects of the maximum number of tests per notification (one vs two tests) for 1-day and 2-day delays, respectively. In subplots (A) and (C), red boxes represent a 1-day delay and blue boxes represent a 2-day delay. In subplots (B) and (D), purple boxes correspond to one test per notification, while pink boxes correspond to two tests. 38

4.8 Box plots of attack rates under different scenarios for individuals under 18 years of age. Subplots (A) and (C) compare the effects of testing delay (1-day vs 2-day) for scenarios with a maximum of one test and up to two tests per notification, respectively. Subplots (B) and (D) compare the effects of the maximum number of tests per notification (one vs two tests) for 1-day and 2-day delays, respectively. In subplots (A) and (C), red boxes represent a 1-day delay and blue boxes represent a 2-day delay. In subplots (B) and (D), purple boxes correspond to one test per notification, while pink boxes correspond to two tests. 39

4.9 Box plots of attack rates under different scenarios for individuals aged 18–65. Subplots (A) and (C) compare the effects of testing delay (1-day vs 2-day) for scenarios with a maximum of one test and up to two tests per notification, respectively. Subplots (B) and (D) compare the effects of the maximum number of tests per notification (one vs two tests) for 1-day and 2-day delays, respectively. In subplots (A) and (C), red boxes represent a 1-day delay and blue boxes represent a 2-day delay. In subplots (B) and (D), purple boxes correspond to one test per notification, while pink boxes correspond to two tests. 40

4.10 Box plots of attack rates under different scenarios for individuals aged 66 years or older. Subplots (A) and (C) compare the effects of testing delay (1-day vs 2-day) for scenarios with a maximum of one test and up to two tests per notification, respectively. Subplots (B) and (D) compare the effects of the maximum number of tests per notification (one vs two tests) for 1-day and 2-day delays, respectively. In subplots (A) and (C), red boxes represent a 1-day delay and blue boxes represent a 2-day delay. In subplots (B) and (D), purple boxes correspond to one test per notification, while pink boxes correspond to two tests. 41

4.11 Relative reductions in the attack rates with respect to the baseline scenario under different scenarios, assuming one test per notification. Subplot (A) represents the total population, (B) corresponds to individuals under 18 years of age, (C) represents individuals aged 18–65, and (D) corresponds to individuals aged 66 years or older. Red boxes represent a 1-day delay between notification and testing, while blue boxes represent a 2-day delay. 42

4.12 Relative reductions in the attack rates with respect to the baseline scenario under different scenarios, assuming up to two tests per notification. Subplot (A) represents the total population, (B) corresponds to individuals under 18 years of age, (C) represents individuals aged 18–65, and (D) corresponds to individuals aged 66 years or older. Red boxes represent a 1-day delay between notification and testing, while blue boxes represent a 2-day delay. 43

4.13 P-values obtained from Welch's t-test comparing 1-day and 2-day delays between notification and testing for scenarios with a maximum of one test per notification across different levels of application coverage. Subplot (A) represents the total population, (B) corresponds to individuals under 18 years of age, (C) represents individuals aged 18–65, and (D) corresponds to individuals aged 66 years or older. 47

4.14 P-values obtained from Welch's t-test comparing 1-day and 2-day delays between notification and the first test for scenarios allowing up to two tests per notification across different levels of application coverage. Subplot (A) represents the total population, (B) corresponds to individuals under 18 years of age, (C) represents individuals aged 18–65, and (D) corresponds to individuals aged 66 years or older. 48

4.15 P-values obtained from Welch's t-test comparing scenarios with a maximum of one test versus up to two tests per notification under a 1-day delay across different levels of application coverage. Subplot (A) represents the total population, (B) corresponds to individuals under 18 years of age, (C) represents individuals aged 18–65, and (D) corresponds to individuals aged 66 years or older. 49

4.16 P-values obtained from Welch's t-test comparing scenarios with a maximum of one test versus up to two tests per notification under a 2-day delay across different levels of application coverage. Subplot (A) represents the total population, (B) corresponds to individuals under 18 years of age, (C) represents individuals aged 18–65, and (D) corresponds to individuals aged 66 years or older. 50

5.1 Temporal incidence of infection for the baseline scenario. The red curve represents the total population, while age-specific subpopulations are shown as follows: green for individuals under 18 years of age, blue for individuals aged 18–65, and purple for individuals aged 66 years or older. 53

5.2 Temporal cumulative incidence for the baseline scenario, expressed as proportions of the corresponding populations. The red curve represents the total population, while age-specific subpopulations are shown as follows: green for individuals under 18 years of age, blue for individuals aged 18–65, and purple for individuals aged 66 years or older. 53

5.3 Incidence of infection under varying levels of application coverage, assuming one test per notification. Panels on the left correspond to a 1-day delay between notification and testing, while panels on the right correspond to a 2-day delay. Subplots (A) and (B) represent the total population, (C) and (D) correspond to individuals under 18 years of age, (E) and (F) represent individuals aged 18–65, and (G) and (H) correspond to individuals aged 66 years or older. 54

5.4 Incidence of infection under varying levels of application coverage, assuming up to two tests per notification. Panels on the left correspond to a 1-day delay between notification and testing, while panels on the right correspond to a 2-day delay. Subplots (A) and (B) represent the total population, (C) and (D) correspond to individuals under 18 years of age, (E) and (F) represent individuals aged 18–65, and (G) and (H) correspond to individuals aged 66 years or older. 55

5.5 Cumulative incidence under varying levels of application coverage, expressed as totals for the corresponding populations, assuming one test per notification. Panels on the left correspond to a 1-day delay between notification and testing, while panels on the right correspond to a 2-day delay. Subplots (A) and (B) represent the total population, (C) and (D) correspond to individuals under 18 years of age, (E) and (F) represent individuals aged 18–65, and (G) and (H) correspond to individuals aged 66 years or older. 56

5.6 Cumulative incidence under varying levels of application coverage, expressed as totals for the corresponding populations, assuming up to two tests per notification. Panels on the left correspond to a 1-day delay between notification and testing, while panels on the right correspond to a 2-day delay. Subplots (A) and (B) represent the total population, (C) and (D) correspond to individuals under 18 years of age, (E) and (F) represent individuals aged 18–65, and (G) and (H) correspond to individuals aged 66 years or older. 57

5.7 Box plots of attack rates under different scenarios at the population level. Subplots (A) and (C) compare the effects of testing delay (1-day vs 2-day) for scenarios with a maximum of one test and two tests per notification, respectively. Subplots (B) and (D) compare the effects of the maximum number of tests per notification (one vs two tests) for 1-day and 2-day delays, respectively. In subplots (A) and (C), red boxes represent a 1-day delay and blue boxes represent a 2-day delay. In subplots (B) and (D), purple boxes correspond to one test per notification, while pink boxes correspond to two tests. 58

5.8 Box plots of attack rates under different scenarios for individuals under 18 years of age. Subplots (A) and (C) compare the effects of testing delay (1-day vs 2-day) for scenarios with a maximum of one test and two tests per notification, respectively. Subplots (B) and (D) compare the effects of the maximum number of tests per notification (one vs two tests) for 1-day and 2-day delays, respectively. In subplots (A) and (C), red boxes represent a 1-day delay and blue boxes represent a 2-day delay. In subplots (B) and (D), purple boxes correspond to one test per notification, while pink boxes correspond to two tests. 59

5.9 Box plots of attack rates under different scenarios for individuals aged 18–65 years. Subplots (A) and (C) compare the effects of testing delay (1-day vs 2-day) for scenarios with a maximum of one test and two tests per notification, respectively. Subplots (B) and (D) compare the effects of the maximum number of tests per notification (one vs two tests) for 1-day and 2-day delays, respectively. In subplots (A) and (C), red boxes represent a 1-day delay and blue boxes represent a 2-day delay. In subplots (B) and (D), purple boxes correspond to one test per notification, while pink boxes correspond to two tests. 60

5.10 Box plots of attack rates under different scenarios for individuals aged 66 years or older. Subplots (A) and (C) compare the effects of testing delay (1-day vs 2-day) for scenarios with a maximum of one test and two tests per notification, respectively. Subplots (B) and (D) compare the effects of the maximum number of tests per notification (one vs two tests) for 1-day and 2-day delays, respectively. In subplots (A) and (C), red boxes represent a 1-day delay and blue boxes represent a 2-day delay. In subplots (B) and (D), purple boxes correspond to one test per notification, while pink boxes correspond to two tests. 61

5.11 Relative reductions in the attack rates with respect to the baseline scenario under different scenarios, assuming one test per notification. Subplot (A) represents the total population, (B) corresponds to individuals under 18 years of age, (C) represents individuals aged 18–65, and (D) corresponds to individuals aged 66 years or older. Red boxes represent a 1-day delay between notification and testing, while blue boxes represent a 2-day delay. 62

5.12 Relative reductions in the attack rates with respect to the baseline scenario under different scenarios, assuming up to two tests per notification. Subplot (A) represents the total population, (B) corresponds to individuals under 18 years of age, (C) represents individuals aged 18–65, and (D) corresponds to individuals aged 66 years or older. Red boxes represent a 1-day delay between notification and testing, while blue boxes represent a 2-day delay. 63

5.13 P-values from Tukey's HSD test comparing application coverage levels under a 1-day delay and one test per notification. Subplot (A) represents the total population, (B) corresponds to individuals under 18 years of age, (C) represents individuals aged 18–65, and (D) corresponds to individuals aged 66 years or older. 67

5.14 P-values from Welch's t-test comparing application coverage levels under a 2-day delay and one test per notification. Subplot (A) represents the total population, (B) corresponds to individuals under 18 years of age, (C) represents individuals aged 18–65, and (D) corresponds to individuals aged 66 years or older. 68

5.15 P-values from Welch's t-test comparing application coverage levels under a 1-day delay and up to two tests per notification. Subplot (A) represents the total population, (B) corresponds to individuals under 18 years of age, (C) represents individuals aged 18–65, and (D) corresponds to individuals aged 66 years or older. 69

5.16 P-values from Welch's t-test comparing application coverage levels under a 2-day delay and up to two tests per notification. Subplot (A) represents the total population, (B) corresponds to individuals under 18 years of age, (C) represents individuals aged 18–65, and (D) corresponds to individuals aged 66 years or older. 70

5.17 P-values from Welch's t-test comparing 1-day and 2-day delays between notification and testing for scenarios with one test per notification across different application coverage levels. Subplot (A) represents the total population, (B) corresponds to individuals under 18 years of age, (C) represents individuals aged 18–65, and (D) corresponds to individuals aged 66 years or older. 71

5.18 P-values from Welch's t-test comparing 1-day and 2-day delays between notification and testing for scenarios allowing up to two tests per notification across different application coverage levels. Subplot (A) represents the total population, (B) corresponds to individuals under 18 years of age, (C) represents individuals aged 18–65, and (D) corresponds to individuals aged 66 years or older. 72

Chapter 1

Introduction

Advances in automation and digital technologies have increasingly influenced decision-making across many aspects of daily life. In public health, these technologies have been adopted to reduce time and resource constraints associated with surveillance, communication, and intervention delivery. Their relevance became particularly evident following the emergence of the coronavirus disease 2019 (COVID-19) pandemic, during which digital tools played a central role in supporting large-scale public health responses [1].

The COVID-19 pandemic was driven by the global spread of severe acute respiratory syndrome coronavirus 2 (SARS-CoV-2), leading the World Health Organization (WHO) to declare a Public Health Emergency of International Concern from January 30th, 2020 to May 5th, 2023 [2]. The prolonged duration of this emergency disrupted established societal and economic activities worldwide, necessitating widespread behavioural and policy adaptations. Travel restrictions were implemented at both international and local levels, public health measures such as mask mandates were enforced, and verifications of health status were required for participation in certain activities [3].

In response to these disruptions and ongoing uncertainty, public health systems sought adaptive strategies to maintain continuity while limiting transmission. Reduced physical accessibility accelerated the adoption of virtual and digital solutions, facilitating communication, coordination, and service delivery at scale. This transition supported the

refinement and expansion of established epidemiological interventions, including contact tracing [4], by enabling more timely and efficient identification of potential exposures.

1.1 Contact Tracing

Contact tracing is the process of identifying and monitoring individuals who have been in close proximity to an infectious person for a sufficiently long duration to pose a risk of transmission [5]. Historically, contact tracing has been conducted manually, relying on interviews with individuals who test positive to elicit information about their recent "close contacts" over a defined exposure window [6]. During the COVID-19 pandemic, for example, the Centers for Disease Control and Prevention defined a close contact as an individual who was within six feet of an infectious person for a cumulative duration of at least 15 minutes over a 24-hour period [7–9]. Identified contacts were subsequently notified of their potential exposure and advised to take appropriate precautions, such as testing or quarantine, irrespective of symptom presentation.

Manual contact tracing offers several advantages. By enabling the targeted identification of exposed individuals, it supports early detection of asymptomatic or presymptomatic infections and reduces onward transmission. In addition, the individualized nature of contact notification allows for greater discretion in communicating exposure risk, which may mitigate stigma and social discomfort associated with confirmed cases. Targeted tracing also reduces the need for population-wide isolation measures, which have been shown to adversely affect mental well-being when prolonged [3, 5]. Despite these strengths, manual contact tracing is subject to important limitations.

A central limitation is its reliance on accurate human recall, which is inherently imperfect [10]. Infected individuals must retrospectively identify contacts based on both proximity and duration criteria, a task that becomes particularly challenging for interactions with unfamiliar individuals or those of shorter duration [11]. Such limitations may result in missed contacts, increasing the risk of ongoing transmission, or conversely, in

unnecessary quarantine when interaction durations are overestimated. Moreover, manual contact tracing is highly time- and labour-intensive, constraining its scalability during periods of widespread transmission. Collectively, these challenges have motivated interest in digital contact tracing (DCT) as a complementary or alternative approach [5, 9].

1.2 Digital Contact Tracing (DCT)

DCT extends traditional contact tracing by using downloadable applications that rely on wireless communication technologies, most commonly Bluetooth, to exchange proximity information between devices [12]. When a user is identified as infectious, the collected proximity data are used to determine recent close contacts and, if those individuals are also users of the application, to notify them of their potential exposure [6]. DCT applications are typically deployed on smartphones or wearable devices, such as smartwatches [12], and are generally implemented using either centralized or decentralized system architectures [13].

In centralized DCT systems, users are assigned anonymous identifiers by a central server that maintains and updates a shared database. When a user reports a positive test result through the application, the server processes stored proximity and duration data to identify and notify close contacts [14]. Applications employing this architecture include COVIDSafe in Australia [13, 14], Bulgaria's ViruSafe [14, 15], and TousAntiCovid in France [14, 16].

Decentralized DCT systems adopt a similar proximity-sensing mechanism but differ in how exposure data are processed and shared. In this framework, the central server receives information only from users who report an infectious status, typically in the form of anonymous identifiers associated with their device. Other users' applications periodically download these identifiers and perform local matching to determine whether a potential exposure has occurred, triggering a notification when a match is detected [14, 17]. Notable examples of decentralized implementations include the Canadian COVID

Alert application [14, 18], Germany's Corona-Warn-App [14, 19], and SwissCovid [14, 20].

Despite addressing several limitations of manual contact tracing, the adoption of DCT during the COVID-19 pandemic introduced new challenges that complicated the evaluation of its real-world effectiveness. Public concerns related to privacy, data security, and distrust in data governance were consistently identified as key barriers to uptake [21, 22]. Limited adoption constrained population-level coverage, reducing the potential impact of DCT even in settings where the underlying technology functioned as intended.

Evidence of these concerns is illustrated by a national survey conducted in Australia in May 2020, which assessed public attitudes toward the COVIDSafe application [23]. Among 1,500 respondents, 44% reported either unwillingness or uncertainty regarding installation. Within this subgroup, concerns about data security accounted for one-quarter of responses, while 11.1% cited lack of trust in government institutions. Technical barriers, including software compatibility and device storage limitations, were also reported, with 24.1% of non-users identifying these issues as factors influencing their decision [23].

Despite these challenges, DCT remains theoretically attractive due to its potential to provide rapid, scalable, and minimally intrusive exposure notification. Its capacity to integrate with complementary interventions, such as self-administered testing and voluntary symptom-based isolation, may reduce demands on public health personnel and healthcare systems, particularly during periods of high incidence [24]. Understanding the conditions under which DCT can meaningfully contribute to outbreak control, both independently and in combination with other interventions, forms a central focus of this thesis.

1.3 Thesis Overview

This study investigates the transmission dynamics of an infectious disease through simulation of viral spread within a population of 10,000 individuals over a period of 365

days. The model, although structurally developed and parameterized with estimates of SARS-CoV-2, preserves generality and allows for the adaptability of the framework. This design choice allows the proposed methodology to be adapted to a wide range of directly transmitted respiratory pathogens through appropriate re-parameterization, including both well-characterized pathogens and emerging or previously unknown diseases. To ensure relevance to public health practice, the framework incorporates intervention strategies that were widely implemented or considered during the COVID-19 pandemic, drawing on established tools from epidemiological modelling.

One foundational component of the modelling framework is the classical Susceptible–Infected–Recovered (SIR) model, which categorizes individuals according to their infection status and associated transmission potential [25]. In this formulation, susceptible individuals (S) are at risk of infection, infected individuals (I) are capable of transmitting the disease, and recovered individuals (R) are assumed to have acquired immunity following infection [25]. In some extensions of the model, the recovered compartment also includes individuals who have died as a result of infection, in which case it is referred to as the *removed* class. Such extensions reflect one of many adaptations of the basic SIR framework developed to better represent specific epidemiological contexts [26–28].

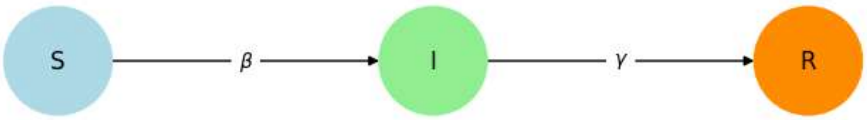

Figure 1.1: Flow diagram of an SIR model with constant transmission and recovery rates, β and γ, respectively.

Another central component of the framework is the inclusion of a hypothetical DCT application operating within the simulated population. The application mirrors the core functionality of real-world DCT systems by notifying users of potential exposure following contact with an infected individual. Upon receiving a positive test result, users are assumed to report their status through the application, which initiates notification of close contacts while the infected individual enters isolation.

This capacity for rapid response aligns naturally with the incorporation of at-home diagnostic testing, the use of which increased substantially during later stages of the COVID-19 pandemic [29]. The model assumes that rapid diagnostic tests are continuously available throughout the simulation period, enabling individuals to promptly verify potential exposure following a notification. This assumption simplifies the modelling framework by eliminating delays associated with laboratory testing, supply shortages, and limited access to professional healthcare services.

To isolate the effects of the intervention strategies under investigation, our model further assumes full compliance with application use for those who have the DCT app, and with testing and isolation requirements. This assumption allows behavioural variability driven by factors such as quarantine fatigue [30] and social isolation [31] to be excluded, thereby facilitating a focused examination of the conditions under which DCT and self-testing/isolation can most effectively reduce transmission. The analysis also explores variation in effectiveness across age groups and evaluates the interaction between DCT and symptom-based isolation as concurrent control measures.

The overarching goal of this thesis is to assess the potential role of DCT when integrated with widespread self-testing and mandated self-isolation for positive cases. By examining the effectiveness and limitations of this combined strategy, we aim to contribute a generalizable modelling framework that can inform preparedness and response strategies for future infectious disease outbreaks.

Chapter 2

Literature Review

Infectious diseases are often characterized by the symptoms they produce; however, this perspective does not fully capture the range of possible clinical presentations. In particular, asymptomatic infections, defined as cases in which individuals are infectious but do not manifest disease-specific symptoms following the incubation period, represent an important and frequently underdetected subgroup [32]. Although the absence of symptoms is generally associated with reduced viral shedding [33], asymptomatic individuals may still be capable of transmitting infection [34]. As a result, such cases can contribute to ongoing transmission without triggering testing or isolation, thereby distorting assessments of population-level disease burden.

This limitation has important implications for contact tracing, as undetected infections may generate transmission chains that remain unobserved for extended periods. The effectiveness of contact tracing strategies may therefore decline as the duration of unrecognized infectiousness increases. In response to this challenge, several studies have proposed mass testing as a complementary intervention to improve case detection and reduce silent transmission within the population [28, 35].

2.1 Asymptomatic Testing

Mass testing refers to the repeated screening of a large proportion of a population regardless of symptom presentation, with the objective of rapidly identifying infectious individuals, including asymptomatic and presymptomatic cases [35–37]. Presymptomatic individuals are defined as those who test positive prior to symptom onset but subsequently develop clinical signs of infection [38]. This section reviews empirical evidence from multiple countries to evaluate the effectiveness of mass testing strategies in altering the trajectory of COVID-19 outbreaks.

One comparative study of interest [39] examined the implementation of mass testing in the United Arab Emirates (UAE) between April and November 2020 and contrasted its outcomes with those observed in Germany and Saudi Arabia, where large-scale testing was introduced in late April and May, respectively. The study also compared these approaches with the strategy adopted in the United Kingdom (UK), which primarily targeted symptomatic individuals. Following the introduction of open public testing in the UAE, the mean number of daily tests increased from 6,357 in late March to 119,713 by November 2020. By November 15, the UAE reported the second highest number of COVID-19 tests per capita globally, exceeding testing rates in the UK, Germany, and Saudi Arabia by factors of approximately three, five, and six per thousand population, respectively.

Despite this substantial difference in testing volume, the UAE maintained a relatively stable average monthly test positivity rate of approximately 1% throughout the study period. Positivity peaked at 3.04% in May before declining to a minimum of 0.3% in August. In contrast, the comparator countries exhibited greater temporal variability. Germany reported a positivity rate of approximately 6% in April, followed by a decline to levels comparable to the UAE between June and September, after which rates increased steadily to nearly 8% by November. The UK experienced markedly higher positivity early in the pandemic, exceeding 20% in April, before declining to approximately 1% during

July and August and subsequently increasing again toward levels similar to Germany. Saudi Arabia showed a distinct pattern, with positivity rising from approximately 6% to a peak of around 14% in June, followed by a sustained decline over the remainder of the observation period, resulting in lower rates than the UAE during the final two months.

The study further assessed mortality outcomes using cumulative deaths per million population. By the end of the study period, the UK reported 766 deaths per million, roughly five times higher than Saudi Arabia (162 per million) and Germany (150 per million), and more than an order of magnitude higher than the UAE (54 per million). When considered alongside consistently low positivity rates, these findings suggest that early and extensive population-level testing may have contributed to improved epidemic control in the UAE. The results also highlight contrasts between countries that implemented broad testing strategies and those that relied primarily on symptom-based testing, underscoring the potential role of mass testing in reducing transmission and mortality during large-scale outbreaks.

Further evidence supporting the utility of repeated testing is presented by Wells et al. [40], which advocates for the implementation of policies centred around rapid antigen (RA) testing. Despite the superior diagnostic accuracy of the RT-PCR testing, advantages such as wider availability, shorter delays in obtaining results, and comparative cost-effectiveness render RA testing as a more practical option for integration with frequent testing strategies, a decision that yielded positive outcomes.

Data relevant to testing and disease dynamics were acquired from several sources, including a case study involving an offshore oil company that required employees to quarantine for approximately 24 hours, until a negative RT-PCR test result was obtained. Individuals were permitted to enter the work environment after this preliminary stage, which was followed by the administration of RA tests every three days for their first nine days on site. This policy was noted to have been enforced at the beginning of the staged vaccination rollout in the United States and therefore, none of the workers would have been vaccinated at the time.

The study estimated that daily RT-PCR testing with a 24-hour turnaround time was required to ensure that the effective reproduction number, R_E, the average amount of infections caused by a single case at a given point in time [41, 42], remained less than 1. Such an outcome signifies that the severity of an outbreak is being reduced [41]. A comparable outcome was deemed possible when RA tests with same-day results were administered every two to three days. Of the 18 types of RA tests considered, none were capable of relaying the desired results when the frequency descended beyond the lower threshold.

On average, RA produced a lower R_E than the RT-PCR testing with a 24-hour delay. For instance, RA administration every two days, in conjunction with immediate symptom-based isolation, resulted in an average reduction of 77.9% in the R_E, compared to 61.3% for the RT-PCR strategy.

As mentioned previously, the primary limitation of RA testing is its reduced diagnostic accuracy relative to RT-PCR tests. False-positive results may lead to unnecessary resource use and workforce disruption, and their likelihood increases with testing frequency. However, repeated testing is still recommended to ameliorate the probability of false negatives, which are particularly problematic in the early stages of infection when viral loads are low. Delaying follow-up testing after an initial negative result allows viral loads to increase, thereby improving detection probability. Importantly, the consequences of false negatives are more severe than those of false positives, as failure to isolate an infectious individual may lead to R_E exceeding 1, triggering an outbreak [40].

2.2 Applications of Mobile Technology During Outbreaks

The COVID-19 pandemic accelerated the deployment of mobile technologies as integral components of public health response strategies worldwide [43]. Governments adopted a range of application-based tools tailored to specific policy objectives, including quarantine monitoring in Hong Kong [43], large-scale collection of behavioural and biological

data in Iceland [43], and digital certification of health status in China through remotely updated reporting systems [43–45]. Similarly, the confirmation of individuals being vaccinated was facilitated through applications such as the Canadian Verify Ontario [46] and CovPassCheck [47], which was employed in Germany. Another example of such technological implementations is the Google Apple Exposure Notification framework, released in April 2020 by the titular companies, with a decentralized architecture [48]. The system possessed the same objectives as other contact tracing platforms but primarily distinguished itself by performing most critical procedures at the operating system level [48]. When combined with other preventive measures, such technologies have been associated with improved access to timely information, enhanced monitoring of population mental health, and the identification of novel predictors relevant to outbreak forecasting and control [24].

Singapore provides a prominent example of integrated mobile technology use through the TraceTogether and SafeEntry systems, examined in detail by Chow et al. [49]. TraceTogether was initially launched on March 20, 2020, as a Bluetooth-based application designed to support manual contact tracing by identifying and notifying individuals potentially exposed to infection. To address accessibility limitations, the system was later extended to include physical tokens for individuals without smartphones. Adoption of TraceTogether was notably high, with 96.3% of locally reported cases between August 24, 2021 and February 17, 2022 registered as active users, a rate likely facilitated by the mandatory venue check-in process implemented through SafeEntry.

SafeEntry required individuals to either scan a QR code or tap a TraceTogether-enabled device upon entering public venues, enabling the recording of location, time of entry, and, when relevant, vaccination status. Following confirmation of a positive test result, application users received a short message service (SMS) code to submit information about close contacts, while token users could present devices at healthcare facilities or arrange collection from their residences. Although the system was widely integrated into daily activities, compliance with data submission following infection was limited,

with only 52.2% of assessed cases completing this step, thus constraining the overall effectiveness of the contact tracing process [49].

Despite these limitations, the study concluded that TraceTogether contributed meaningfully to outbreak control efforts. Automated health risk warnings and quarantine orders were issued based on estimated exposure risk, with health risk warnings prompting users to obtain a negative rapid antigen test result and quarantine orders mandating a 14-day isolation period. During the study period, automated health risk warnings yielded a test positivity rate of 3.6%, compared with 6.2% for health risk warnings and 12.5% for quarantine orders generated through manual contact tracing supported by the application. Importantly, the median processing time for automated notifications was 18.3 hours, compared to 28.1 hours for manual tracing, representing a reduction of approximately 35%, and underscoring the potential time efficiency of DCT systems [49].

Mobile technology also played a role in outbreak response during the 2014-2016 West African Ebola outbreak, the largest one on record, which resulted in 28,656 confirmed infections and 11,325 deaths [50]. Sierra Leone was disproportionately affected, reporting 8,706 cases and 3,956 fatalities [50]. In response, DCT tools were explored as a supplement to existing manual processes, leading to the development of the Ebola Contact Tracing application [51].

A study conducted in Port Loko District evaluated the deployment of this application among 26 contact tracing coordinators and 86 contact tracers [51]. The digital system was introduced to augment a paper-based workflow in which suspected cases identified through investigation were tested, and confirmed cases initiated contact tracing via a physical daily reporting form. Manual procedures were found to be limited by substantial time demands and frequent documentation errors, including incomplete and inaccurate records. The digital application addressed these issues through automated data validation, time-stamping of entries, and immediate transmission of information to the district Ebola Response Centre.

Comparative analysis of digital and paper-based contact tracing conducted between

April 13 and August 31, 2015 demonstrated improved data completeness and follow-up using the digital system. Under the paper-based approach, records were returned for only 38.5% of 408 contacts and several contained insufficient information for effective monitoring. In contrast, 62.5% of the 556 contacts associated with 16 digitally monitored cases were successfully visited and assessed by contact tracers, indicating enhanced operational performance relative to traditional methods [51].

2.3 Previous Models

A 2021 study by Barrat et al. [5] investigated the effectiveness of manual and digital contact tracing in settings designed to approximate communities transitioning toward normal activity following the relaxation of lockdown measures. The analysis focused on two empirical contact networks comprising approximately 200 individuals in a school environment and 700 individuals in an office environment, respectively. Disease transmission dynamics were simulated using a compartmental framework adapted from earlier work by Di Domenico et al. [52], incorporating high-resolution temporal and spatial contact data.

Although both datasets were used to evaluate the impact of digital contact tracing, the data collection mechanisms differed between settings. In the school environment, participants were provided with smartphones and required to install a dedicated application capable of detecting nearby Bluetooth devices, thereby identifying close contacts based on signal strength [5, 53]. In the office environment, contact data were collected using wearable proximity sensors employing low-power radio communication, with a temporal resolution of 20 seconds, allowing identification of close contacts among individuals equipped with the devices.

The modelling framework extended the classical SIR structure by incorporating additional health states, including exposed (E) and isolated (Q) compartments, and subdividing the infected class into presymptomatic (P), asymptomatic (I_a), mildly symptomatic (I_m),

and severely symptomatic (I_s) subpopulations. Transitions from the exposed compartment into I_a, I_m, or I_s occurred with probabilities p_a, p_m, and $1 - p_a - p_m$, respectively. Susceptible individuals could either become infected and enter the exposed compartment or be identified as close contacts and placed in isolation. Individuals in the E, I_a, I_m, and I_s compartments could also transition into isolation following contact tracing. Upon completion of the isolation period, individuals who remained uninfected returned to the susceptible class, while those who recovered or died entered the recovered (R) compartment. Severely symptomatic individuals were assumed to transition exclusively into isolation, whereas asymptomatic and mildly symptomatic individuals could recover directly.

Simulations were initiated by randomly selecting a single infected individual to seed transmission. Manual contact tracing was modelled by defining close contacts as individuals whose cumulative interaction duration with an infected case exceeded a threshold θ_{ct} within the 48 hours preceding case detection. To account for practical limitations of manual tracing, two additional parameters were included: p_{ct}, representing the proportion of contacts successfully identified, and τ_{ct}, representing a two-day delay between case confirmation and isolation of contacts. Digital contact tracing followed a similar exposure criterion, with contacts defined by interactions exceeding a threshold θ_{app} during the 48 hours prior to a positive test. Adoption was captured through the parameter p_{app}, denoting the proportion of the population using the application, while τ_{dct} represented the delay between contact notification and isolation, ranging from 0 to 2 days. A key distinction between manual and digital tracing in the model was the assumption that digital systems identify all close contacts of participating users without recall error.

The study found that when manual contact tracing was implemented in isolation, reductions in final epidemic size increased approximately linearly with p_{ct}. In contrast, reductions associated with digital contact tracing exhibited a quadratic dependence on application adoption. While improvements in manual tracing effectiveness substantially enhanced outbreak control, the addition of digital contact tracing consistently yielded further reductions in epidemic size. These gains were attributed primarily to shorter delays

between case detection and contact isolation enabled by digital systems [5].

Chapter 3

Methodology

This chapter describes the structure and implementation of the agent-based model used in this study. The model evaluates scenarios with and without self-isolation following exposure notifications. Agent behaviour is partially determined by age, which influences patterns of social contact represented through an age-structured contact matrix, as well as the probability of using the DCT application.

Seven health states are included in the model, with transitions between states triggered by infection events originating from susceptible individuals. These transitions collectively determine the transmission dynamics of the simulated outbreak and allow estimation of epidemiological quantities such as the basic reproduction number (R_0).

Disease progression is modelled by assigning durations of residence in infectious compartments based on probability distributions. These stochastic durations enable the simulation to capture variability in the natural history of infection across individuals.

3.1 Study Design

Agent-based models simulate events by considering interactions of individuals with each other and their environment, rather than a system of equations [54, 55]. Agents are assigned personal attributes, such as age, health status and whether they use the application, which could influence behavioral dynamics and, thus, the trajectory of the outbreak. The

computational nature of the framework results in mathematical intractability [56], but allows for a simpler compartmental structure to assess transmission dynamics than what would likely arise from a deterministic approach, as shown in Figure 3.1.

Monte Carlo simulations were performed to capture several possible variations of the progression of the event [57] and averaged to determine a probable outcome. This is important because multiple components of our model, including the estimation of certain parameters, such as infectious periods, which were sampled from probability distributions or the likelihood of symptom development, incorporate randomness. A total of 1,000 simulations is generally considered sufficient to account for the effects of noise and stochasticity.

3.2 Assumptions

The model relies on several simplifying assumptions to ensure computational tractability while capturing the essential features of infectious disease transmission. The primary assumptions are:

- Given the short timelines for simulating a single outbreak, demographic processes such as births, migration, and natural mortality are not included.
- Only individuals between the ages of 18 and 65 are eligible to use the DCT application.
- Diagnostic tests are assumed to be readily available throughout the simulation period.
- Diagnostic tests are assumed to have perfect specificity (i.e., no false positives).
- All symptomatic individuals are assumed to experience the same degree of symptom severity.

- Individuals who recover from infection remain immune for the remainder of the simulation.

3.3 Model Structure

The simulations in this study are based on a compartmental agent-based framework consisting of the seven health states illustrated in Figure 3.1. In addition to health status, individuals are categorized according to whether they use the digital contact tracing application. Specifically, the population is divided into two groups: application users and non-users. The corresponding model variables are described in Table 3.1.

To account for age-dependent behaviour and disease outcomes, the population is further stratified into three age groups: individuals younger than 18 years, individuals aged 18–65 years, and those aged 66 years or older.

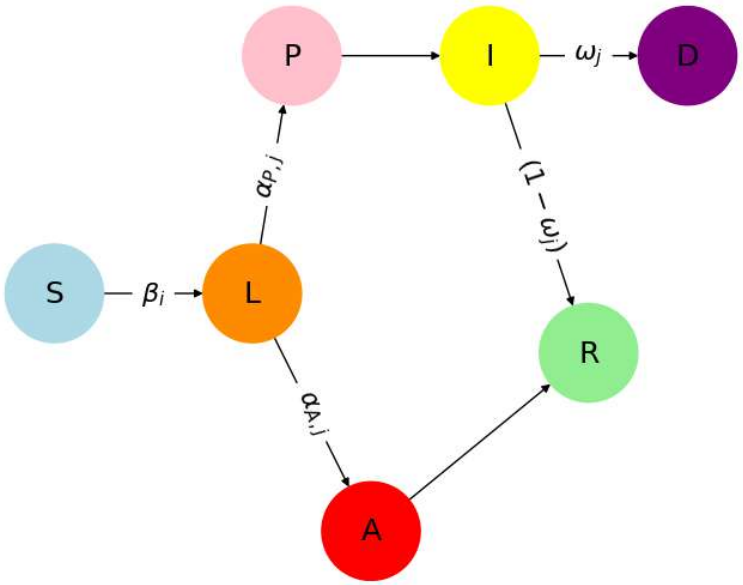

Figure 3.1: Flow diagram displaying the dynamics of the disease outbreak.

Table 3.1: Description of the model variables.

Variable	Description
S	Susceptible individuals
L	Latent individuals
A	Asymptomatic individuals
P	Presymptomatic individuals
I	Symptomatic individuals
R	Recovered individuals
D	Deceased individuals due to infection
N_a	Individuals who use the DCT application
N_m	Individuals who do not use the DCT application

Susceptible Class

The simulation begins with the selection of a random individual to enter the latent state, initiating the transmission process within the population. Infection occurs through direct contact between susceptible and infectious individuals. The probability of transmission depends on the infectious state of the transmitting individual, represented by the parameter β_i in Figure 3.1, where i denotes the infectious compartment. Transmission from asymptomatic, symptomatic and presymptomatic individuals occurs with probabilities of β_A, β_I and β_P, respectively.

Latent Class

The latency period represents the time between infection and the onset of infectiousness [58]. In the model, individuals remain in the latent compartment for a duration between 1 and 6 days. After this period, individuals transition to either the presymptomatic or asymptomatic class. These transitions occur with age-dependent probabilities $\alpha_{P,j}$ and $\alpha_{A,j}$, respectively, where j denotes the age group of the individual.

Presymptomatic Class

The presymptomatic compartment contains individuals who have completed the latent stage and will subsequently develop symptoms, after the end of the incubation period [59, 60]. Individuals remain infectious during this stage, and the duration of the presymptomatic period is sampled from a gamma distribution for each infectious individual independently. After this period, individuals progress to the symptomatic compartment.

Asymptomatic Class

Asymptomatic individuals remain infectious throughout their infection but do not develop observable symptoms. Although their transmission potential is generally lower than that of symptomatic individuals due to lower viral loads, asymptomatic cases can still contribute to disease spread. Because these individuals do not experience symptoms, they may not seek testing in the absence of exposure notifications, which increases the likelihood of undetected transmission [61]. The duration of the asymptomatic infectious period is sampled from a gamma distribution for each individual independently, after which individuals recover from the virus.

Symptomatic Class

Symptomatic individuals exhibit clinical signs of infection following the presymptomatic stage [62]. In the absence of behavioural restrictions, individuals in this compartment are typically major contributors to transmission due to higher viral loads. The duration of the symptomatic period is also sampled from a gamma distribution for each individual independently. At the end of this period, individuals either die with probability, ω_j, where j denotes the age group, or recover.

Recovered Class

Recovered individuals have cleared the infection and are assumed to acquire immunity for the remainder of the simulation. Under the modelling assumptions that immunity does not

wane and that death occurs only as a result of infection, individuals do not transition out of the recovered compartment.

Deceased Class

Deaths in the model occur only among symptomatic individuals. This simplification isolates mortality directly attributable to infection and allows clearer interpretation of disease-related outcomes in the simulated population.

Application Users

An important parameter of the model is μ, representing the proportion of the population that installs and uses the digital contact tracing application. The application serves two primary functions: enabling infected individuals to report their positive test results and notifying close contacts of potential exposure. To isolate the effects of the intervention, the model assumes full compliance among application users. Specifically, users are assumed to perform diagnostic tests when notified of exposure, potentially with some delays from the time of notification, report positive results through the application, and adhere to isolation requirements for the full duration of the prescribed period.

The demographic composition of application users is also considered in the model. Application adoption is restricted to individuals between the ages of 18 and 65 years. Individuals younger than 18 are excluded from the users population of DCT due to lower expected smartphone ownership and limited independence in decision-making. Individuals older than 65 are also excluded due to lower average familiarity with mobile technologies and reduced levels of daily social interaction relative to younger age groups [63, 64].

3.4 Intervention Strategies

3.4.1 Strategy I: Use of DCT Only

In the first intervention strategy, disease control relies exclusively on DCT. When an infectious DCT user interacts with another application user within the defined proximity threshold, both devices register the encounter as a potential close contact. If an individual subsequently tests positive and reports this result through the application, all recorded close contacts from the preceding three days receive exposure notifications.

Upon receiving a notification, individuals are instructed to perform a diagnostic test which may be performed with a delay of 1–2 days, depending on the simulated scenario, regardless of whether they are indeed infected. Individuals who test positive regardless of their symptom status isolate for seven days and report the result through the application, triggering notifications to their own close contacts from the previous three days. This recursive process allows exposure notifications to propagate through the contact network.

The three-day lookback period is intended to capture interactions occurring during the incubation period, which also accounts for the presymptomatic stage of infection [60], thereby improving the identification of exposed and potentially infectious individuals.

If the initial test following notification is negative, some policy scenarios would require a second confirmatory test two days later. Individuals who test negative twice do not isolate or perform additional tests. If the second test is positive, the individual enters isolation and reports the result through the application. The second test serves as a precaution against false-negative results, while the model assumes that false-positive results do not occur. Test sensitivity is based on Abbott-Panbio^{TM} RA tests, and may depend on the duration of the incubation period of the specific agent and the amount of time that has passed since infection [65].

Application users who are clinically symptomatic will test themselves independently of exposure notifications. In this case, testing occurs one day after symptom onset, or at least two days after any previous test. If the initial symptom-driven test is negative, a second

test may be required depending on the simulated policy. Individuals who test positive isolate and notify their contacts from the preceding three days through the application.

3.4.2 Strategy II: DCT and Symptom-Based Isolation

The second intervention strategy combines digital contact tracing with symptom-based isolation. Under this policy, all symptomatic individuals initiate a five-day isolation period at the onset of symptoms, regardless of whether they use the application. This approach reflects mitigation strategies previously explored for respiratory diseases such as COVID-19 and influenza [66–69].

If an individual is already isolating due to exposure notification and a positive test result, the isolation period is extended to ensure that at least five days of isolation occur following symptom onset. Asymptomatic application users who test positive continue to follow the seven-day isolation period defined in Strategy I.

The epidemiological outcomes associated with Strategy I are presented in Chapter 4, while the results for Strategy II are discussed in Chapter 5.

3.5 Model Parameters

3.5.1 Disease and Framework Parameters

The transmission dynamics in the model are determined by a set of epidemiological and behavioural parameters. Some parameters are assumed to be constant across all individuals, while others vary according to the age group of the agents involved. Parameters that do not depend on age are summarized in Table 3.2. These include quantities that define the baseline disease progression and the operational features of the modelling framework.

Age-dependent parameters are presented in Tables 3.3 and 3.4. These parameters capture differences across age groups in disease progression and clinical outcomes following infection.

Table 3.2: Age-independent disease-related parameters.

Parameter	Description	Value	Source
β_A	Transmission probability for the asymptomatic stage	0.0312	[28, 70–72]
β_P	Transmission probability for the presymptomatic stage	0.12	Calibrated to $R_0 = 2.24$ [28]
β_I	Transmission probability for the symptomatic stage	0.1068	[28, 70–72]
a (days)	Duration of the asymptomatic period	Gamma(shape: 5, scale: 1)	[73]
p (days)	Duration of the presymptomatic period	Gamma(shape: 1.058, scale: 2.174) [1, 3]	[28]
s (days)	Duration of the symptomatic period	Gamma(shape: 2.768, scale: 1.1563)	[73]
i_p (days)	Incubation period	LogNormal(shape: 1.434, scale: 0.661) [4, 7]	[70, 74]
τ	Duration of the simulation	365 days	Assumed
i	Initial number of infected individuals	1 person	Assumed
δ	Minimum isolation period for symptomatic individuals (Strategy II)	5 days	Assumed
ζ	Minimum isolation period for asymptomatic individuals	7 days	Assumed
c	Reduction in number of daily contacts for isolated individuals	0.72	[75–77]

Table 3.3: Variations of the probabilities with which individuals transition out of the latent class with respect to age.

Parameter	0–4	5–19	20–49	50–64	65–79	80+	Source
$\alpha_{P,j}$, Probability of latent individuals from age group j entering the presymptomatic class	0.7	0.623	0.672	0.672	0.812	0.812	[78–81]
$\alpha_{A,j}$, Probability of latent individuals from age group j entering the asymptomatic class	0.3	0.377	0.328	0.328	0.188	0.188	[78–81]

Table 3.4: Variations of the probabilities with which individuals transition into the deceased class with respect to age.

Parameter	0–34	35–54	55–69	70–84	85+	Source
ω_j, Probability of symptomatic individuals from age group j entering the deceased class	0.00001	0.00015	0.00165	0.0321	0.3048	[27, 70, 82]

Table 3.5: Parameters related to testing and contact tracing.

Parameter	Description	Value	Comment
ϕ	Lookback period for contact tracing	3 days	Assumed
μ	Proportion of the eligible population that installs the application	$0-1$	Varied
b	Interval between the first and second tests following a notification	2 days	Assumed
u	Delay between exposure notification and testing	$1-2$ days	Varied
n	Maximum number of tests performed following a notification	$1-2$ tests	Varied
κ	Diagnostic test sensitivity	$0-1$	[65]
λ	Relative reduction in test sensitivity for asymptomatic infections	0.5	Assumed

3.5.2 Testing and Contact Tracing Parameters

Testing and digital contact tracing constitute the primary intervention mechanisms examined in this study. The parameters governing these processes are summarized in Table 3.5.

3.5.3 Contact Matrix

To represent age-specific patterns of social interaction within the population, we incorporated an age-structured contact matrix, denoted by CM. The matrix is defined over five age groups: 0–4, 5–19, 20–49, 50–64, and 65+ years. Each age group corresponds to both a row and a column of the matrix. The entry $CM_{i,j}$ represents the proportion of daily contacts of an individual in age group i that occur with individuals in age group j. These values therefore characterize the mixing patterns between age groups in the simulated population [65].

For each agent, the total number of daily contacts is sampled from an age-specific negative binomial distribution [70, 76, 77]. Contacts are then allocated across age groups according to the proportions specified in the contact matrix. The same procedure is applied to individuals in isolation; however, their contact rates are reduced to reflect decreased social interaction during isolation.

$$
CM = \begin{array}{c} \begin{array}{ccccc} 0-4 & 5-19 & 20-49 & 50-64 & 65+ \end{array} \\ \left[\begin{array}{ccccc} 0.25 & 0.132 & 0.44 & 0.144 & 0.034 \\ 0.0264 & 0.43 & 0.404 & 0.108 & 0.0316 \\ 0.03 & 0.13 & 0.602 & 0.179 & 0.059 \\ 0.026 & 0.086 & 0.456 & 0.3 & 0.132 \\ 0.012 & 0.052 & 0.303 & 0.266 & 0.367 \end{array}\right] \end{array} \begin{array}{l} \textbf{Age} \\ 0-4 \\ 5-19 \\ 20-49, \\ 50-64 \\ 65+ \end{array}
$$

3.6 Computational Implementation

The simulations were implemented using an agent-based modelling framework. In this approach, each individual in the population is represented as an agent with a set of attributes that influence interactions with other agents and the surrounding environment, according to the assumptions of the model [54]. The model was implemented in the Julia programming language, and each scenario was evaluated using 1,000 Monte Carlo simulations.

Each simulation represents a stochastic realization of the epidemic over a 365-day period. Random seeds were assigned according to the simulation index to ensure reproducibility while allowing independent random sampling across simulations. Simulation outputs were processed using the high-performance computing cluster of York University's Agent-Based Modelling Laboratory. The resulting data were then analyzed in R using RStudio. For each scenario, the mean daily incidence (i.e., the average number of new infections per day) was computed across all simulations to characterize the typical epidemic trajectory.

The basic reproduction number (R_0) represents the expected number of infections generated by a single individual in a fully susceptible population [83]. In the context of our model, the quantity was estimated in the scenario without interventions by tracking the number of secondary infections caused by the initially infected individual across the

simulations and computing the average. In our literature, the studies generally considered values that ranged from 2 to 2.5 [27, 28, 84], and to align with these sources, the calculations were repeated several times with varying probabilities of presymptomatic transmission until an R_0 of 2.24 was obtained. The effective reproduction number for the baseline of the second strategy was calculated in a similar manner, but with the incorporation of symptom-based isolation.

Subsequent statistical analysis was conducted in R using bootstrap resampling. For each simulation, the total number of infections over the course of the outbreak was first computed. The attack rate for each simulation was then obtained by dividing this value by the population size. Bootstrap sampling with replacement (1,000 iterations) was applied to the resulting distribution to estimate variability in the attack rate across simulations [85].

The attack rate is defined as the proportion of the population infected during the outbreak [86]. Distributions of attack rates across scenarios were visualized using notched box plots. In addition, the relative reduction in attack rate associated with each level of application adoption was calculated relative to the corresponding baseline scenario. The relative reduction is defined as:

$$RR = \frac{A_0 - A_S}{A_0},$$

where RR is the relative reduction in attack rate, A_0 represents the attack rate under the baseline scenario, and A_S is the attack rate for the intervention scenario being assessed. These results were also visualized using box plots.

Finally, statistical tests were performed in R to assess the distributional properties of the bootstrapped estimates and to evaluate statistically significant differences between scenarios. A significance level of $\alpha = 0.05$ was used for all tests, corresponding to a 95% confidence level.

Chapter 4

Digital Contact Tracing with Self-Testing

This chapter presents the simulation results for the intervention strategy in which the initiation of the 7-day isolation period depends on application users receiving a positive diagnostic test result. Epidemic dynamics are first illustrated using time series plots of daily incidence. Following bootstrap resampling, attack rates and the corresponding relative reductions are compared across scenarios using box plots. Finally, statistical tests are performed to identify significant differences between the outcomes of the various policy scenarios.

4.1 Outline of Policy Scenarios

The baseline scenario corresponds to the absence of digital contact tracing, where the application is not deployed within the population. This scenario serves as the reference case and is first examined using time series plots of daily incidence. Subsequent scenarios introduce the application into the population and modify selected model parameters to evaluate the effects of different policy assumptions.

A total of 16 scenarios are considered, generated by varying key parameters of the

intervention strategy. These variations are described below.

1. **Application Coverage**

   The proportion of individuals aged 18–65 who install the application is varied from 20% to 80% in increments of 20%. This range reflects plausible levels of adoption and allows evaluation of how application uptake influences epidemic dynamics. In particular, the analysis examines the relationship between adoption levels and the incidence of infection, defined as the number of new infections occurring within a given time period [87].

2. **Delay Between Notification and Testing**

   Another parameter considered is the delay between receiving an exposure notification and performing a diagnostic test. Although the model assumes that rapid tests are generally available, practical constraints may prevent individuals from testing immediately after receiving a notification. In addition, diagnostic sensitivity may depend on the time elapsed since infection. To capture these considerations, two delays are evaluated: testing 1 day after notification and testing 2 days after notification.

3. **Maximum Number of Tests per Notification**

   The model assumes that diagnostic tests do not produce false-positive results but may produce false negatives. Test sensitivity may depend on factors such as time since infection and viral load, which often manifests in symptom severity. To account for this possibility, one scenario requires individuals who receive a negative result following exposure notification to perform a second test two days later. This scenario is compared with an alternative in which only a single test is required after notification, allowing assessment of the effect of confirmatory testing on epidemic outcomes.

4.2 Baseline Scenario

The presymptomatic transmission probability, $\beta_P = 0.12$, was calibrated to produce a basic reproduction number of $R_0 = 2.24$ in the baseline scenario, where no interventions are implemented. The parameter values listed in Tables 3.2–3.5 were used to generate the baseline epidemic trajectories shown in Figures 4.1 and 4.2. These figures illustrate the evolution of daily incidence and cumulative incidence across the simulated population and within age-specific subpopulations. Cumulative incidence is defined as the proportion of a population that becomes infected during a specified period of time [88, 89]. In this analysis, cumulative incidence is calculated relative to the size of each corresponding population subgroup.

Figure 4.1 shows that the population-level incidence reaches a peak of approximately 190 infections per day around day 60 of the simulation. The cumulative incidence curve in Figure 4.2 reaches approximately 59.8% of the population after 166 days, indicating that, on average, 5,980 of the 10,000 agents become infected during the simulated outbreak.

Age-specific results reveal differences in epidemic progression across demographic groups. For example, individuals aged 66 years and older exhibited the lowest cumulative incidence (41.7% of their population size), with a peak incidence occurring later than the other groups. This pattern may reflect the smaller size of this subpopulation (1,708 individuals) and potentially lower daily contact rates for older individuals [64].

In contrast, the 18–65 age group exhibited epidemic dynamics that closely mirror those of the overall population. This group represents the largest proportion of the simulated population (6,386 individuals), which may contribute to higher contact frequencies and transmission opportunities. The cumulative incidence in this group reached approximately 64.1%.

The remaining age group, consisting of individuals younger than 18 years (1,906 agents), had a cumulative incidence of 61.7%. This value is closer to that of the 18–65 group than to the oldest age group, despite the smaller population size.

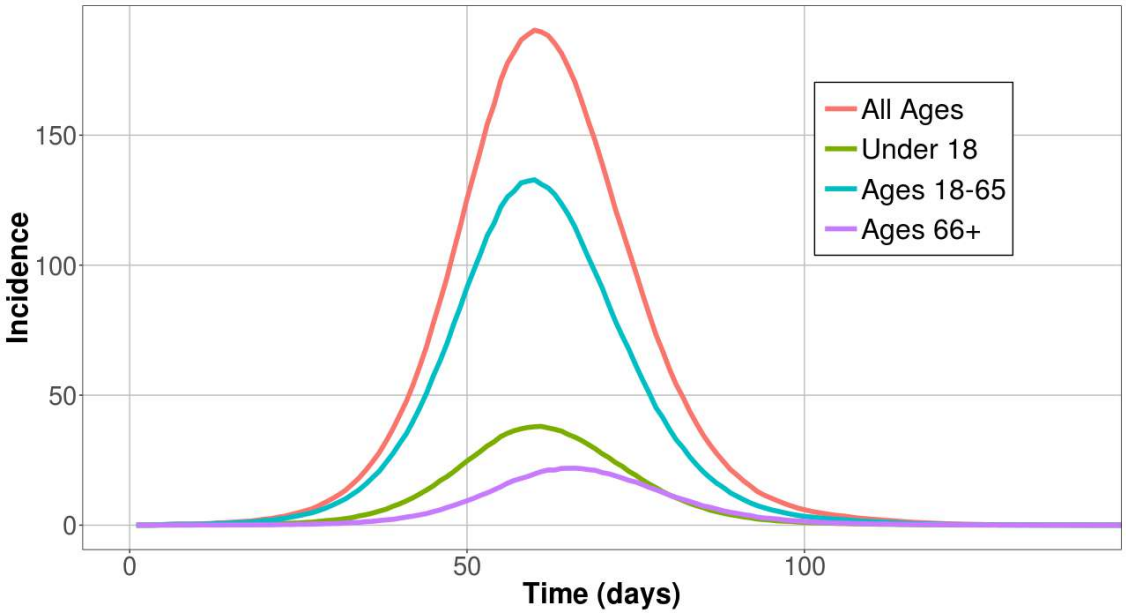

Figure 4.1: Daily incidence in the baseline scenario for the total population (red) and age-specific subpopulations: under 18 years (green), 18–65 years (blue), and over 65 years (purple).

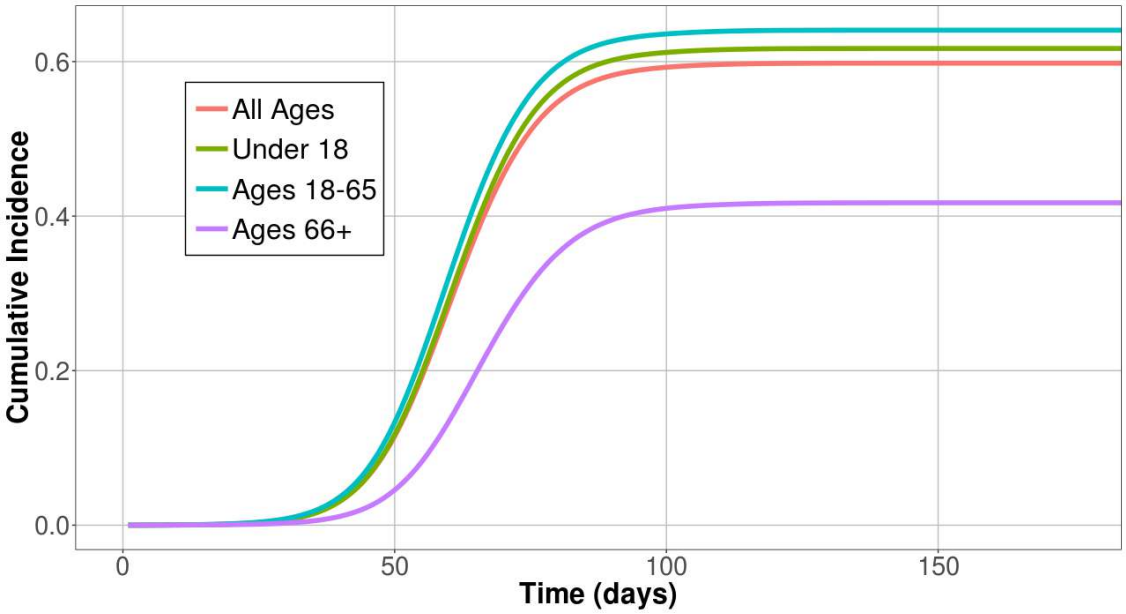

Figure 4.2: Cumulative incidence in the baseline scenario for the total population (red) and age-specific subpopulations, expressed as proportions of the corresponding population sizes: under 18 years (green), 18–65 years (blue), and over 65 years (purple).

4.3 Assessment of Scenarios

Using the calibrated value of R_0, we examined epidemic trajectories and attack rates under varying levels of application adoption. Time series of daily incidence are first compared across scenarios, followed by analysis of attack rates derived from the simulations.

Attack rates are summarized using notched box plots constructed from 1,000 bootstrap samples. The notches represent approximate 95% confidence intervals around the median, allowing visual comparison between distributions. Mean values are indicated by circles, and the whiskers extend to the 2.5^{th} and 97.5^{th} percentiles. Results are grouped by application coverage, enabling comparison of attack rates across scenarios with different testing delays and maximum numbers of tests per notification, while all other parameters are held constant.

4.3.1 Time Series

We begin by examining the temporal evolution of incidence over the 365-day simulation period. Across all scenarios, increasing application adoption is associated with a reduction in transmission intensity. This pattern is observed across all age groups, including those not eligible to use the application, reflecting indirect effects of reduced transmission within the population. In scenarios without application use, no intervention is applied, and the epidemic follows its natural course.

As application coverage increases, the incidence curves shift to the right and exhibit lower peak values, indicating slower epidemic growth and delayed peak incidence. This trend is consistent across all parameter combinations considered.

These patterns are also reflected in the cumulative incidence curves shown in Figures 4.5 and 4.6. In each subplot, higher levels of application coverage are associated with lower plateau values of cumulative incidence. A rightward shift of the curves is also observed, indicating a delay in the progression of the outbreak. These effects are examined further through analysis of attack rates in the following section.

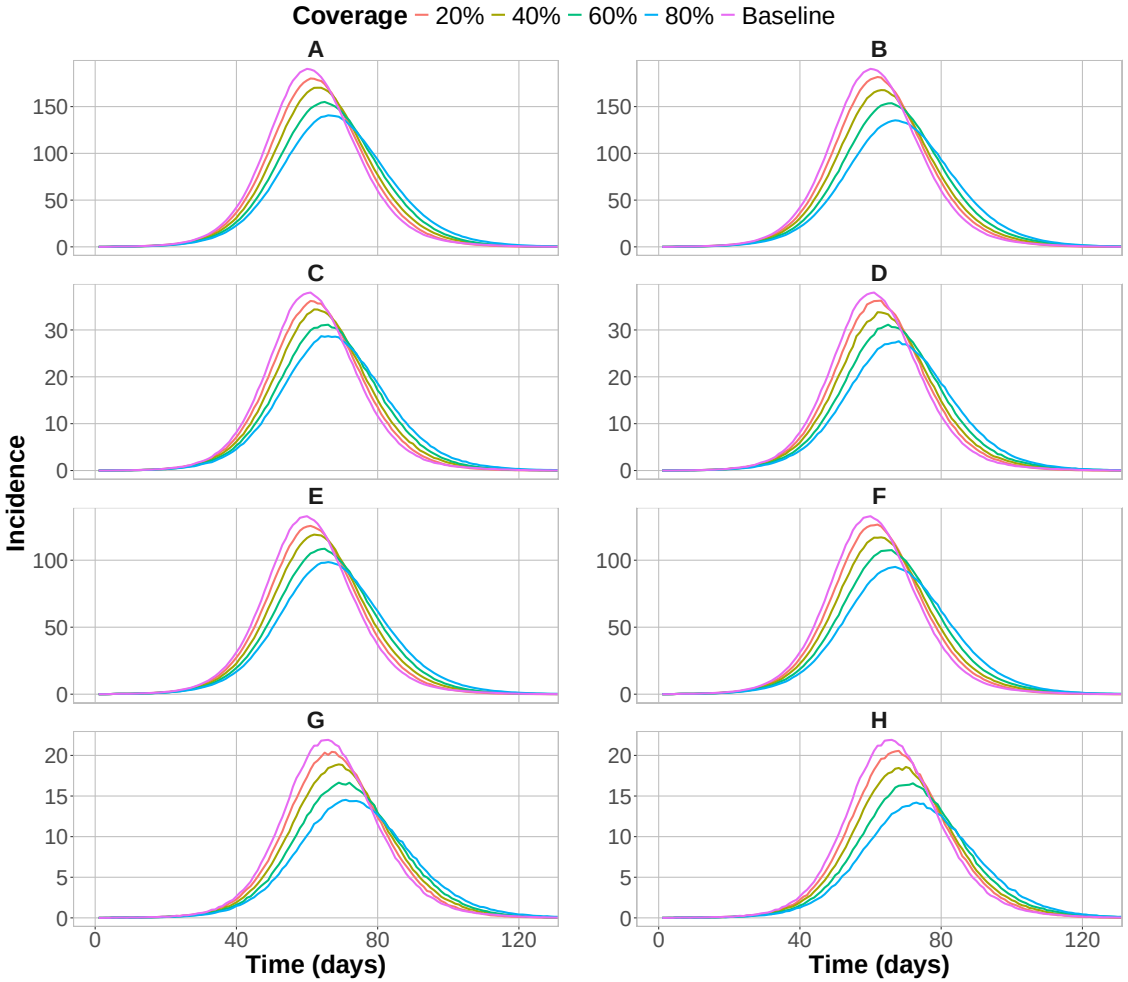

Figure 4.3: Incidence of infection under varying levels of application coverage, assuming one test per notification. Panels on the left correspond to a 1-day delay between notification and testing, while panels on the right correspond to a 2-day delay. Subplots (A) and (B) represent the total population, (C) and (D) correspond to individuals under 18 years of age, (E) and (F) represent individuals aged 18–65, and (G) and (H) correspond to individuals aged 66 years or older.

4.3.2 Attack Rates

Box plots provide a clearer representation of the reduction in attack rates associated with increasing application coverage. They also facilitate comparison between scenarios with different testing delays (1-day vs. 2-day delay following notification) and different limits on the number of tests per notification.

Figure 4.7 presents the population-level results. In the baseline scenario, the mean attack rate is ∼59.4%, with a median of ∼59.3%. In subplot (A), which considers a maximum of one test per notification, a longer delay of 2 days before testing is generally

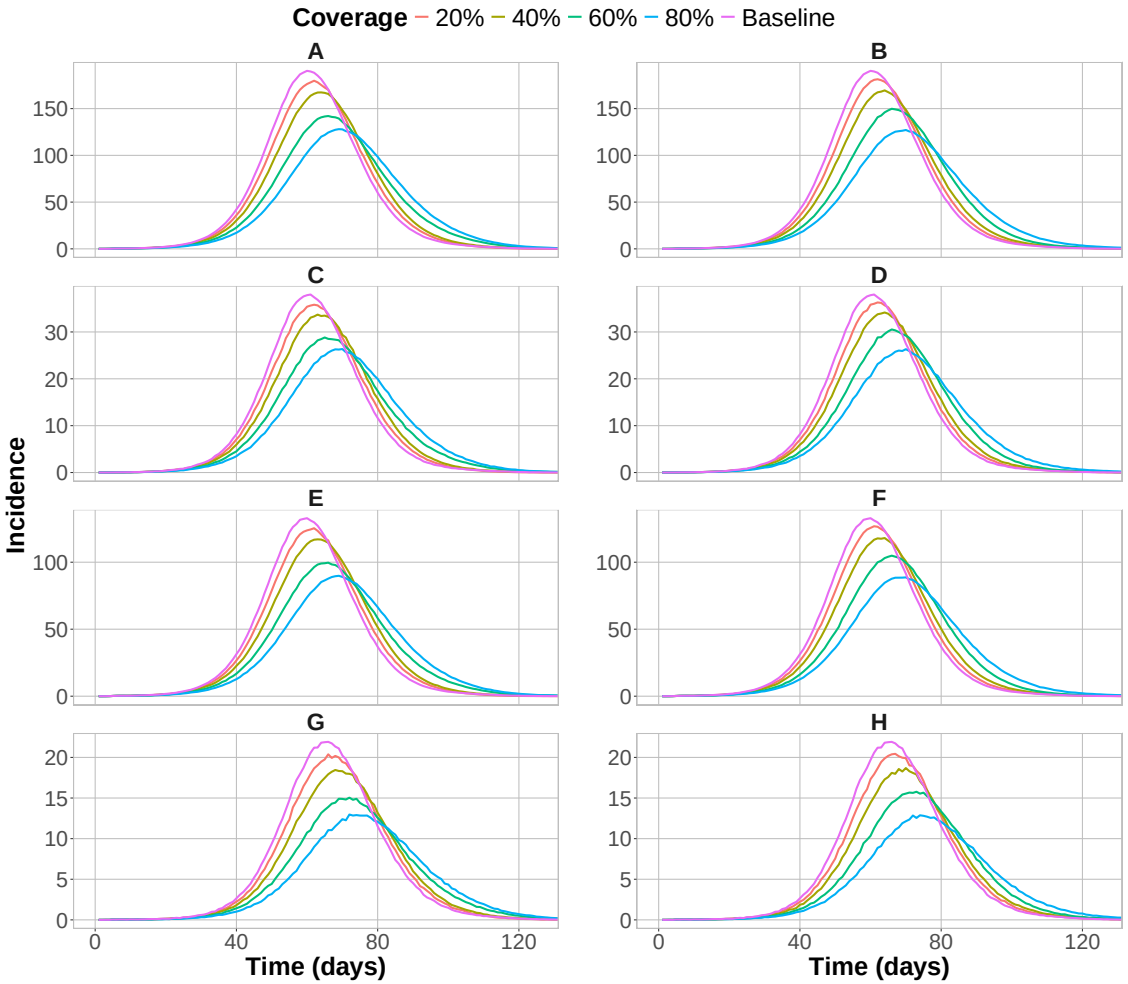

Figure 4.4: Incidence of infection under varying levels of application coverage, assuming up to two tests per notification. Panels on the left correspond to a 1-day delay between notification and testing, while panels on the right correspond to a 2-day delay. Subplots (A) and (B) represent the total population, (C) and (D) correspond to individuals under 18 years of age, (E) and (F) represent individuals aged 18–65, and (G) and (H) correspond to individuals aged 66 years or older.

associated with lower attack rates compared to a 1-day delay. This pattern is reflected in the lower positions of both the means and medians for the 2-day delay (blue boxes) relative to the 1-day delay (red boxes) across most levels of application coverage.

The difference between the two delays is most pronounced at 40% and 80% application coverage, while greater overlap between the notches is observed at 20% and 60% coverage. Across all scenarios, the lowest attack rates occur at 80% application adoption. At this level, the mean and median attack rates are $\sim$51.9% and $\sim$51.8% for a 1-day delay, and $\sim$50.3% and $\sim$50.2% for a 2-day delay, respectively.

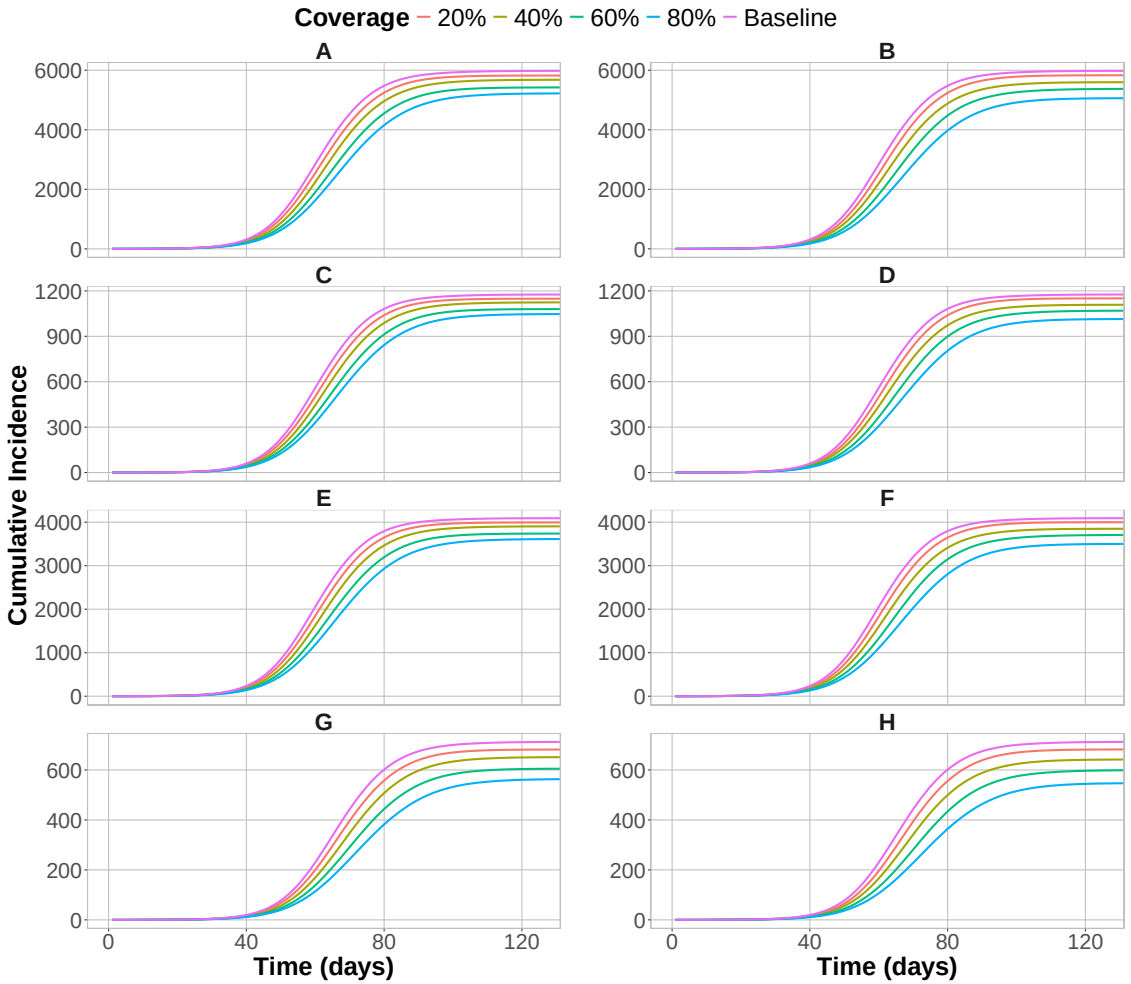

Figure 4.5: Cumulative incidence of infection under varying levels of application coverage, expressed as totals of the corresponding populations, assuming one test per notification. Panels on the left correspond to a 1-day delay between notification and testing, while panels on the right correspond to a 2-day delay. Subplots (A) and (B) represent the total population, (C) and (D) correspond to individuals under 18 years of age, (E) and (F) represent individuals aged 18–65, and (G) and (H) correspond to individuals aged 66 years or older.

In subplot (C), which allows for a second test following an initial negative result, greater overlap between the notches is observed compared to subplot (A), indicating smaller differences between the distributions. In particular, the results at 40% application coverage appear more similar across testing delays than in the single-test scenario. The largest difference is observed at 60% application coverage. At this level, the mean attack rate for a 2-day delay is $\sim$52.5%, compared to $\sim$51.9% for a 1-day delay. The corresponding medians are $\sim$52.2% and $\sim$51.7%, respectively. As in the previous case, the lowest attack rates occur at 80% application coverage. The mean attack rates are $\sim$49.2% for a

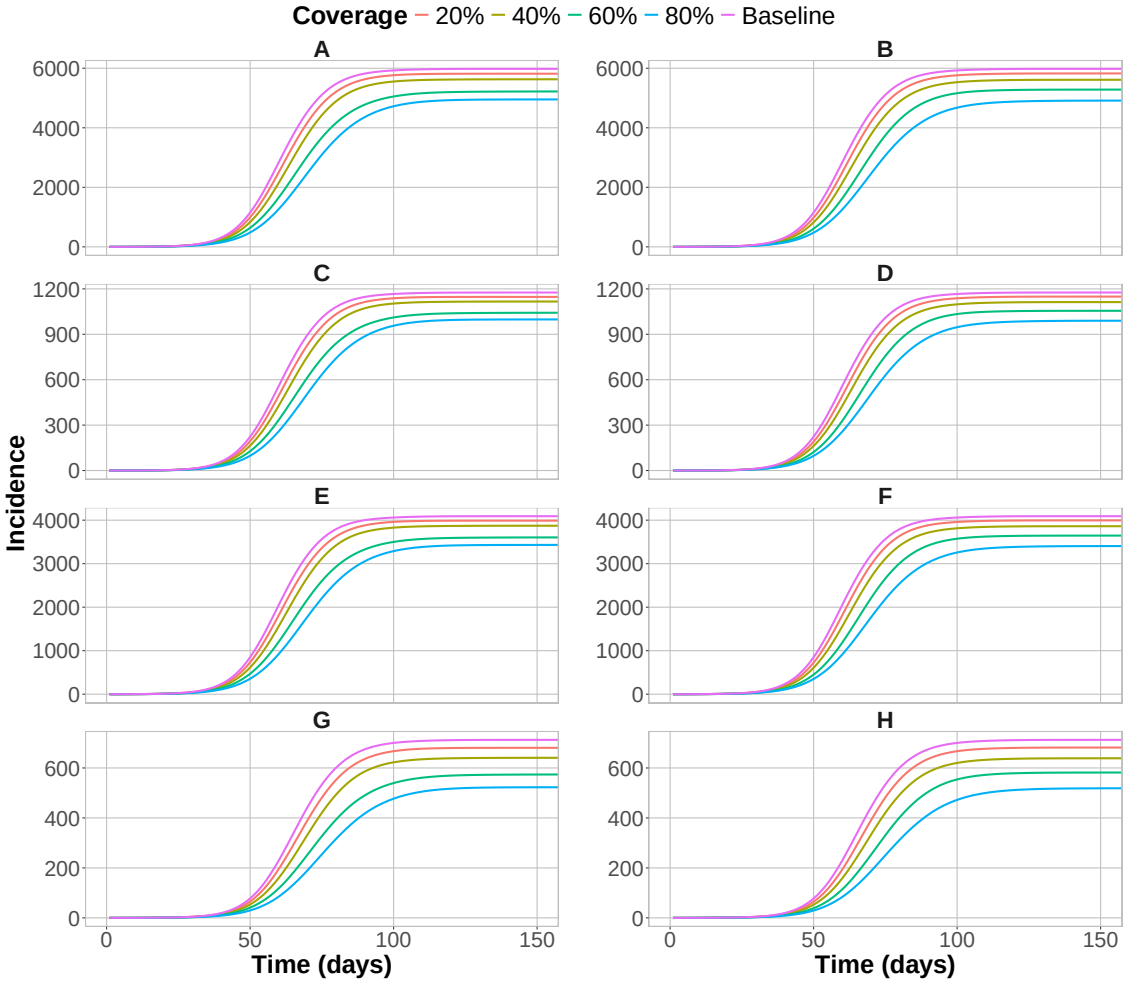

Figure 4.6: Cumulative incidence of infection under varying levels of application coverage, presented as totals of the corresponding populations, assuming up to two tests per notification. Panels on the left correspond to a 1-day delay between notification and testing, while panels on the right correspond to a 2-day delay. Subplots (A) and (B) represent the total population, (C) and (D) correspond to individuals under 18 years of age, (E) and (F) represent individuals aged 18–65, and (G) and (H) correspond to individuals aged 66 years or older.

1-day delay and ∼48.9% for a 2-day delay, with corresponding medians of ∼49.1% and ∼48.8%.

Subplots (B) and (D) compare the distributions corresponding to a maximum of one test (purple) and two tests (pink) per notification, under testing delays of 1 day and 2 days, respectively. In both cases, substantial overlap between the distributions is observed at application coverage levels below 50%, indicating limited differences between the testing strategies.

At higher levels of application coverage, the distributions become more distinct, with

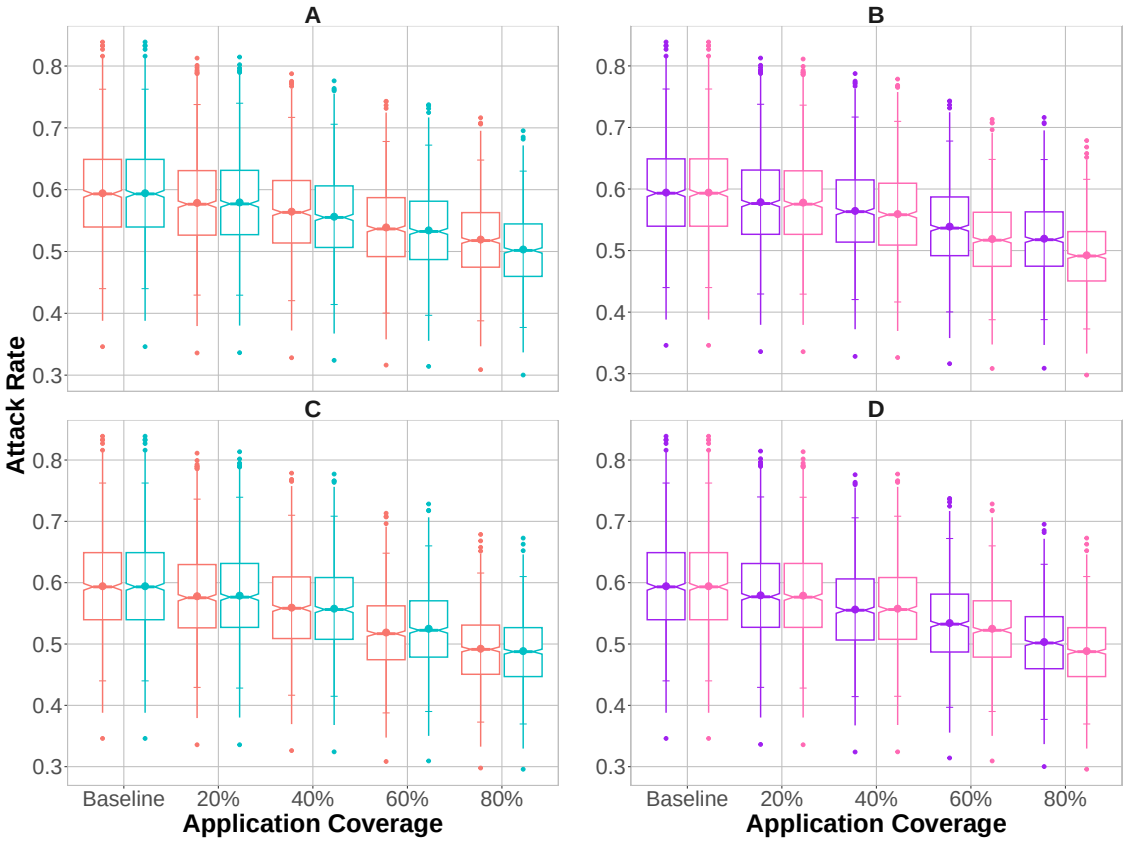

Figure 4.7: Box plots of attack rates under different scenarios at the population level. Subplots (A) and (C) compare the effects of testing delay (1-day vs 2-day) for scenarios with a maximum of one test and up to two tests per notification, respectively. Subplots (B) and (D) compare the effects of the maximum number of tests per notification (one vs two tests) for 1-day and 2-day delays, respectively. In subplots (A) and (C), red boxes represent a 1-day delay and blue boxes represent a 2-day delay. In subplots (B) and (D), purple boxes correspond to one test per notification, while pink boxes correspond to two tests.

reduced overlap between the notches. This suggests that the impact of allowing a second test becomes more pronounced as application adoption increases.

These patterns are also observed in Figures 4.8–4.10, which present results for the three age groups in ascending order. For individuals younger than 18 years, the baseline mean and median attack rates are ∼61.3% and ∼61.2%, respectively. Under the scenario with a maximum of two tests and a 2-day delay, these values decrease to ∼51.6% and ∼51.5% at 80% application coverage. A similar trend is observed for the 18–65 age group, where the mean and median attack rates decrease from ∼63.7% and ∼63.5% to ∼53.0% and ∼52.8%, respectively, under the same scenario. For individuals aged 66 years or older, the mean and median attack rates decrease from ∼41.4% and ∼41.3% to ∼30.2% and

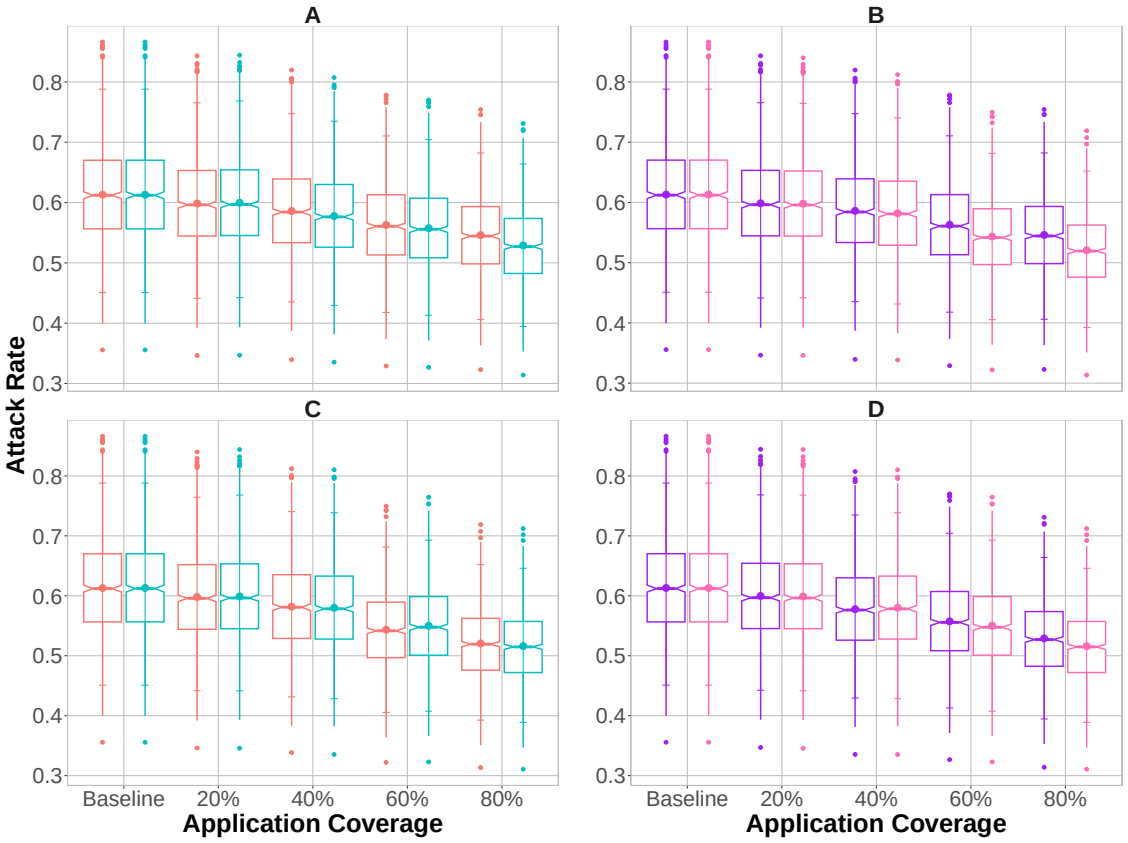

Figure 4.8: Box plots of attack rates under different scenarios for individuals under 18 years of age. Subplots (A) and (C) compare the effects of testing delay (1-day vs 2-day) for scenarios with a maximum of one test and up to two tests per notification, respectively. Subplots (B) and (D) compare the effects of the maximum number of tests per notification (one vs two tests) for 1-day and 2-day delays, respectively. In subplots (A) and (C), red boxes represent a 1-day delay and blue boxes represent a 2-day delay. In subplots (B) and (D), purple boxes correspond to one test per notification, while pink boxes correspond to two tests.

$\sim$30.2%, respectively. Overall, increasing application coverage and the use of additional testing are associated with reductions in attack rates across all age groups.

To further quantify the effects of the application coverage relative to the baseline, we assessed the relative reduction in attack rate presented in Chapter 4.3.3.

4.3.3 Relative Reductions in Attack Rates

Consistent with the previous results, relative reductions in attack rate increase with higher levels of application coverage. Figure 4.11 presents the results for scenarios with a maximum of one test per notification, where red boxes correspond to a 1-day testing delay

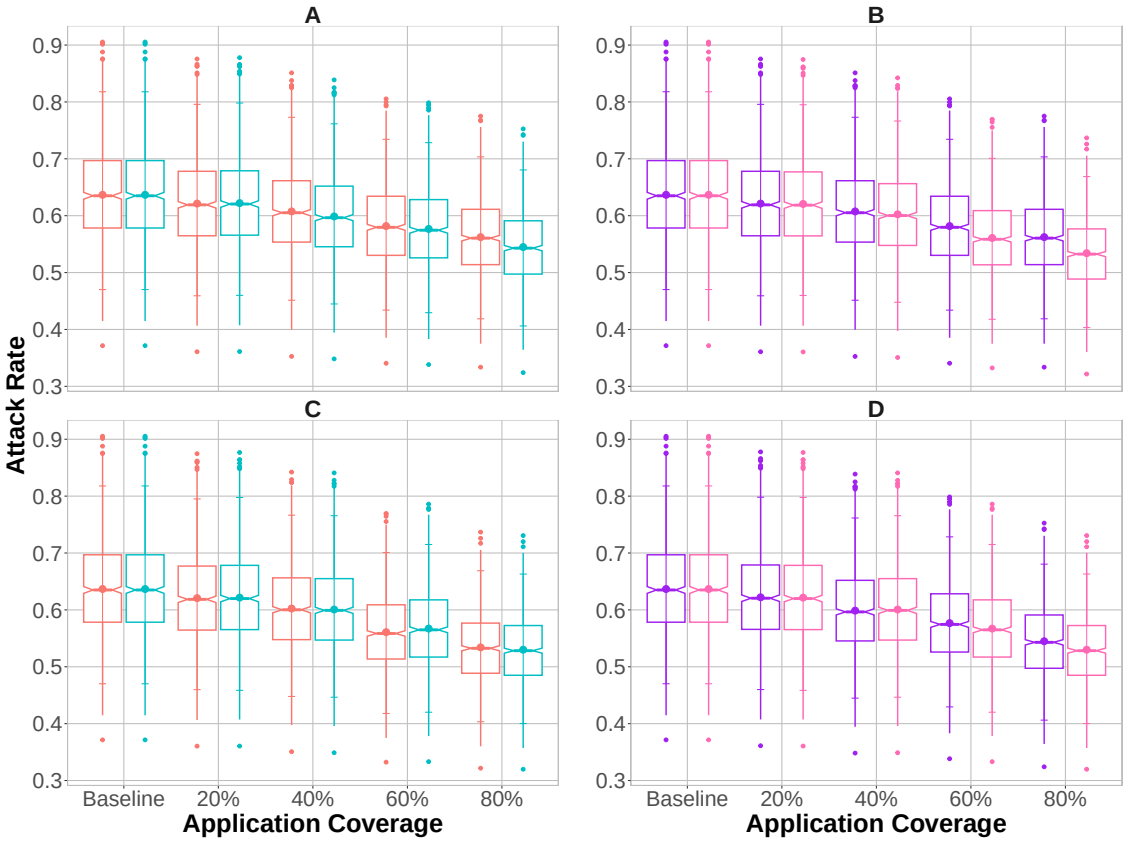

Figure 4.9: Box plots of attack rates under different scenarios for individuals aged 18–65. Subplots (A) and (C) compare the effects of testing delay (1-day vs 2-day) for scenarios with a maximum of one test and up to two tests per notification, respectively. Subplots (B) and (D) compare the effects of the maximum number of tests per notification (one vs two tests) for 1-day and 2-day delays, respectively. In subplots (A) and (C), red boxes represent a 1-day delay and blue boxes represent a 2-day delay. In subplots (B) and (D), purple boxes correspond to one test per notification, while pink boxes correspond to two tests.

and blue boxes correspond to a 2-day delay.

Subplot (A) shows the population-level results. In general, larger reductions are observed when a 2-day delay is applied. At 20% application coverage, the mean and median reductions are similar across delays, with values of $\sim$2.6% and $\sim$2.7% for a 1-day delay, and $\sim$2.5% and $\sim$2.6% for a 2-day delay. At 80% coverage, the reductions increase substantially, reaching $\sim$12.4% and $\sim$12.8% for a 1-day delay, and $\sim$15.1% and $\sim$15.4% for a 2-day delay.

Similar trends are observed across age groups. For individuals younger than 18 years, the mean and median reductions increase from $\sim$2.3% and $\sim$2.4% at 20% coverage to $\sim$10.7% and $\sim$11.1% at 80% coverage for a 1-day delay. When the delay is extended to 2

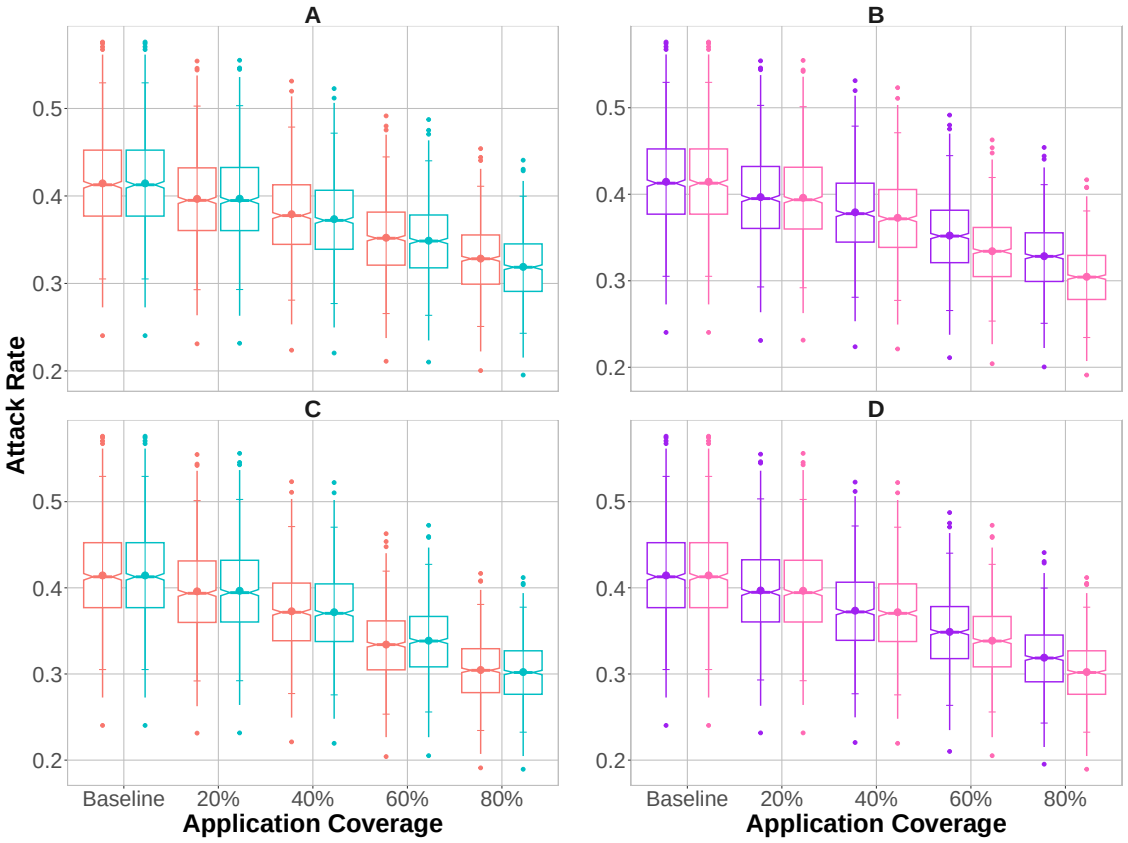

Figure 4.10: Box plots of attack rates under different scenarios for individuals aged 66 years or older. Subplots (A) and (C) compare the effects of testing delay (1-day vs 2-day) for scenarios with a maximum of one test and up to two tests per notification, respectively. Subplots (B) and (D) compare the effects of the maximum number of tests per notification (one vs two tests) for 1-day and 2-day delays, respectively. In subplots (A) and (C), red boxes represent a 1-day delay and blue boxes represent a 2-day delay. In subplots (B) and (D), purple boxes correspond to one test per notification, while pink boxes correspond to two tests.

days, these values increase from ∼2.2% and ∼2.2% to ∼13.5% and ∼13.9%, respectively.

For the 18–65 age group, the mean and median reductions increase from ∼2.4% and ∼2.5% at 20% coverage to ∼11.5% and ∼11.9% at 80% coverage for a 1-day delay, and from ∼2.3% and ∼2.4% to ∼14.2% and ∼14.6% for a 2-day delay.

For individuals aged 66 years or older, reductions are larger in magnitude. At 20% coverage, the mean and median reductions are ∼4.3% and ∼4.3% for a 1-day delay, and ∼4.2% and ∼4.3% for a 2-day delay. At 80% coverage, these values increase to ∼20.5% and ∼20.8% for a 1-day delay, and ∼22.8% and ∼23.1% for a 2-day delay.

When a second test is required following an initial negative result, the difference between scenarios with 1-day and 2-day testing delays becomes less pronounced, consistent

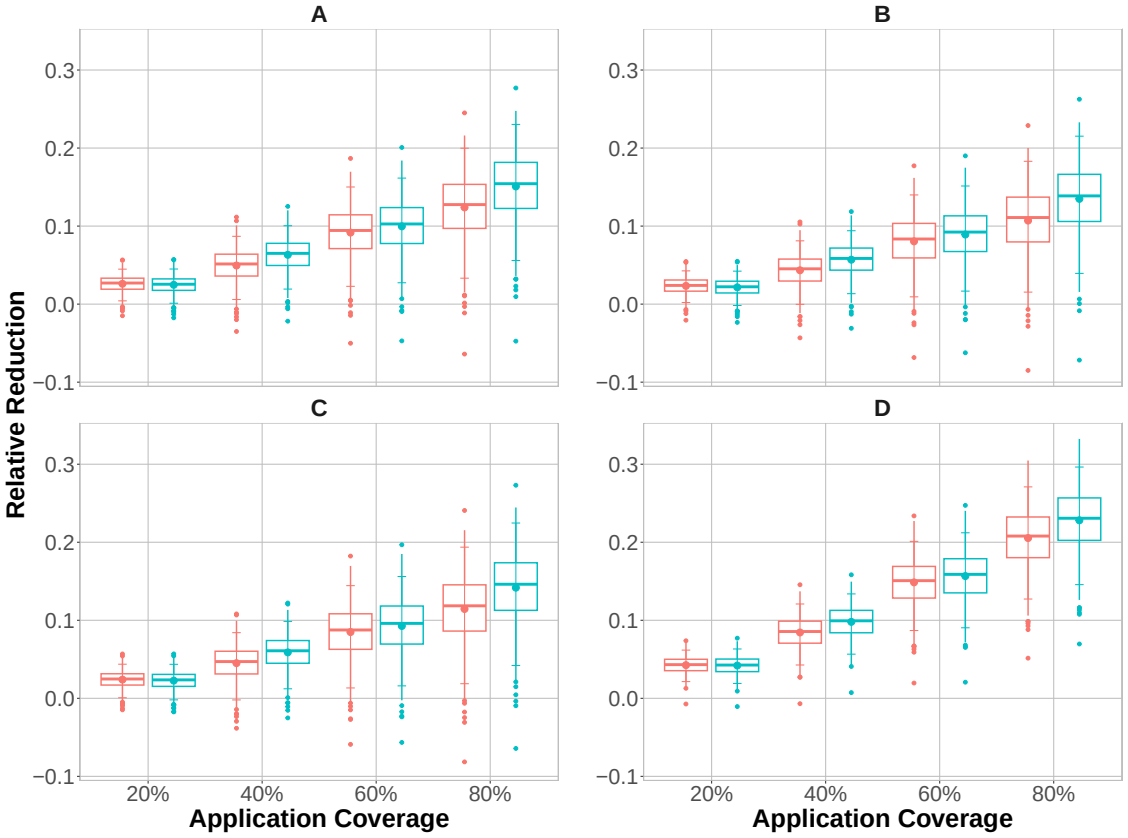

Figure 4.11: Relative reductions in the attack rates with respect to the baseline scenario under different scenarios, assuming one test per notification. Subplot (A) represents the total population, (B) corresponds to individuals under 18 years of age, (C) represents individuals aged 18–65, and (D) corresponds to individuals aged 66 years or older. Red boxes represent a 1-day delay between notification and testing, while blue boxes represent a 2-day delay.

with the patterns observed in the attack rates. However, at 60% application coverage, the 1-day delay scenario yields slightly higher reductions.

At the population level, increasing application coverage leads to substantial improvements in relative reduction. For a 1-day delay, the mean and median reductions increase from ∼2.7% and ∼2.8% at 20% coverage to ∼16.8% and ∼17.2% at 80% coverage. For a 2-day delay, the corresponding values increase from ∼2.6% and ∼2.6% to ∼17.5% and ∼17.9%.

Similar trends are observed across age groups. For individuals younger than 18 years, the mean and median reductions increase from ∼2.4% and ∼2.5% to ∼14.8% and ∼15.2%, respectively, for a 1-day delay. With a 2-day delay, these values increase from ∼2.3% and ∼2.3% to ∼15.5% and ∼15.9%.

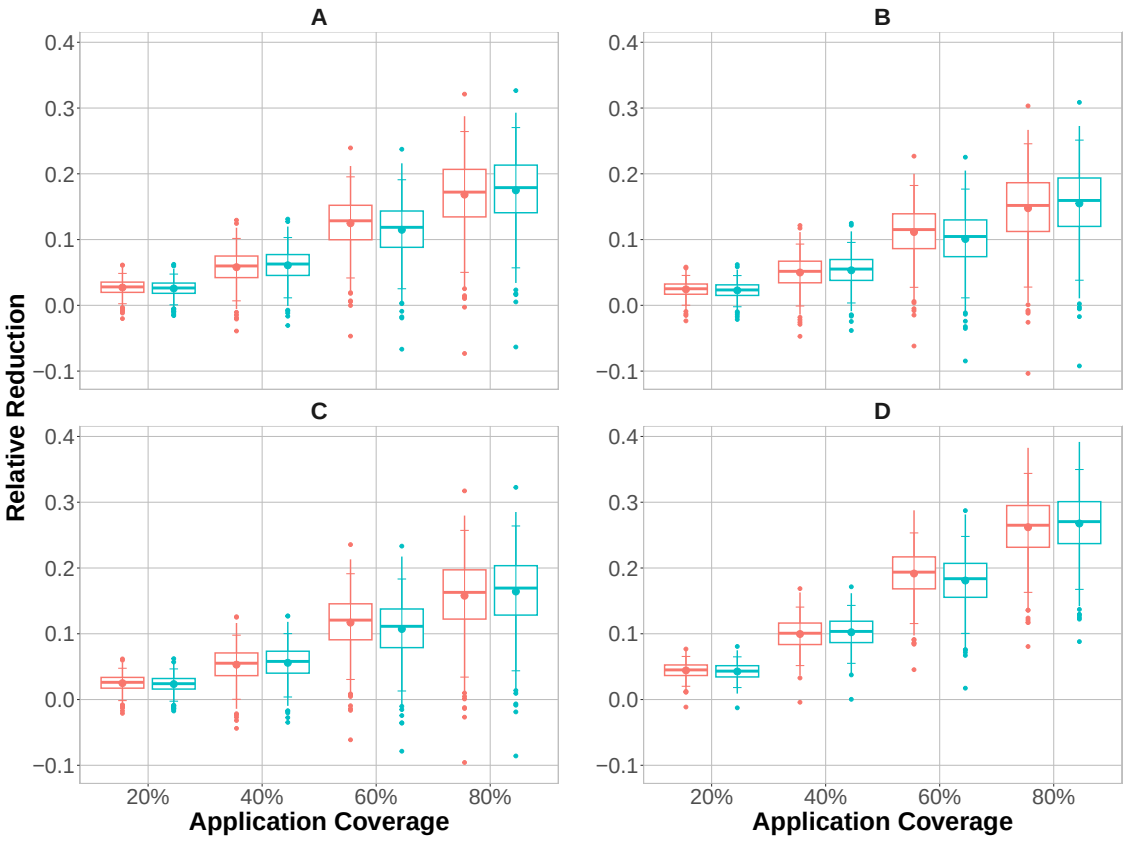

Figure 4.12: Relative reductions in the attack rates with respect to the baseline scenario under different scenarios, assuming up to two tests per notification. Subplot (A) represents the total population, (B) corresponds to individuals under 18 years of age, (C) represents individuals aged 18–65, and (D) corresponds to individuals aged 66 years or older. Red boxes represent a 1-day delay between notification and testing, while blue boxes represent a 2-day delay.

For the 18–65 age group, the mean and median reductions increase from ∼2.5% and ∼2.6% at 20% coverage to ∼15.8% and ∼16.3% at 80% coverage for a 1-day delay. For a 2-day delay, the corresponding values increase from ∼2.4% and ∼2.4% to ∼16.4% and ∼17.0%.

For individuals aged 66 years or older, larger reductions are observed. With a 1-day delay, the mean and median reductions increase from ∼4.4% and ∼4.5% to ∼26.2% and ∼26.5%. With a 2-day delay, these values increase from ∼4.3% and ∼4.3% to ∼26.8% and ∼27.1%.

Overall, scenarios allowing up to two tests per notification tend to produce larger relative reductions in attack rate than the corresponding single-test scenarios at higher levels of application coverage (e.g., 60% and 80%). In addition, the 66+ age group

consistently exhibits the largest reductions, while the younger age groups display more similar outcomes across scenarios.

4.4 Statistical Analysis

To further characterize the simulation outputs, particularly the distributions of attack rates, statistical analyses were performed. These analyses aim to assess the distributional properties of the data and to evaluate differences between scenarios.

4.4.1 Shapiro-Wilk Test

The Shapiro–Wilk test was used to assess whether the data follow a normal distribution. The null hypothesis of the test is that the data are normally distributed. At a significance level of $\alpha = 0.05$, a p-value less than 0.05 leads to rejection of the null hypothesis, indicating that the data deviate from normality. Otherwise, there is insufficient evidence to reject the assumption of normality [90].

The results of the Shapiro–Wilk tests are presented in Tables 4.1–4.4 and are used to determine whether parametric or non-parametric statistical methods are appropriate for subsequent analysis.

Table 4.1: P-values for the Shapiro-Wilk test (all age groups).

	No Coverage	20% Coverage	40% Coverage	60% Coverage	80% Coverage
1 test, 1 day delay	0.3256	0.3358	0.351	0.3577	0.3894
1 test, 2 days delay	0.3256	0.3201	0.3476	0.3404	0.3898
2 tests, 1 day delay	0.3256	0.332	0.322	0.3764	0.4164
2 tests, 2 days delay	0.3256	0.3051	0.3153	0.3114	0.4152

Table 4.2: P-values for the Shapiro-Wilk test (individuals under 18 years of age).

	No Coverage	20% Coverage	40% Coverage	60% Coverage	80% Coverage
1 test, 1 day delay	0.3102	0.3174	0.3072	0.3358	0.375
1 test, 2 days delay	0.3102	0.2912	0.329	0.3602	0.3597
2 tests, 1 day delay	0.3102	0.3085	0.3122	0.3667	0.3753
2 tests, 2 days delay	0.3102	0.2836	0.29	0.3036	0.3909

Table 4.3: P-values for the Shapiro-Wilk test (individuals 18–65 years of age).

	No Coverage	20% Coverage	40% Coverage	60% Coverage	80% Coverage
1 test, 1 day delay	0.386	0.32	0.3453	0.3464	0.3976
1 test, 2 days delay	0.386	0.3059	0.332	0.351	0.3932
2 tests, 1 day delay	0.386	0.3604	0.3265	0.3838	0.412
2 tests, 2 days delay	0.386	0.2998	0.326	0.3179	0.4037

Table 4.4: P-values for the Shapiro-Wilk test (individuals aged 66 years or older).

	No Coverage	20% Coverage	40% Coverage	60% Coverage	80% Coverage
1 test, 1 day delay	0.1936	0.2379	0.2481	0.239	0.2506
1 test, 2 days delay	0.1936	0.239	0.2448	0.2136	0.2249
2 tests, 1 day delay	0.1936	0.2392	0.2459	0.2544	0.2746
2 tests, 2 days delay	0.1936	0.2291	0.2294	0.1858	0.2619

Based on the p-values recorded in Tables 4.1–4.4, which range from 0.1858 to 0.4164, we fail to reject the null hypothesis that the data are normally distributed across scenarios. Before selecting an appropriate statistical test for comparing scenarios, we assessed the homogeneity of variances across groups defined according to the testing delay (1 or 2 days) and the maximum number of tests permitted per notification.

4.4.2 Fligner-Killeen Test

The Fligner-Killeen test is used to assess the equality of variances across multiple groups. It is a non-parametric method and is robust to deviations from normality [91].

The resulting p-values are presented in Table 4.5. At a significance level of $\alpha = 0.05$, a p-value less than 0.05 leads to rejection of the null hypothesis of equal variances. Otherwise, there is insufficient evidence to conclude that the variances differ across groups.

Table 4.5: P-values for the Fligner-Killeen test.

	All Ages	Under 18	Ages $18-65$	Ages 66+
1 test, 1 day delay	1.131×10^{-9}	6.566×10^{-8}	6.148×10^{-9}	$< 2.2 \times 10^{-16}$
1 test, 2 days delay	9.35×10^{-13}	8.949×10^{-11}	7.188×10^{-12}	$< 2.2 \times 10^{-16}$
2 tests, 1 day delay	$< 2.2 \times 10^{-16}$	3.215×10^{-16}	$< 2.2 \times 10^{-16}$	$< 2.2 \times 10^{-16}$
2 tests, 2 days delay	$< 2.2 \times 10^{-16}$	2.603×10^{-15}	$< 2.2 \times 10^{-16}$	$< 2.2 \times 10^{-16}$

Given that the p-values across all groups range from less than 2.2×10^{-16} to 6.566×10^{-8}, we reject the null hypothesis of equal variances in all cases. This indicates that at least one group has a variance that differs from the others. Combined with the earlier assessment of approximate normality and the independence of observations, we therefore employed Welch's t-test, which does not assume equal variances [92].

4.4.3 Welch's t-test

Welch's t-test is used to compare the means of two independent groups under the assumption of approximate normality, without requiring equal variances. The null hypothesis is that the group means are equal [93].

We applied this test to compare attack rates across different levels of application coverage within each scenario. The results show that, within each scenario, all pairwise comparisons across coverage levels yield p-values below the significance threshold. This indicates that different levels of application coverage are associated with statistically significant differences in attack rates.

We then compared scenarios with the same application coverage and number of tests per notification, but different delays between exposure notification and testing.

According to Figure 4.13, when individuals are required to perform only 1 test per notification, there is no statistically significant difference between a 1-day and 2-day testing delay at 20% and 60% application coverage, as the corresponding p-values exceed the significance level of 0.05. At 40% and 80% coverage, the differences between the two delays are more apparent in the attack rates, as the p-values reside below the significance threshold, indicating that these differences are statistically significant.

Figure 4.14 presents a slightly different pattern. When individuals are allowed to take up to two tests per notification, there is no statistically significant difference between 1-day and 2-day delays at 20%, 40%, and 80% application coverage, as the corresponding p-values exceed the significance level. This pattern is consistent across age groups, with the exception of the 18–65 group, where the comparison at 60% coverage is also not

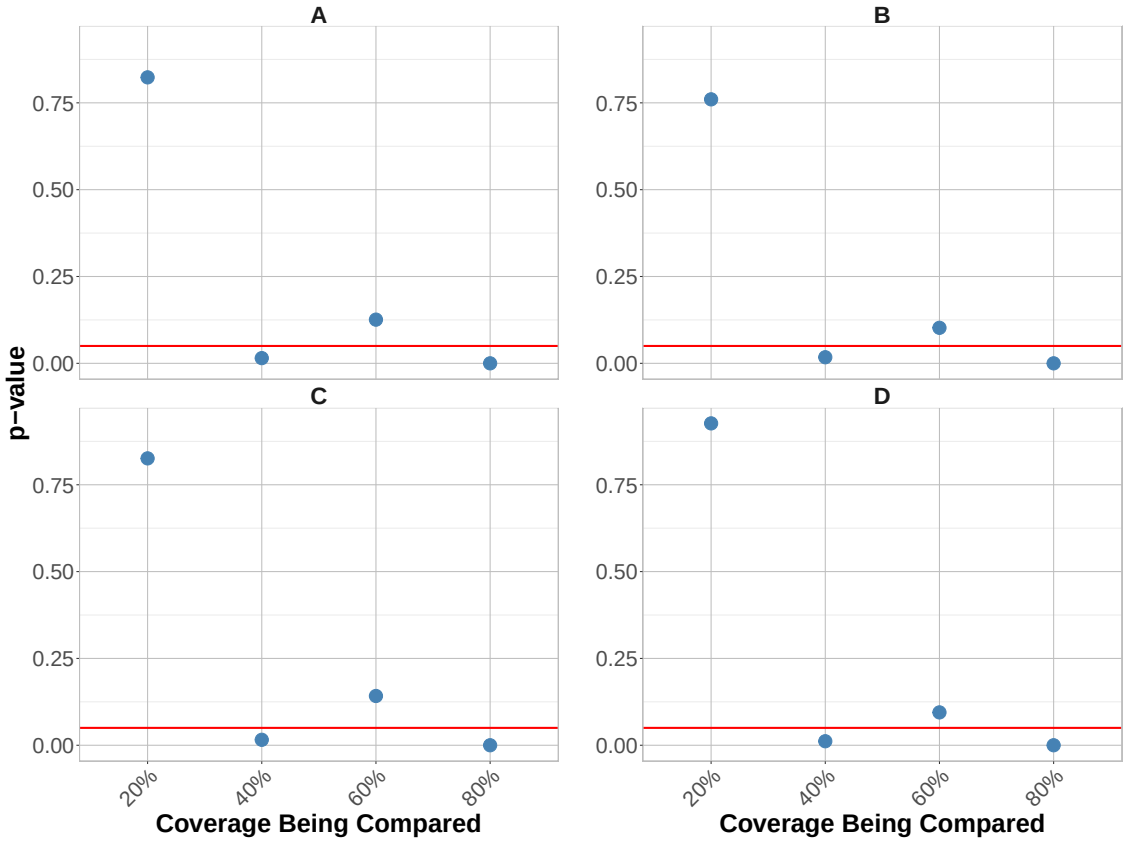

Figure 4.13: P-values obtained from Welch's t-test comparing 1-day and 2-day delays between notification and testing for scenarios with a maximum of one test per notification across different levels of application coverage. Subplot (A) represents the total population, (B) corresponds to individuals under 18 years of age, (C) represents individuals aged 18–65, and (D) corresponds to individuals aged 66 years or older.

statistically significant, with the p-value slightly above the threshold of 0.05. These findings are consistent with the patterns observed in Chapter 4.3.2.

Overall, 5 out of 8 comparisons between testing delays do not show statistically significant differences. This suggests that the timing of testing (1 versus 2 days after notification) may have a limited effect on outbreak dynamics under the conditions considered.

We next assessed differences between scenarios allowing a maximum of one versus two tests per notification using the same statistical approach.

With the exception of the comparison for 40% coverage for the 66+ age group under a 1-day delay, a consistent pattern is observed across Figures 4.15 and 4.16. Specifically, no statistically significant differences are detected between scenarios at coverage levels below 50%, whereas for 60% and 80% coverage, the corresponding p-values fall below

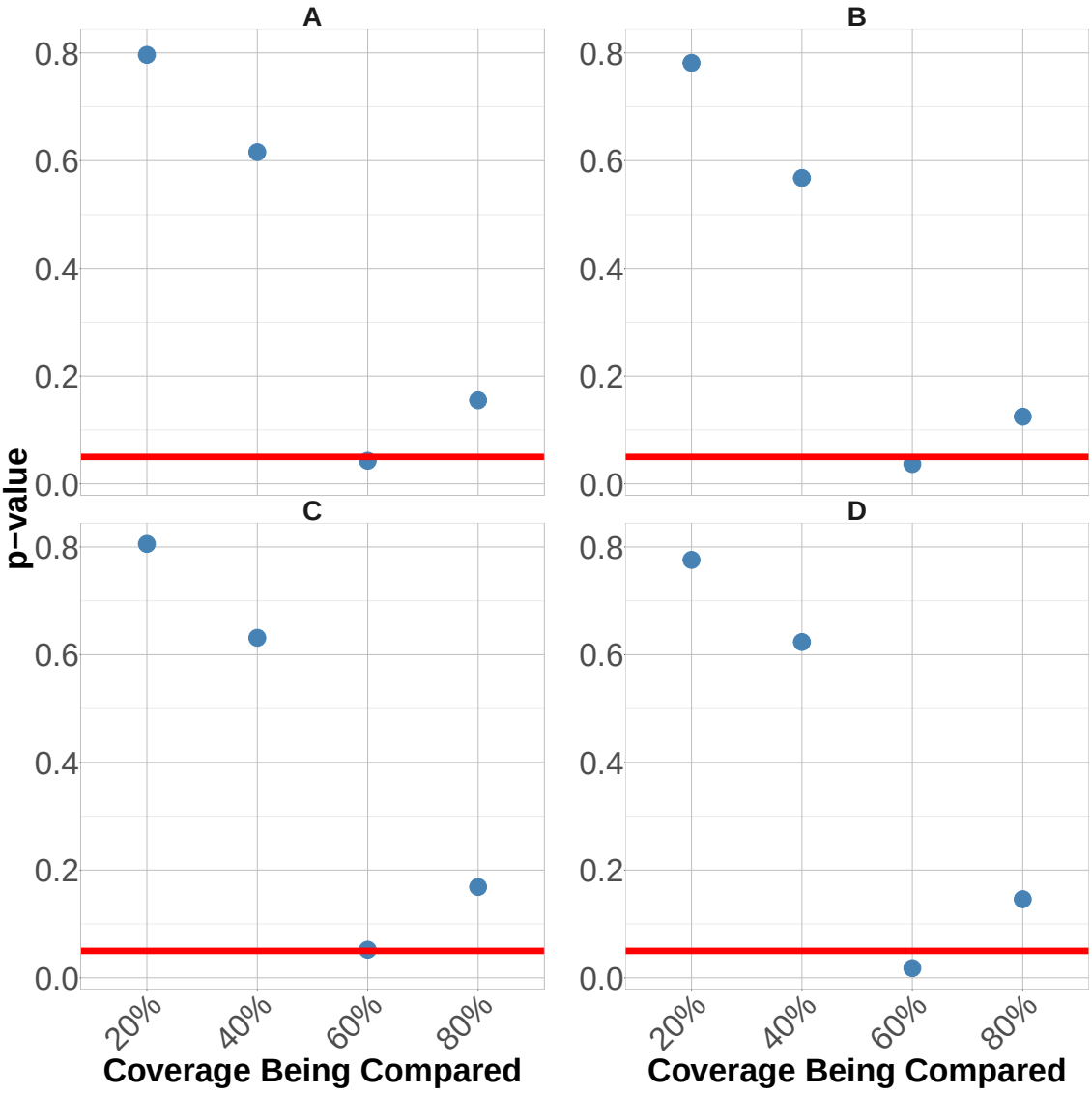

Figure 4.14: P-values obtained from Welch's t-test comparing 1-day and 2-day delays between notification and the first test for scenarios allowing up to two tests per notification across different levels of application coverage. Subplot (A) represents the total population, (B) corresponds to individuals under 18 years of age, (C) represents individuals aged 18–65, and (D) corresponds to individuals aged 66 years or older.

the significance threshold of 0.05.

These results suggest that allowing a second test may provide additional benefit at higher levels of application coverage, while its impact is less pronounced at lower levels of adoption.

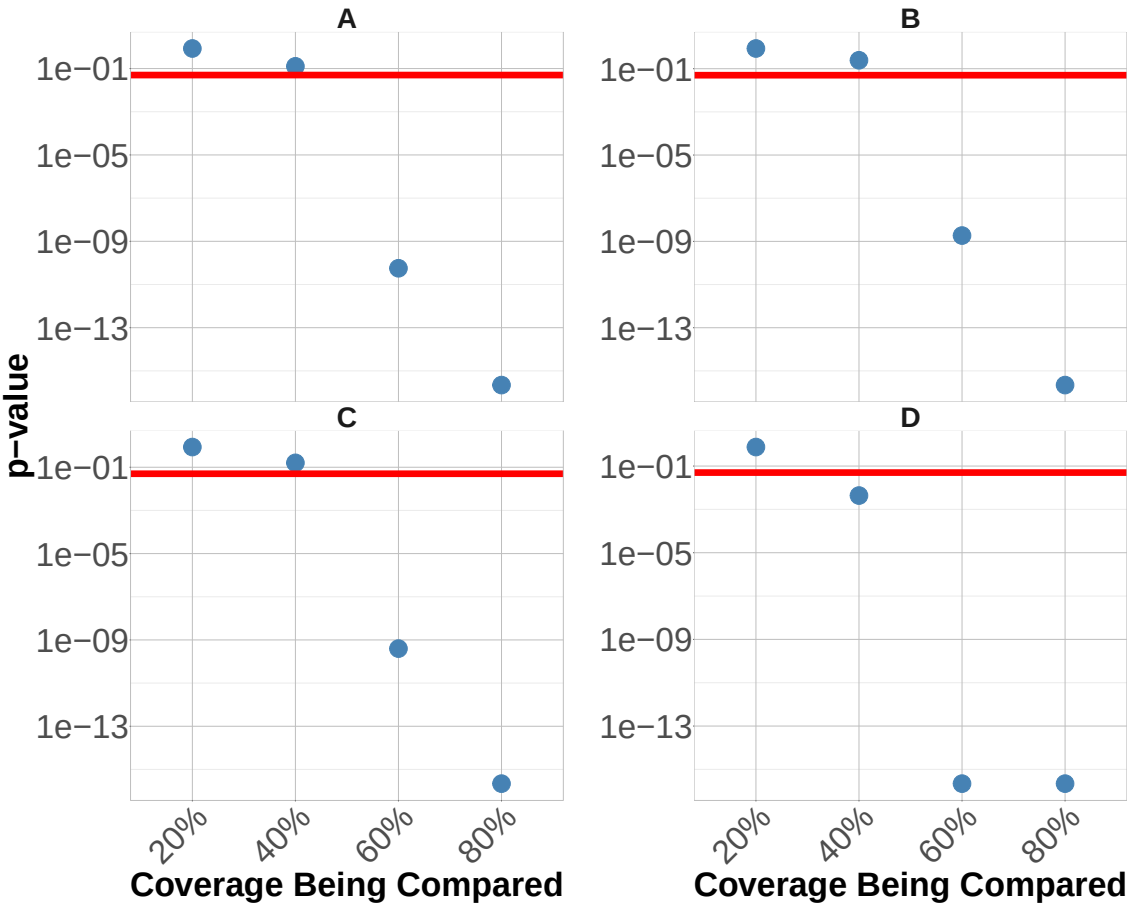

Figure 4.15: P-values obtained from Welch's t-test comparing scenarios with a maximum of one test versus up to two tests per notification under a 1-day delay across different levels of application coverage. Subplot (A) represents the total population, (B) corresponds to individuals under 18 years of age, (C) represents individuals aged 18–65, and (D) corresponds to individuals aged 66 years or older.

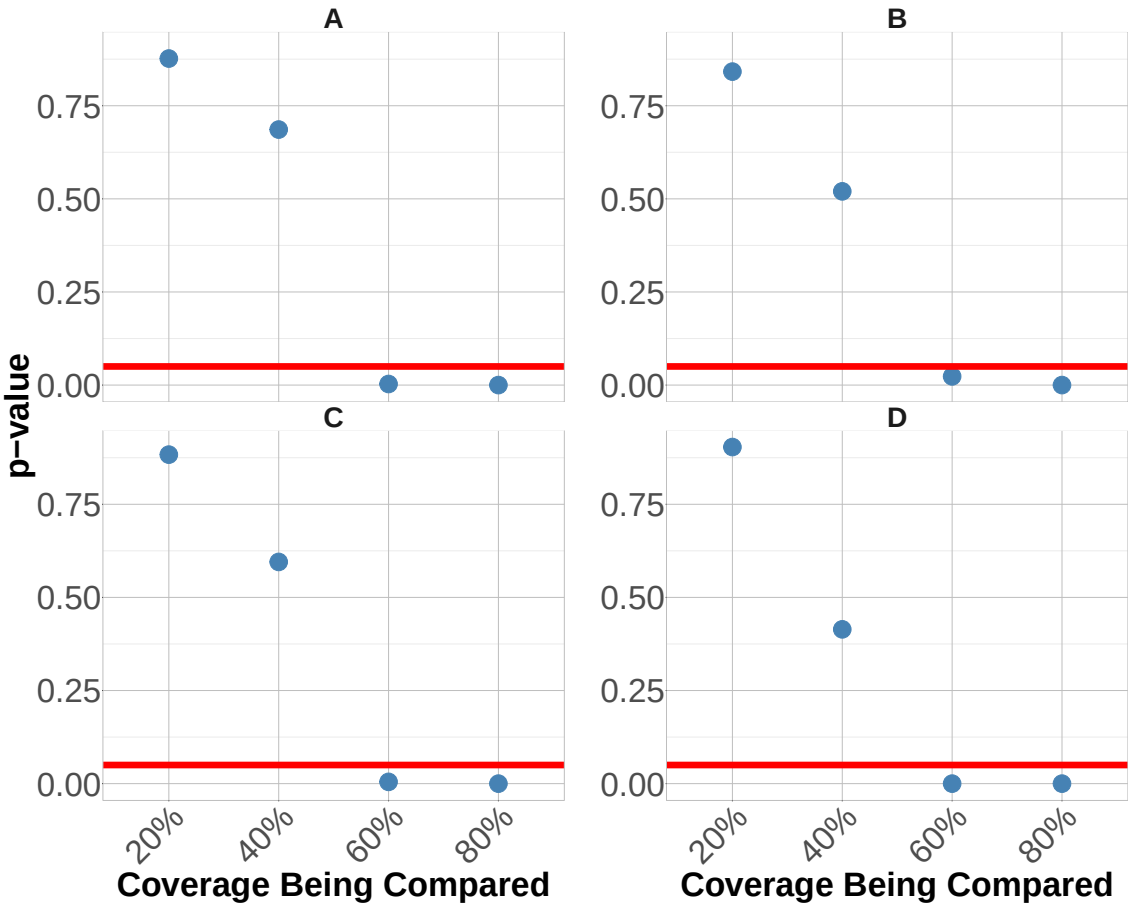

Figure 4.16: P-values obtained from Welch's t-test comparing scenarios with a maximum of one test versus up to two tests per notification under a 2-day delay across different levels of application coverage. Subplot (A) represents the total population, (B) corresponds to individuals under 18 years of age, (C) represents individuals aged 18–65, and (D) corresponds to individuals aged 66 years or older.

Chapter 5

Digital Contact Tracing with Self-Testing and Symptom-Based Isolation

In this chapter, we analyze the outcomes of the second intervention strategy. In this setting, symptomatic individuals initiate a 5-day isolation period upon the onset of symptoms, while asymptomatic individuals who receive a positive test result isolate for 7 days. If symptoms develop during an ongoing isolation period, the individual remains in isolation for 5 days from symptom onset. Similarly, individuals who develop symptoms after completing isolation immediately re-enter isolation for the same duration.

Epidemic dynamics are first examined using time series plots of daily incidence. Following bootstrap resampling, attack rates and corresponding relative reductions are compared across scenarios using box plots. Finally, statistical tests are performed to identify significant differences between policy outcomes.

5.1 Baseline Scenario

The baseline scenario excludes the use of the application and considers only symptom-based isolation. Under these conditions, an effective reproduction number of $R_E = 1.51$ is obtained. Parameter values are taken from Tables 3.2–3.5 and are used to generate the epidemic trajectories analyzed in this chapter.

At the population level, the peak incidence is approximately 72 infections, occurring around day 85 of the simulation. This corresponds to a total of approximately 3,584 infections over the course of the outbreak. Compared to the baseline scenario without interventions presented in Chapter 4.2, this represents a relative reduction of $\sim$39.2% in the attack rate.

Age-stratified results show consistent patterns. The 18–65 age group exhibits the highest cumulative incidence ($\sim$39.8%), while individuals aged 66 years or older experience the lowest cumulative incidence ($\sim$19.3%) and a delayed peak in incidence. The under-18 age group has a cumulative incidence of $\sim$37.3%, which is closer to that of the 18–65 group than to the oldest age group.

5.2 Assessment of Scenarios

We examine the scenarios across the four populations, varying both the delay between notification and testing (1 or 2 days) and the maximum number of tests permitted per notification. Epidemic dynamics are analyzed using time series plots of incidence and cumulative incidence, while attack rates and corresponding relative reductions are summarized using box plots based on 1,000 bootstrap samples.

5.2.1 Time Series

Figures 5.3–5.6 illustrate the temporal evolution of incidence and cumulative incidence under the considered scenarios. Compared to the results presented in Chapter 4.3.1, a

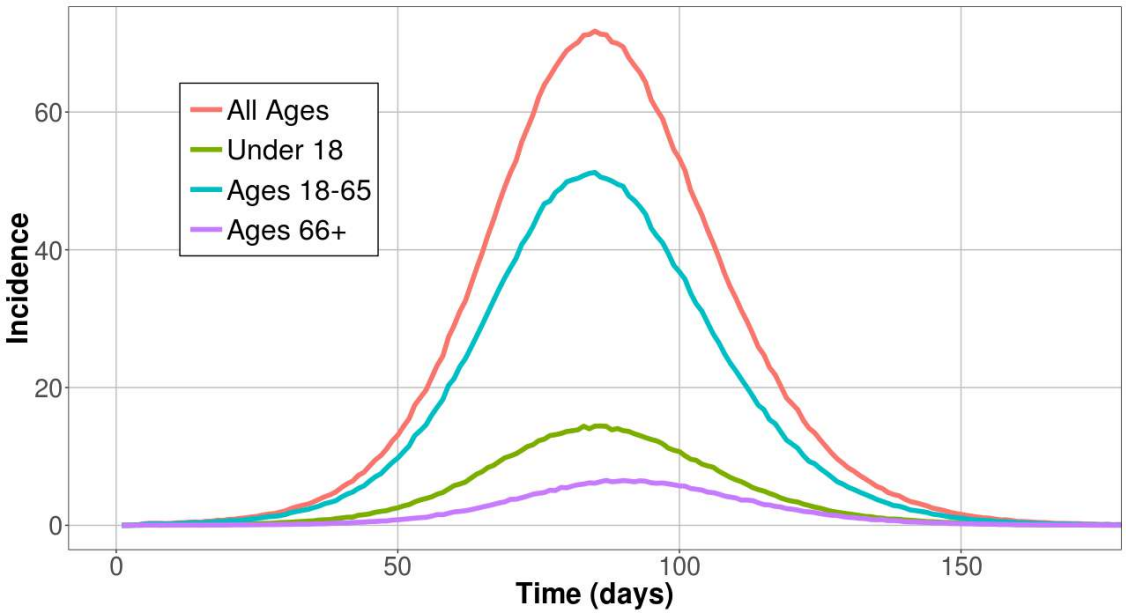

Figure 5.1: Temporal incidence of infection for the baseline scenario. The red curve represents the total population, while age-specific subpopulations are shown as follows: green for individuals under 18 years of age, blue for individuals aged 18–65, and purple for individuals aged 66 years or older.

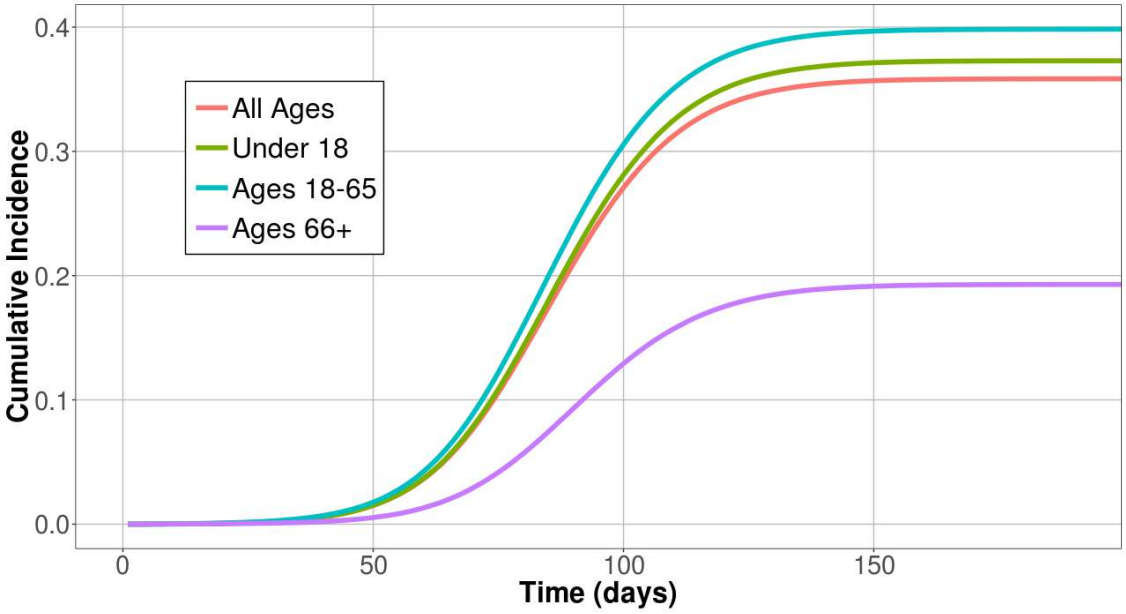

Figure 5.2: Temporal cumulative incidence for the baseline scenario, expressed as proportions of the corresponding populations. The red curve represents the total population, while age-specific subpopulations are shown as follows: green for individuals under 18 years of age, blue for individuals aged 18–65, and purple for individuals aged 66 years or older.

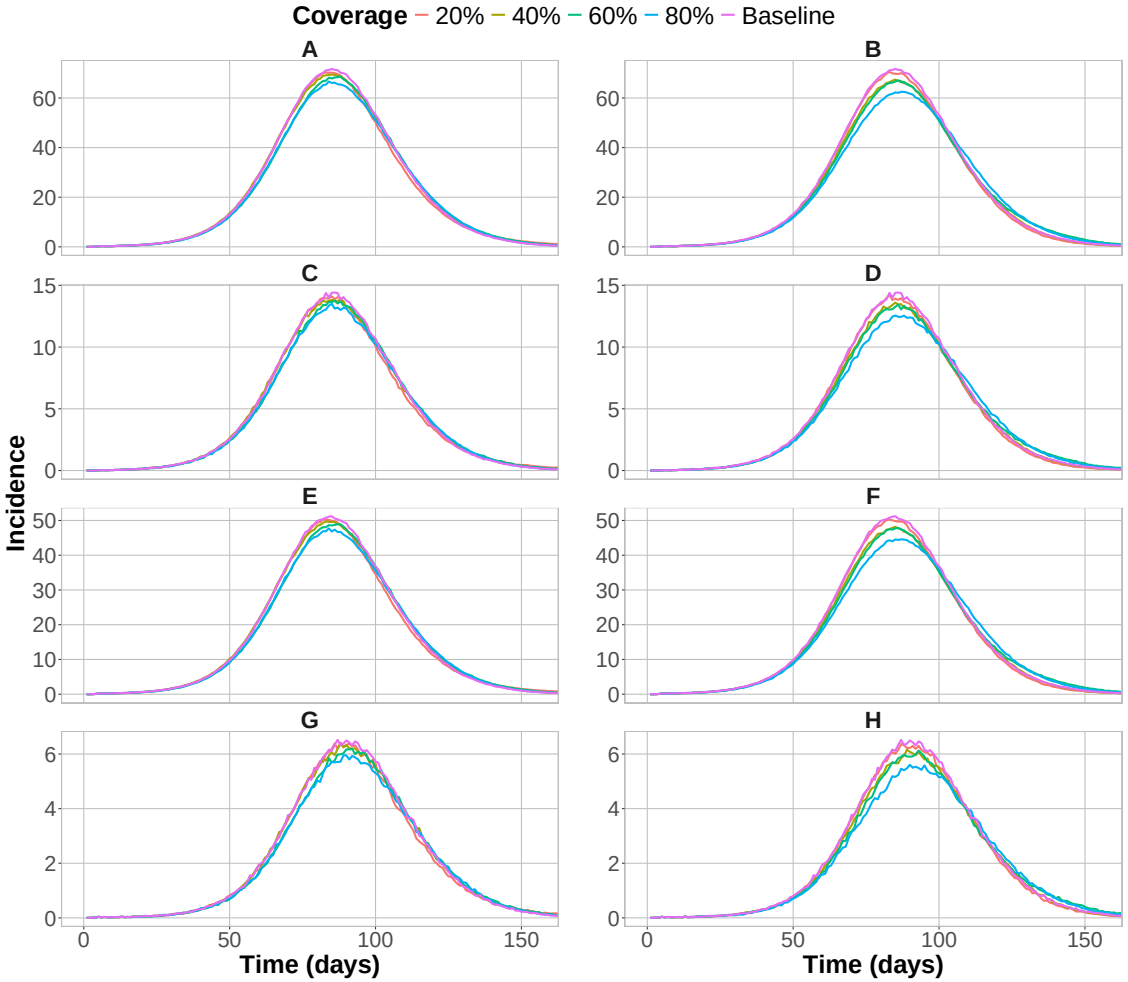

Figure 5.3: Incidence of infection under varying levels of application coverage, assuming one test per notification. Panels on the left correspond to a 1-day delay between notification and testing, while panels on the right correspond to a 2-day delay. Subplots (A) and (B) represent the total population, (C) and (D) correspond to individuals under 18 years of age, (E) and (F) represent individuals aged 18–65, and (G) and (H) correspond to individuals aged 66 years or older.

greater degree of overlap is observed between the incidence curves across different levels of application coverage.

Although higher levels of application coverage are generally associated with lower incidence, this relationship is less pronounced than in the previous chapter. In particular, the rightward shift in peak incidence observed with increasing coverage is less distinct. In contrast, the effect of symptom-based isolation is evident, as reflected by the reduced incidence levels relative to the baseline. The combined impact of symptom-based isolation and digital contact tracing is further examined in the subsequent sections of this chapter.

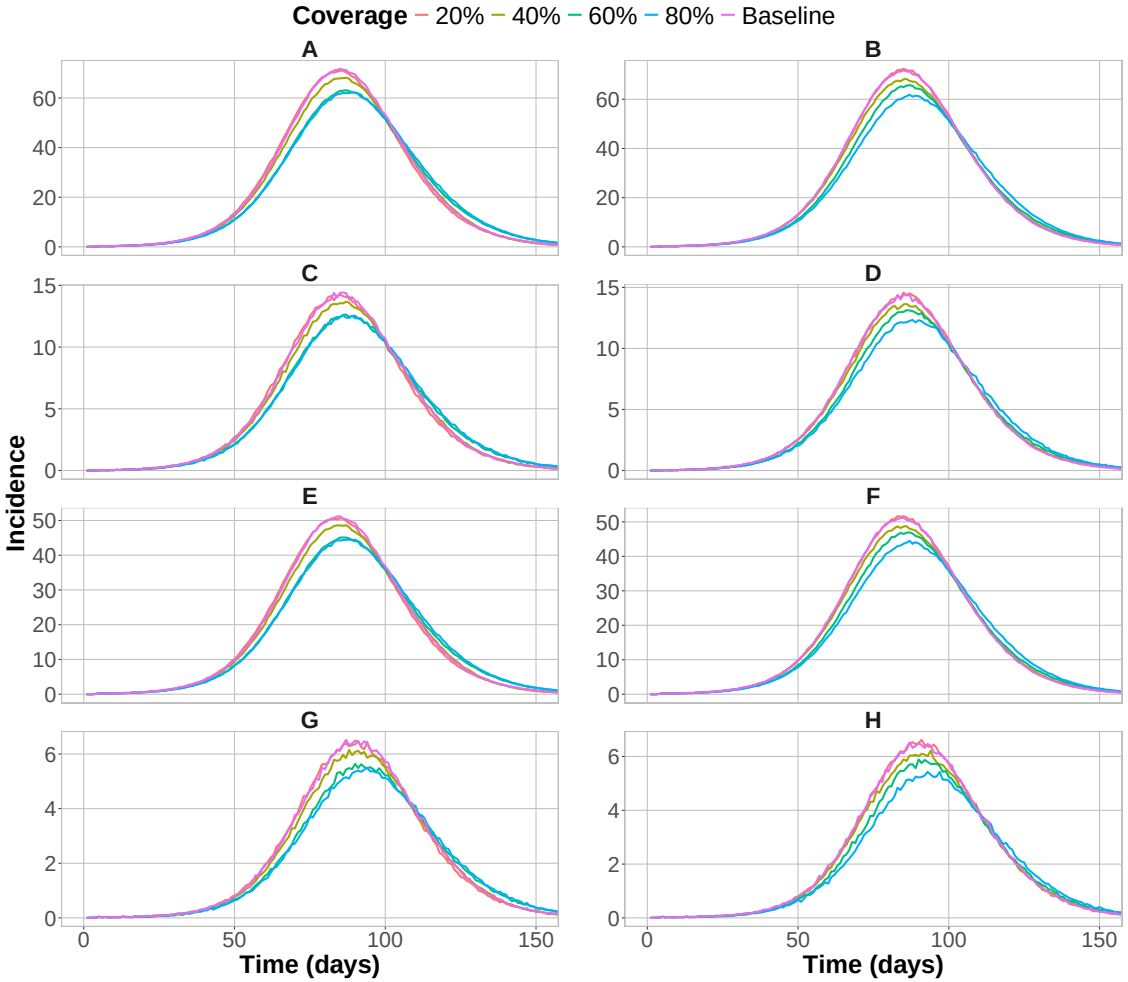

Figure 5.4: Incidence of infection under varying levels of application coverage, assuming up to two tests per notification. Panels on the left correspond to a 1-day delay between notification and testing, while panels on the right correspond to a 2-day delay. Subplots (A) and (B) represent the total population, (C) and (D) correspond to individuals under 18 years of age, (E) and (F) represent individuals aged 18–65, and (G) and (H) correspond to individuals aged 66 years or older.

5.2.2 Attack Rates

Figure 5.7 summarizes the attack rates across the different intervention scenarios at the population level. In contrast to the patterns observed in Chapter 4.3.2, the relationship between attack rate and application coverage is less consistent under this strategy.

In subplot (A), for scenarios with a maximum of one test per notification, non-monotonic patterns are observed. For example, at a 1-day delay, 40% coverage results in higher mean attack rates than 20% coverage, and at a 2-day delay, 60% coverage exceeds 40%. A similar pattern is observed in subplot (C), where two tests per notification are allowed. In

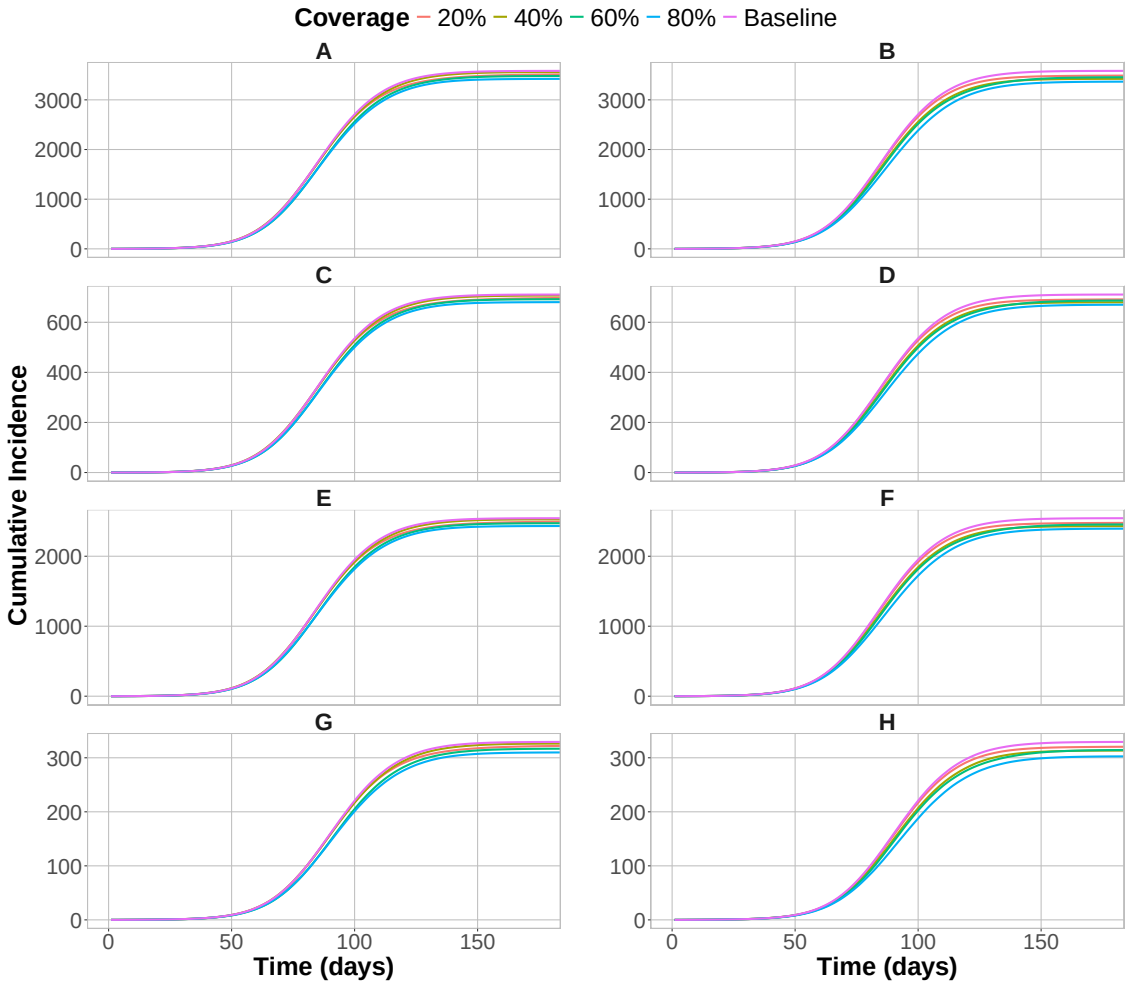

Figure 5.5: Cumulative incidence under varying levels of application coverage, expressed as totals for the corresponding populations, assuming one test per notification. Panels on the left correspond to a 1-day delay between notification and testing, while panels on the right correspond to a 2-day delay. Subplots (A) and (B) represent the total population, (C) and (D) correspond to individuals under 18 years of age, (E) and (F) represent individuals aged 18–65, and (G) and (H) correspond to individuals aged 66 years or older.

this case, the mean and median attack rates at 80% coverage for a 1-day delay exceed those at 60% coverage. For a 2-day delay, attack rates at 20% coverage are also higher than those of the baseline in some instances. These results indicate that increasing application coverage does not consistently lead to reductions in attack rate under this intervention strategy.

Consistent with the time series analysis, overall attack rates are substantially lower than in the previous chapter. The baseline scenario yields a mean attack rate of ∼35.7% and a median of ∼35.6%. Furthermore, the range of variation across scenarios is reduced.

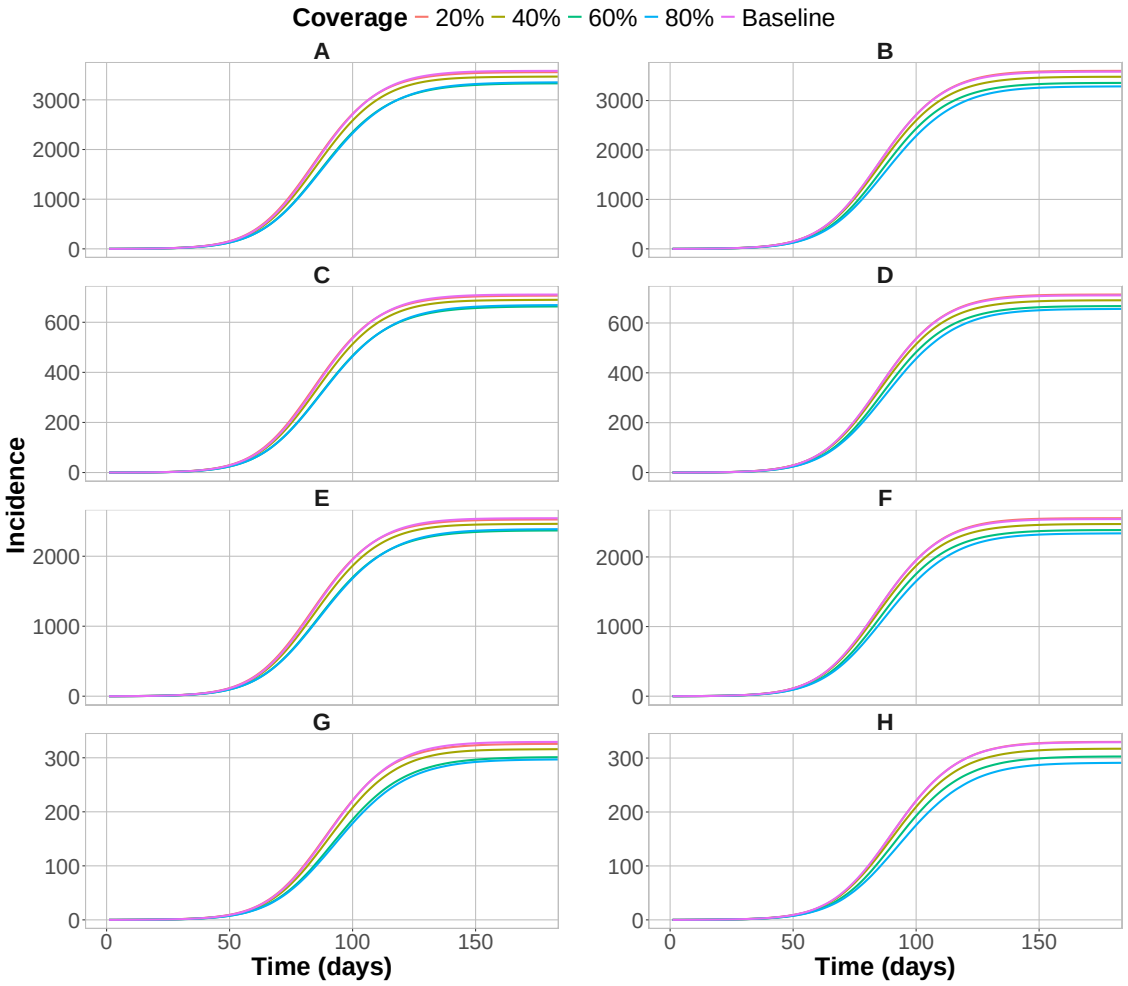

Figure 5.6: Cumulative incidence under varying levels of application coverage, expressed as totals for the corresponding populations, assuming up to two tests per notification. Panels on the left correspond to a 1-day delay between notification and testing, while panels on the right correspond to a 2-day delay. Subplots (A) and (B) represent the total population, (C) and (D) correspond to individuals under 18 years of age, (E) and (F) represent individuals aged 18–65, and (G) and (H) correspond to individuals aged 66 years or older.

For example, at 80% coverage with a 1-day delay and a single test, the mean and median attack rates are ∼34.1% and ∼34.0%, respectively, compared to ∼33.6% and ∼33.4% for a 2-day delay.

When two tests are considered, the lowest attack rates are observed at 60% coverage for a 1-day delay (mean ∼33.2%, median ∼33.1%), and at 80% coverage for a 2-day delay (mean ∼32.8%, median ∼32.7%). The highest values corresponding to a 2-day delay are ∼35.9% and ∼35.8%, observed for 20% coverage.

Comparing testing delays in scenarios with a single test per notification, a 2-day delay

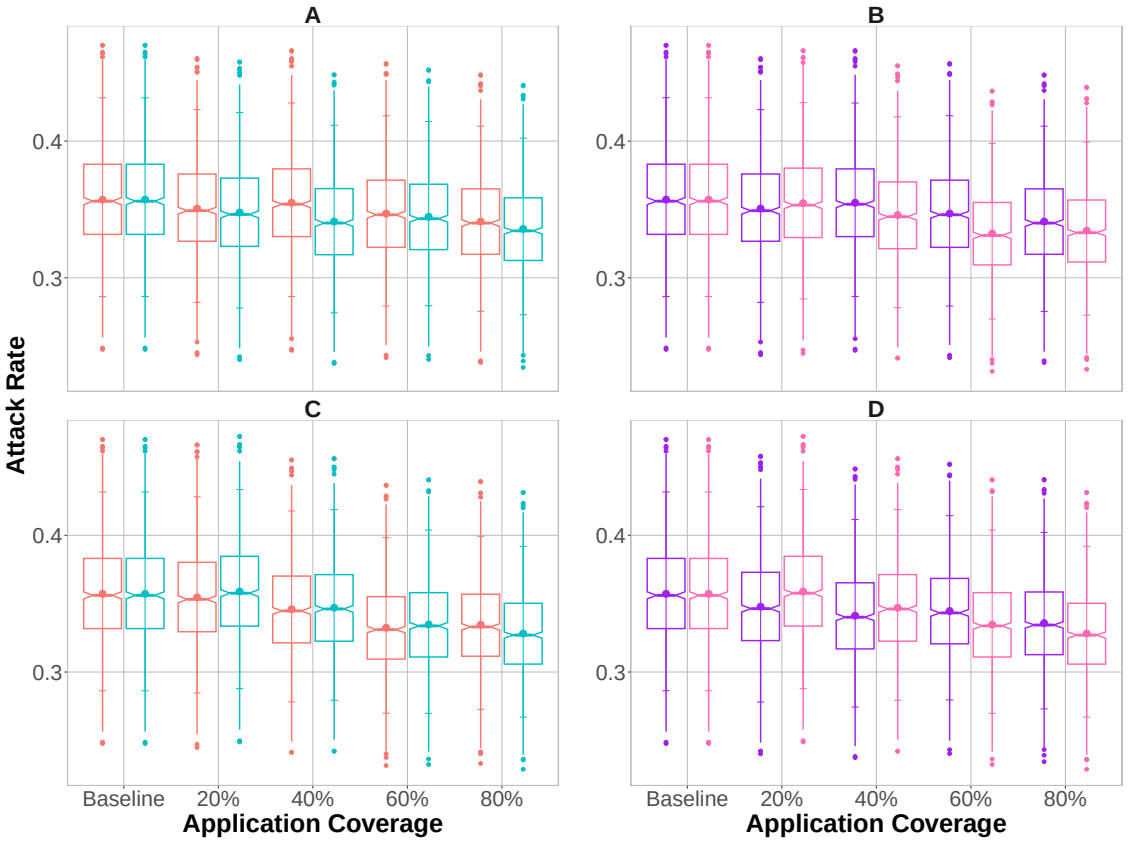

Figure 5.7: Box plots of attack rates under different scenarios at the population level. Subplots (A) and (C) compare the effects of testing delay (1-day vs 2-day) for scenarios with a maximum of one test and two tests per notification, respectively. Subplots (B) and (D) compare the effects of the maximum number of tests per notification (one vs two tests) for 1-day and 2-day delays, respectively. In subplots (A) and (C), red boxes represent a 1-day delay and blue boxes represent a 2-day delay. In subplots (B) and (D), purple boxes correspond to one test per notification, while pink boxes correspond to two tests.

is generally associated with lower attack rates, despite some overlap between distributions, particularly at 20% and 60% application coverage.

When two tests are implemented, the overlap between distributions shifts, with greater similarity observed at 40% coverage. In most cases, the 1-day delay yields lower attack rates than the 2-day delay, with the exception of the 80% coverage scenario.

Across both delay scenarios, allowing an additional test is associated with lower average attack rates at higher levels of application coverage (60% and 80%). A similar effect is observed at 40% coverage for a 1-day delay. In contrast, at 20% coverage, scenarios allowing two tests tend to produce slightly higher attack rates.

These trends are also observed in the age-stratified results shown in Figures 5.8–5.10.

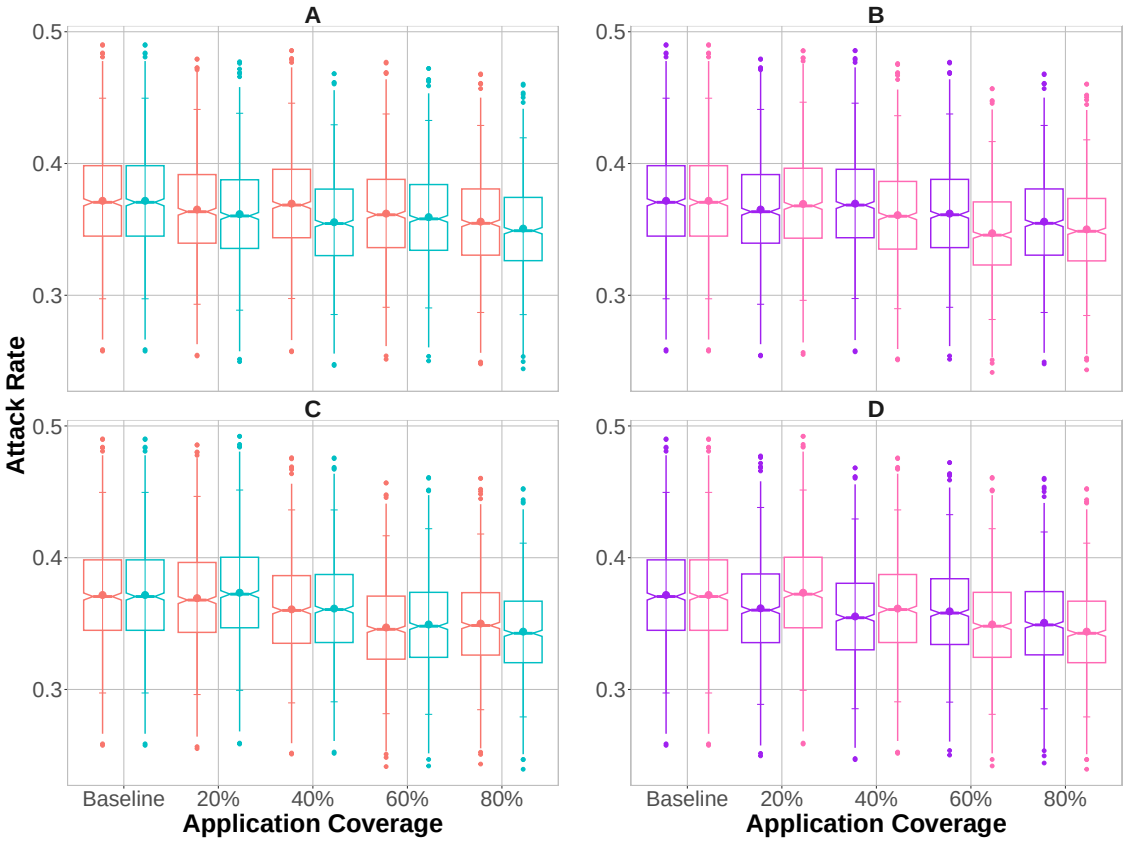

Figure 5.8: Box plots of attack rates under different scenarios for individuals under 18 years of age. Subplots (A) and (C) compare the effects of testing delay (1-day vs 2-day) for scenarios with a maximum of one test and two tests per notification, respectively. Subplots (B) and (D) compare the effects of the maximum number of tests per notification (one vs two tests) for 1-day and 2-day delays, respectively. In subplots (A) and (C), red boxes represent a 1-day delay and blue boxes represent a 2-day delay. In subplots (B) and (D), purple boxes correspond to one test per notification, while pink boxes correspond to two tests.

For individuals under 18 years of age, the baseline mean and median attack rates are $\sim$37.2% and $\sim$37.1%, respectively. Under the scenario with 20% coverage, a 2-day delay, and two tests, these values increase slightly to $\sim$37.3% and $\sim$37.2%. The lowest attack rates are observed at 80% coverage under the same assumptions, with mean and median values of $\sim$34.4% and $\sim$34.3%, respectively.

For the 18–65 age group, the baseline mean and median attack rates are $\sim$39.7% and $\sim$39.5%, respectively, representing the highest burden among the age groups. The largest attack rates are observed at 20% application coverage under scenarios with a 2-day delay and two tests, with mean and median values of $\sim$39.9% and $\sim$39.7%. The lowest values occur at 80% coverage, with corresponding mean and median attack rates of $\sim$36.6% and

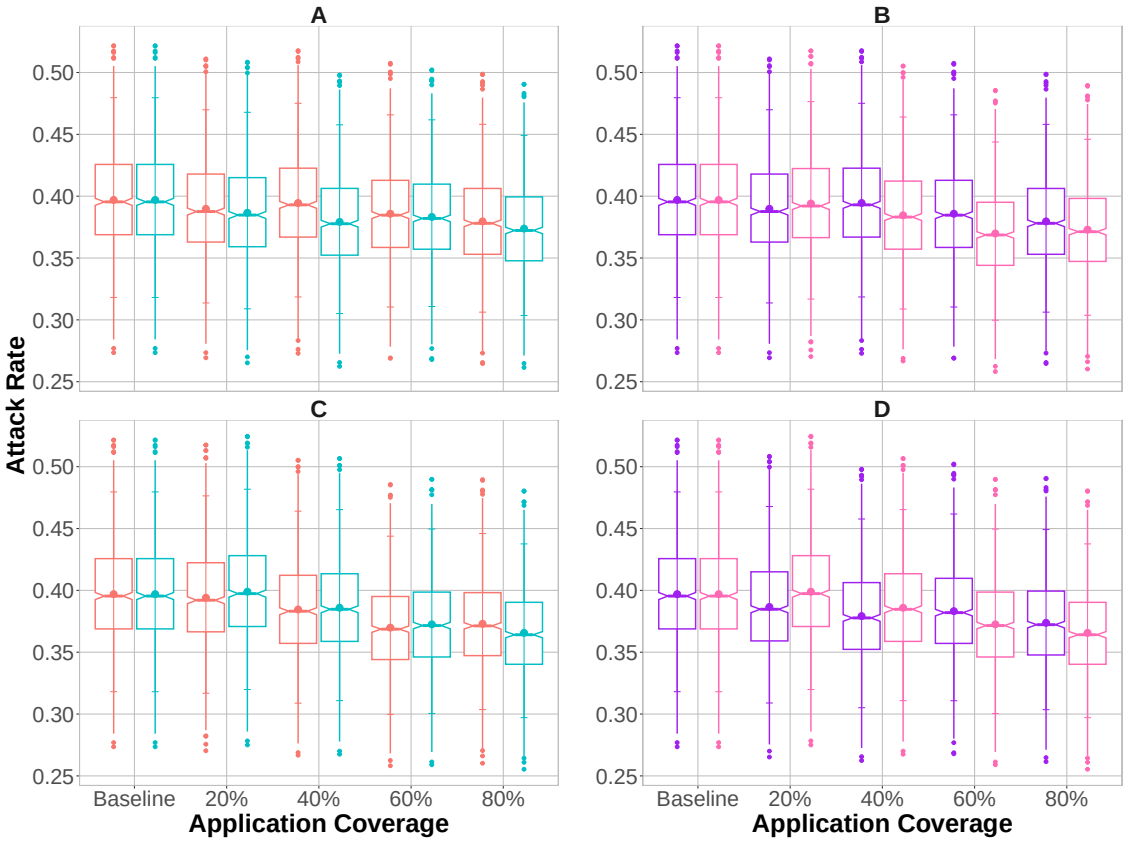

Figure 5.9: Box plots of attack rates under different scenarios for individuals aged 18–65 years. Subplots (A) and (C) compare the effects of testing delay (1-day vs 2-day) for scenarios with a maximum of one test and two tests per notification, respectively. Subplots (B) and (D) compare the effects of the maximum number of tests per notification (one vs two tests) for 1-day and 2-day delays, respectively. In subplots (A) and (C), red boxes represent a 1-day delay and blue boxes represent a 2-day delay. In subplots (B) and (D), purple boxes correspond to one test per notification, while pink boxes correspond to two tests.

$\sim$36.4%.

For individuals aged 66 years or older, the baseline mean and median attack rates are $\sim$19.2% and $\sim$19.2%, respectively, representing the lowest levels among the age groups. Across scenarios, attack rates range from $\sim$19.3% and $\sim$19.2% at 20% coverage to $\sim$17.1% and $\sim$17.0% at 80% coverage. Both pairs of values were captured when up to two tests were permitted, alongside a 2-day testing delay. This is the only age group where the mean and median attack rates at 60% coverage exceed those at 80% with two tests and a 1-day delay.

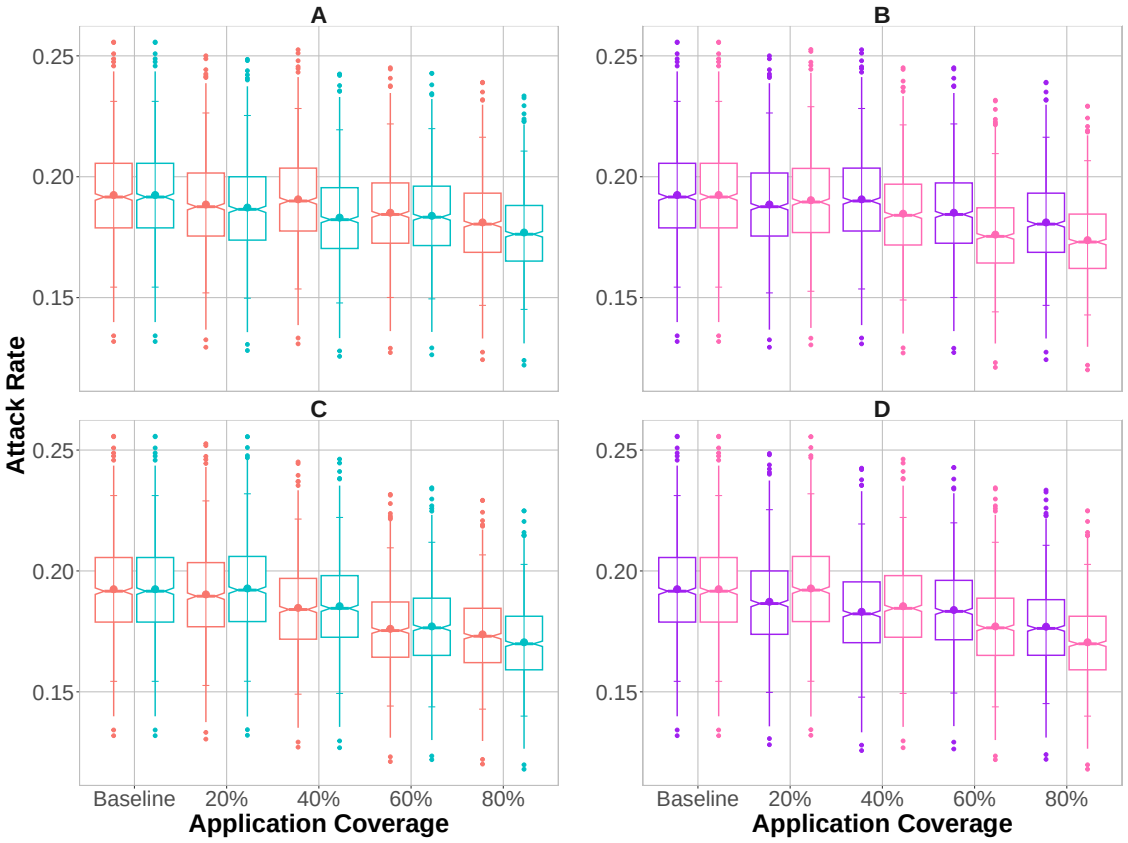

Figure 5.10: Box plots of attack rates under different scenarios for individuals aged 66 years or older. Subplots (A) and (C) compare the effects of testing delay (1-day vs 2-day) for scenarios with a maximum of one test and two tests per notification, respectively. Subplots (B) and (D) compare the effects of the maximum number of tests per notification (one vs two tests) for 1-day and 2-day delays, respectively. In subplots (A) and (C), red boxes represent a 1-day delay and blue boxes represent a 2-day delay. In subplots (B) and (D), purple boxes correspond to one test per notification, while pink boxes correspond to two tests.

5.2.3 Relative Reductions in Attack Rates

The non-monotonic patterns observed in Chapter 5.2.2 are also reflected in the relative reductions in attack rates. Figure 5.11 compares reductions across levels of application coverage for 1-day and 2-day testing delays, when one test is allowed per notification.

At the population level, reductions do not increase uniformly with application coverage. For example, at a 1-day delay, the mean reduction at 20% coverage exceeds that at 40%, with the latter yielding the lowest values (mean $\sim$0.6%, median $\sim$0.6%). Similarly, for a 2-day delay, reductions at 40% coverage exceed those at 60%. However, the largest reductions are consistently observed at 80% coverage, with mean and median values of

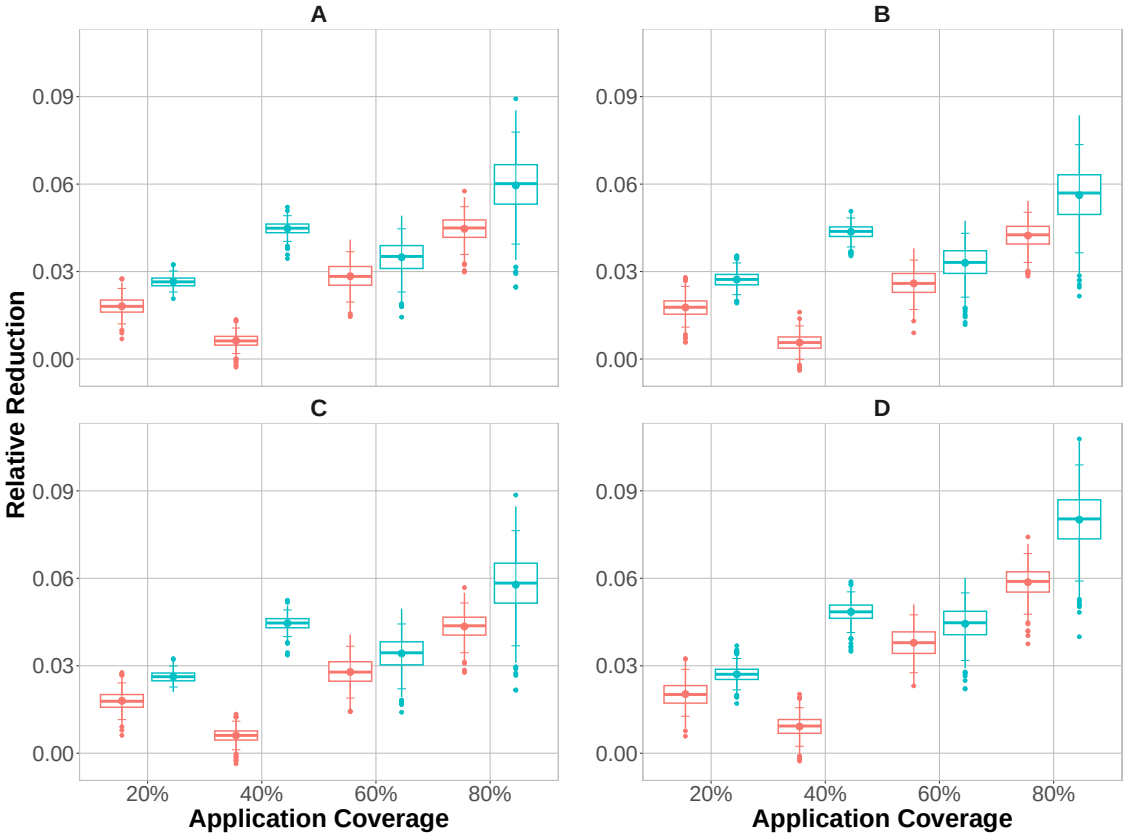

Figure 5.11: Relative reductions in the attack rates with respect to the baseline scenario under different scenarios, assuming one test per notification. Subplot (A) represents the total population, (B) corresponds to individuals under 18 years of age, (C) represents individuals aged 18–65, and (D) corresponds to individuals aged 66 years or older. Red boxes represent a 1-day delay between notification and testing, while blue boxes represent a 2-day delay.

∼6.0% and ∼6.0% for a 2-day delay, and ∼4.5% and ∼4.5% for a 1-day delay. The smallest reductions occur at 20% coverage for a 2-day delay (mean and median ∼2.7%).

These patterns are also observed across age groups. For individuals under 18 years of age, the largest reductions occur at 80% coverage with a 2-day delay (mean ∼5.6%, median ∼5.7%), while the smallest reductions (∼2.7%) are observed at 20% coverage. For a 1-day delay, reductions increase from ∼0.6% and ∼0.6% at 40% coverage to ∼4.2% and ∼4.3% at 80% coverage.

For the 18–65 age group, mean reductions increase from ∼0.6% (1-day delay) and ∼2.6% (2-day delay) at lower coverage levels to ∼4.4% and ∼5.8% at 80% coverage. The corresponding medians follow a similar pattern.

For individuals aged 66 years or older, reductions are larger in magnitude. For a 1-day

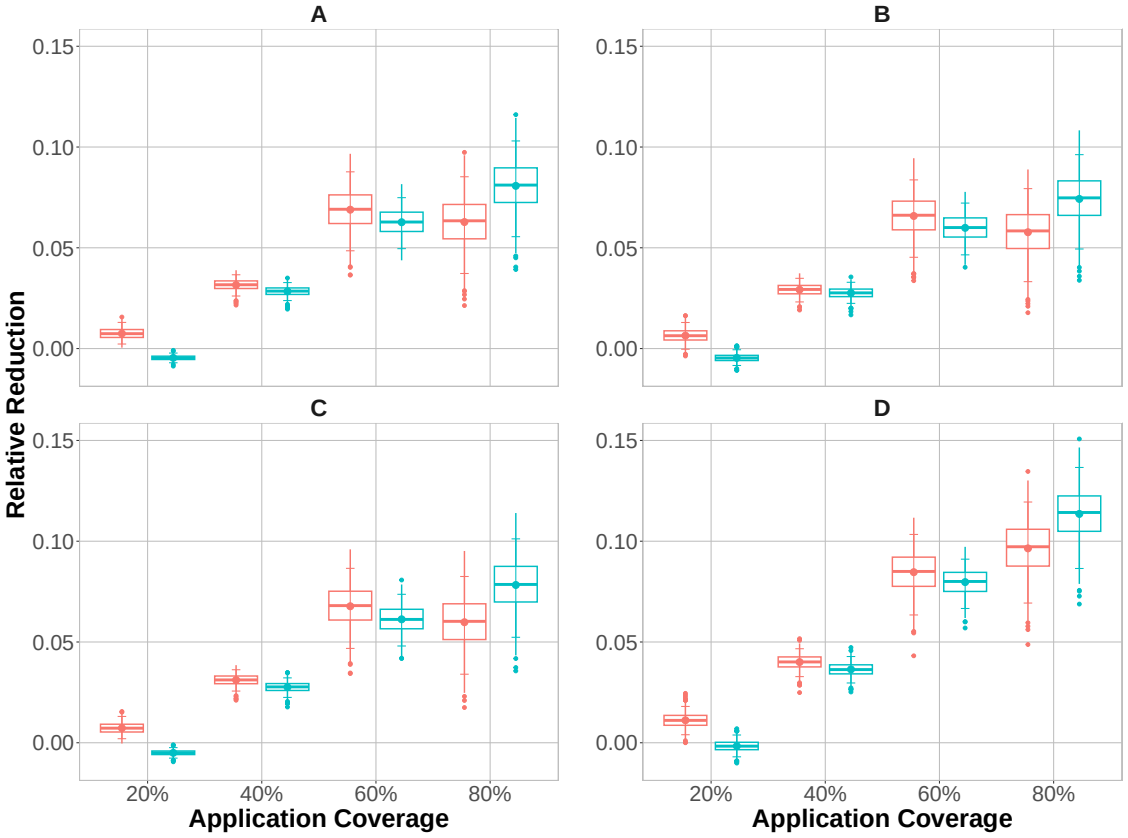

Figure 5.12: Relative reductions in the attack rates with respect to the baseline scenario under different scenarios, assuming up to two tests per notification. Subplot (A) represents the total population, (B) corresponds to individuals under 18 years of age, (C) represents individuals aged 18–65, and (D) corresponds to individuals aged 66 years or older. Red boxes represent a 1-day delay between notification and testing, while blue boxes represent a 2-day delay.

delay, mean and median reductions increase from ∼0.9% and ∼0.9% to ∼5.9% and ∼5.9%. For a 2-day delay, they increase from ∼2.7% to ∼8.0% and ∼8.0%.

Figure 5.12 presents results for scenarios allowing two tests per notification. In subplot (A), for a 1-day delay, the largest reductions are observed at 60% coverage (mean ∼6.9%, median ∼6.9%), while the smallest occur at 20% coverage (mean ∼0.8%, median ∼0.7%). For a 2-day delay, reductions range from negative values at 20% coverage (mean ∼−0.5%, median ∼−0.5%) to the highest values at 80% coverage (mean ∼8.1%, median ∼8.1%).

Subplot (B) displays the relative reductions in attack rates for individuals under 18 years of age. For a 1-day delay, reductions increase from mean and median values of ∼0.6% at 20% coverage to ∼6.6% and ∼6.6% at 60% coverage. For a 2-day delay, reductions increase from negative values at 20% coverage (mean ∼−0.5%, median ∼−0.5%) to

$\sim$7.4% and $\sim$7.5% at 80% coverage.

A similar pattern is observed for the 18–65 age group. For a 1-day delay, reductions increase from $\sim$0.7% and $\sim$0.7% at 20% coverage to $\sim$6.8% and $\sim$6.8% at 60% coverage. For a 2-day delay, reductions range from $\sim -0.5\%$ at 20% coverage to $\sim$7.8% and $\sim$7.9% at 80% coverage.

For individuals aged 66 years or older, reductions are larger in magnitude. For a 1-day delay, mean and median reductions increase from $\sim$1.1% at 20% coverage to $\sim$9.6% and $\sim$9.7% at 80% coverage. For a 2-day delay, reductions increase from $\sim -0.2\%$ and $\sim -0.2\%$ at 20% coverage to $\sim$11.4% and $\sim$11.4% at 80% coverage, indicating a stronger response to the intervention in this age group.

5.3 Statistical Analysis

To further characterize the simulation outputs, particularly the attack rates, we employed statistical techniques to assess distributional properties and evaluate differences between scenarios.

5.3.1 Shapiro-Wilk Test

We first applied the Shapiro-Wilk test to assess the normality of the data. The null hypothesis states that the data are normally distributed. At a significance level of 0.05, a p-value below 0.05 leads to rejection of the null hypothesis in favor of non-normality, whereas a p-value above 0.05 indicates insufficient evidence to reject normality [90].

The results are presented in Tables 5.1–5.4 and are used to guide the selection of appropriate statistical tests in subsequent analyses.

Table 5.1: P-values for the Shapiro-Wilk test (all age groups).

	No Coverage	20% Coverage	40% Coverage	60% Coverage	80% Coverage
1 test, 1 day delay	0.2272	0.2381	0.2539	0.2528	0.259
1 test, 2 days delay	0.2272	0.237	0.2404	0.2751	0.3282
2 tests, 1 day delay	0.2272	0.2293	0.2324	0.3379	0.3688
2 tests, 2 days delay	0.2272	0.2354	0.235	0.2918	0.3585

Table 5.2: P-values for the Shapiro-Wilk test (individuals under 18 years of age).

	No Coverage	20% Coverage	40% Coverage	60% Coverage	80% Coverage
1 test, 1 day delay	0.2297	0.2322	0.2763	0.256	0.239
1 test, 2 days delay	0.2297	0.2475	0.23	0.2784	0.3276
2 tests, 1 day delay	0.2297	0.2252	0.2402	0.3316	0.3909
2 tests, 2 days delay	0.2297	0.2235	0.2471	0.2885	0.365

Table 5.3: P-values for the Shapiro-Wilk test (individuals aged 18–65 years).

	No Coverage	20% Coverage	40% Coverage	60% Coverage	80% Coverage
1 test, 1 day delay	0.2292	0.2381	0.2415	0.2385	0.2503
1 test, 2 days delay	0.2292	0.2339	0.2423	0.2385	0.2914
2 tests, 1 day delay	0.2292	0.2311	0.229	0.3079	0.3401
2 tests, 2 days delay	0.2292	0.2421	0.2322	0.2613	0.3359

Table 5.4: P-values for the Shapiro-Wilk test (individuals aged 66 years or older).

	No Coverage	20% Coverage	40% Coverage	60% Coverage	80% Coverage
1 test, 1 day delay	0.4083	0.455	0.4915	0.4375	0.4497
1 test, 2 days delay	0.4083	0.4279	0.4358	0.5134	0.4191
2 tests, 1 day delay	0.4083	0.4448	0.4823	0.4599	0.465
2 tests, 2 days delay	0.4083	0.4567	0.4487	0.4395	0.4392

Based on the p-values reported in the tables, which range from 0.2235 to 0.5134, the test fails to reject the null hypothesis of normality, indicating no evidence against the assumption that the data are normally distributed. Before selecting an appropriate statistical test for comparing scenarios, we next assessed the homogeneity of variances across groups. These groups are defined according to the testing delay (1 or 2 days) and the maximum number of tests permitted per notification.

5.3.2 Fligner-Killeen Test

Table 5.5: P-values for the Fligner-Killeen test.

	All Ages	Under 18	Ages 18-65	Over 66
1 test, 1 day delay	0.3274	0.4172	0.3279	0.131
1 test, 2 days delay	0.01279	0.01961	0.01378	0.001059
2 tests, 1 day delay	0.0001046	0.0002733	0.0001332	4.934×10^{-7}
2 tests, 2 days delay	7.623×10^{-5}	0.0002602	9.415×10^{-5}	1.558×10^{-7}

For the scenario with a 1-day delay and one test per notification, the p-values exceed 0.05, indicating no evidence against the assumption of equal variances across groups.

In contrast, all other scenarios yield p-values below 0.05, suggesting heterogeneity of variances. Accordingly, for the case in which the assumption of equal variances holds, we applied a one-way analysis of variance (ANOVA) to assess differences in group means.

5.3.3 One-Way ANOVA Test

The One-way ANOVA test assumes that the data are normally distributed and that variances are equal across the groups being compared. The null hypothesis states that all group means are equal. At a significance level of 0.05, a p-value below 0.05 leads to rejection of the null hypothesis, indicating that at least one group mean differs from the others [94]. The results are presented in the Table 5.6.

Table 5.6: P-values for the One-Way ANOVA test.

	All Ages	Under 18	Ages 18-65	Over 66
1 test, 1 day delay	$< 2 \times 10^{-16}$	$< 2 \times 10^{-16}$	$< 2 \times 10^{-16}$	$< 2 \times 10^{-16}$

Since all of the p-values are less than 0.05, we reject the null hypothesis that all group means are equal for each population considered. To identify which group means differ, we performed Tukey's Honestly Significant Difference (HSD) test.

5.3.4 Tukey's HSD Test

While the One-way ANOVA test determines whether at least one group mean differs, Tukey's HSD test provides pairwise comparisons to identify which specific group means are significantly different. At a significance level of 0.05, a p-value below 0.05 leads to rejection of the null hypothesis that the group means are equal [95, 96]. The results of these tests are presented in Figure 5.13.

For the scenario with one test per notification and a 1-day delay, no statistically significant differences are observed in the population-level means between the baseline and 40% coverage, 20% and 40% coverage, or 20% and 60% coverage. A similar pattern is observed for the under 18 and 18–65 age groups. However, for individuals aged 66 years

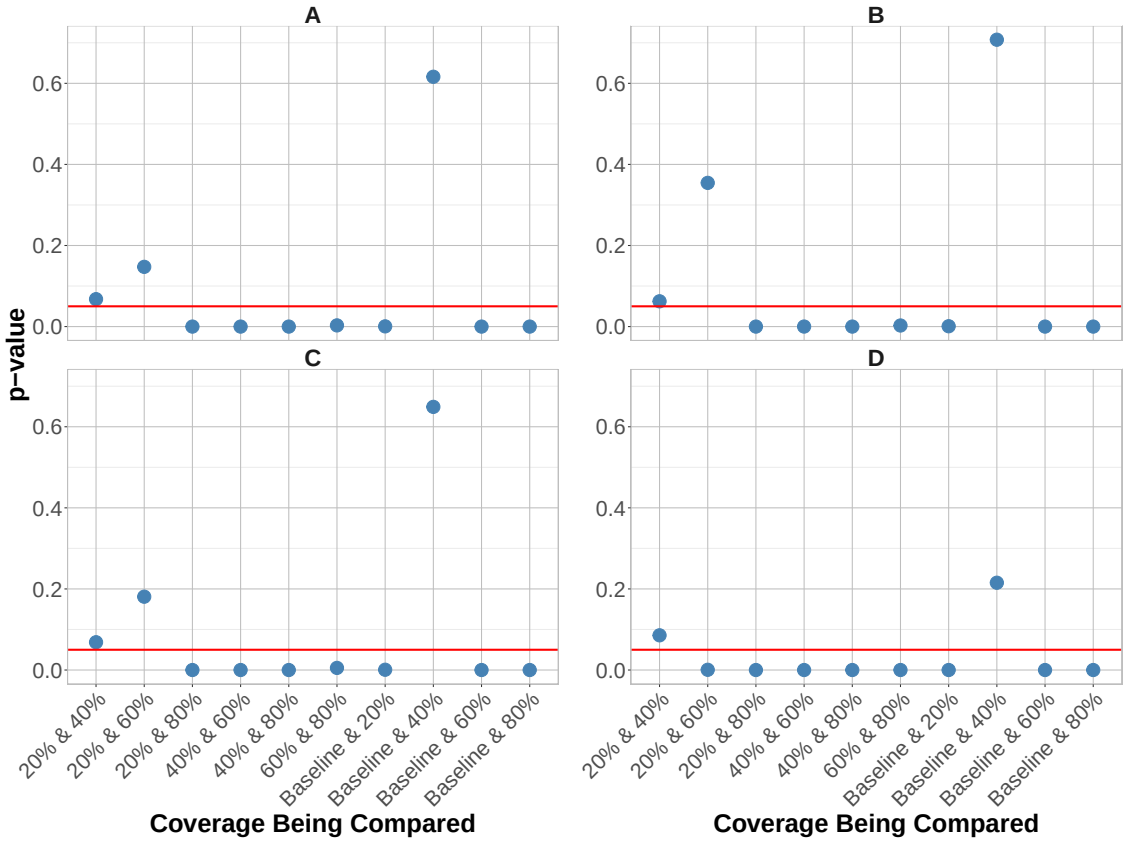

Figure 5.13: P-values from Tukey's HSD test comparing application coverage levels under a 1-day delay and one test per notification. Subplot (A) represents the total population, (B) corresponds to individuals under 18 years of age, (C) represents individuals aged 18–65, and (D) corresponds to individuals aged 66 years or older.

or older, the comparison between 20% and 60% coverage yields a p-value below 0.05, indicating a statistically significant difference between these groups.

5.3.5 Welch's t-test

The Fligner-Killeen test indicates that, for the remaining scenarios, the assumption of equal variances is violated across application coverage levels. Accordingly, Welch's t-test was used to compare group means. The results are presented in Figures 5.14–5.16.

Figure 5.14 presents comparisons across application coverage levels for scenarios with one test per notification and a 2-day delay. For the under 18 and 18–65 age groups, no statistically significant difference is observed between 20% and 60% coverage. At the population level, this comparison yields a p-value slightly below 0.05, indicating

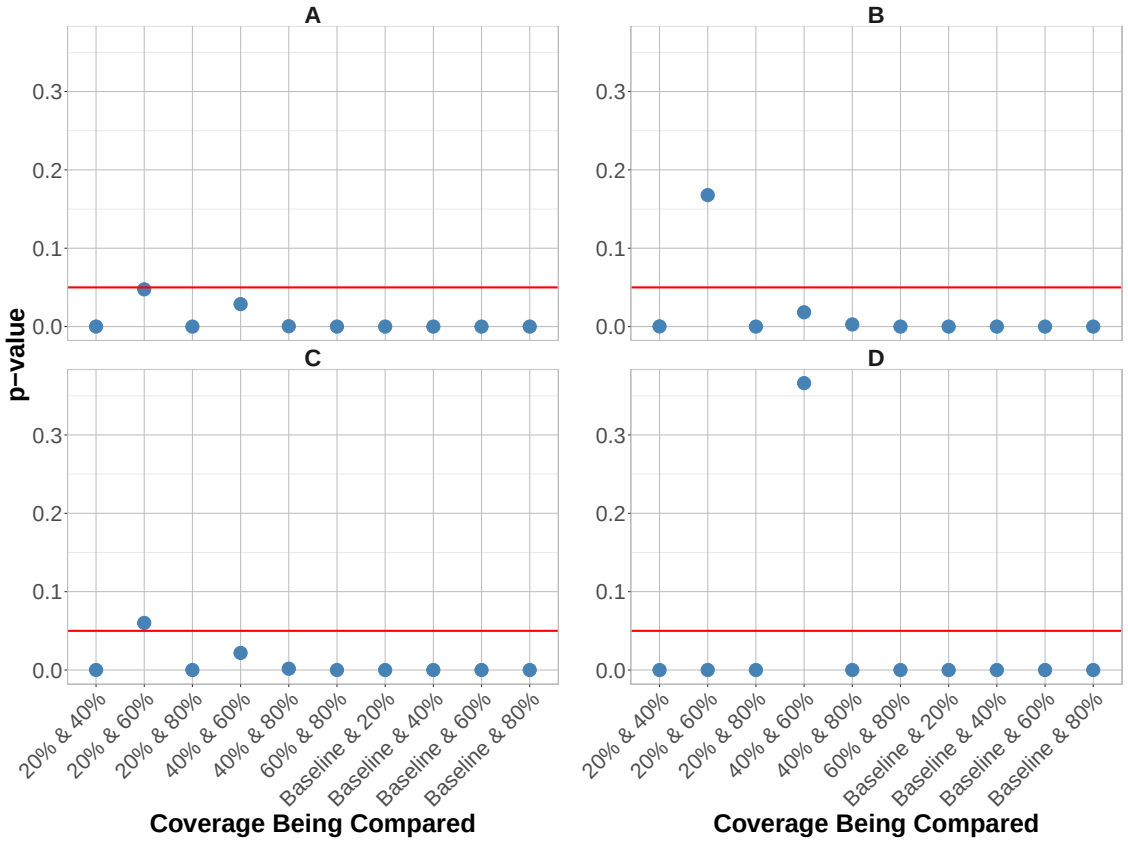

Figure 5.14: P-values from Welch's t-test comparing application coverage levels under a 2-day delay and one test per notification. Subplot (A) represents the total population, (B) corresponds to individuals under 18 years of age, (C) represents individuals aged 18–65, and (D) corresponds to individuals aged 66 years or older.

a marginally significant difference. For individuals aged 66 years and older, only the comparison between 40% and 60% coverage is not statistically significant.

Figure 5.15 considers scenarios allowing two tests per notification with a 1-day delay. At the population level and for the under 18 age group, no statistically significant differences are observed between the baseline and 20% coverage, or between 60% and 80% coverage. For the 18–65 group, this occurs only for the comparison between 20% and 60% coverage, while for individuals aged 66 years or older, all pairwise comparisons are statistically significant.

When the delay is extended to 2 days (Figure 5.16), a consistent pattern emerges in which no statistically significant difference is observed between the baseline and 20% coverage across all populations. These findings are consistent with the results of

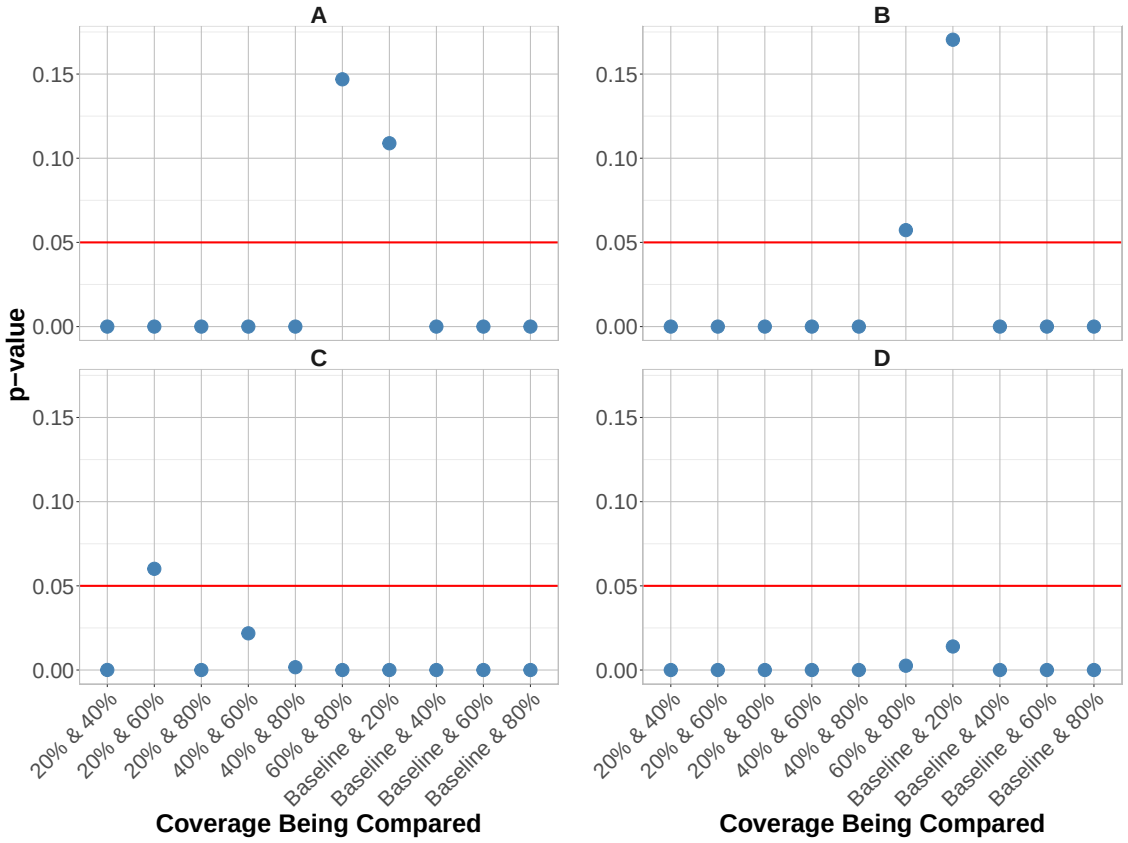

Figure 5.15: P-values from Welch's t-test comparing application coverage levels under a 1-day delay and up to two tests per notification. Subplot (A) represents the total population, (B) corresponds to individuals under 18 years of age, (C) represents individuals aged 18–65, and (D) corresponds to individuals aged 66 years or older.

Tukey's HSD test and support earlier observations of substantial overlap across application coverage levels. In contrast to Chapter 4, where isolation depended solely on positive test results, the inclusion of symptom-based isolation appears to reduce the differences between scenarios.

Figures 5.17 and 5.18 compare testing delays (1-day vs 2-day) for scenarios with a maximum of one and two tests per notification, respectively. In both cases, no statistically significant difference is observed at 60% coverage across all age groups. This also extends to 40% coverage when two tests are considered. Additionally, for scenarios with one test per notification, no significant difference between delays is observed at 20% coverage for all age groups except individuals under 18 years of age.

Overall, 4 out of 8 comparisons show no statistically significant difference between

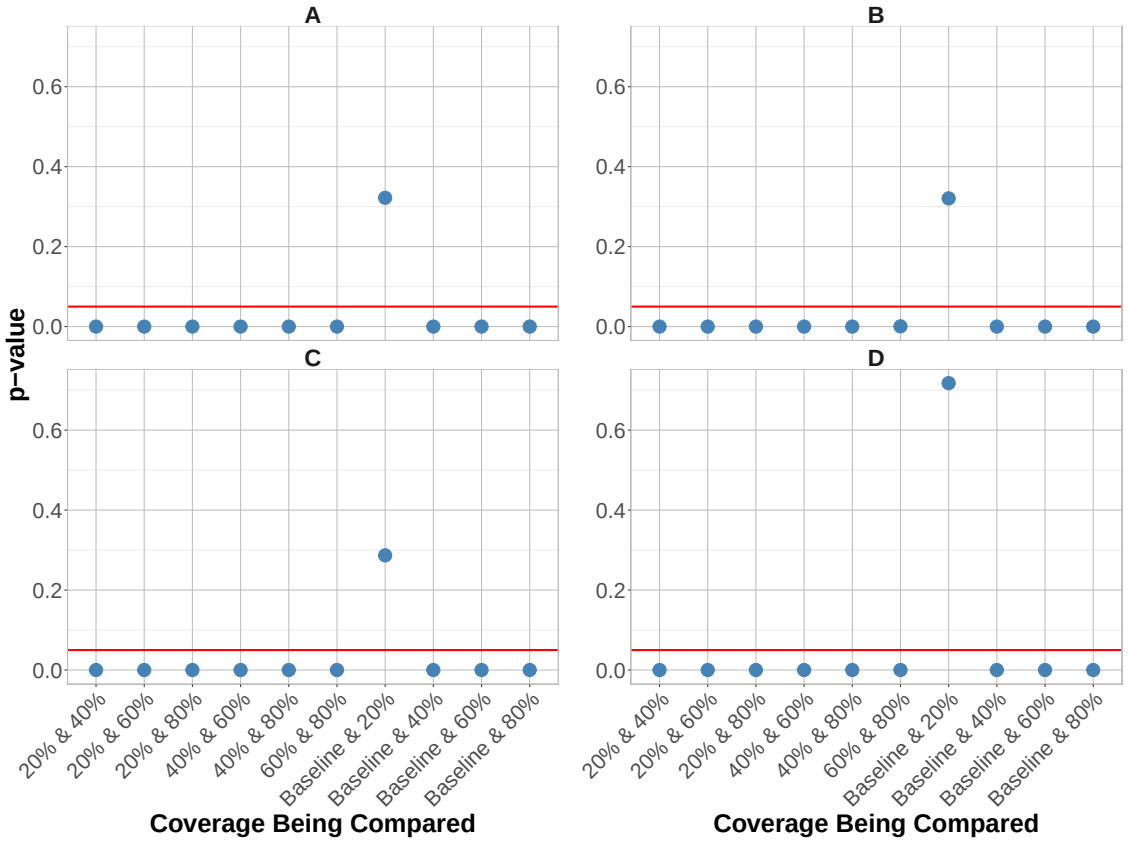

Figure 5.16: P-values from Welch's t-test comparing application coverage levels under a 2-day delay and up to two tests per notification. Subplot (A) represents the total population, (B) corresponds to individuals under 18 years of age, (C) represents individuals aged 18–65, and (D) corresponds to individuals aged 66 years or older.

testing delays. Together with the corresponding results in Chapter 4, this suggests that the timing of testing (1-day versus 2-day delay) has a limited effect on outbreak dynamics under the conditions considered.

Finally, Welch's t-test indicates that allowing two tests per notification leads to statistically significant differences in mean attack rates across all coverage levels when testing delays are held constant. Consistent with earlier results, scenarios permitting a second test are associated with lower attack rates at higher levels of application coverage (60% and 80%), and at 40% coverage under a 1-day delay. In contrast, at lower coverage levels, scenarios with a single test per notification tend to yield lower attack rates. These findings suggest that the effectiveness of permitting an additional test depends on the level of application coverage, with greater benefit observed at higher adoption levels.

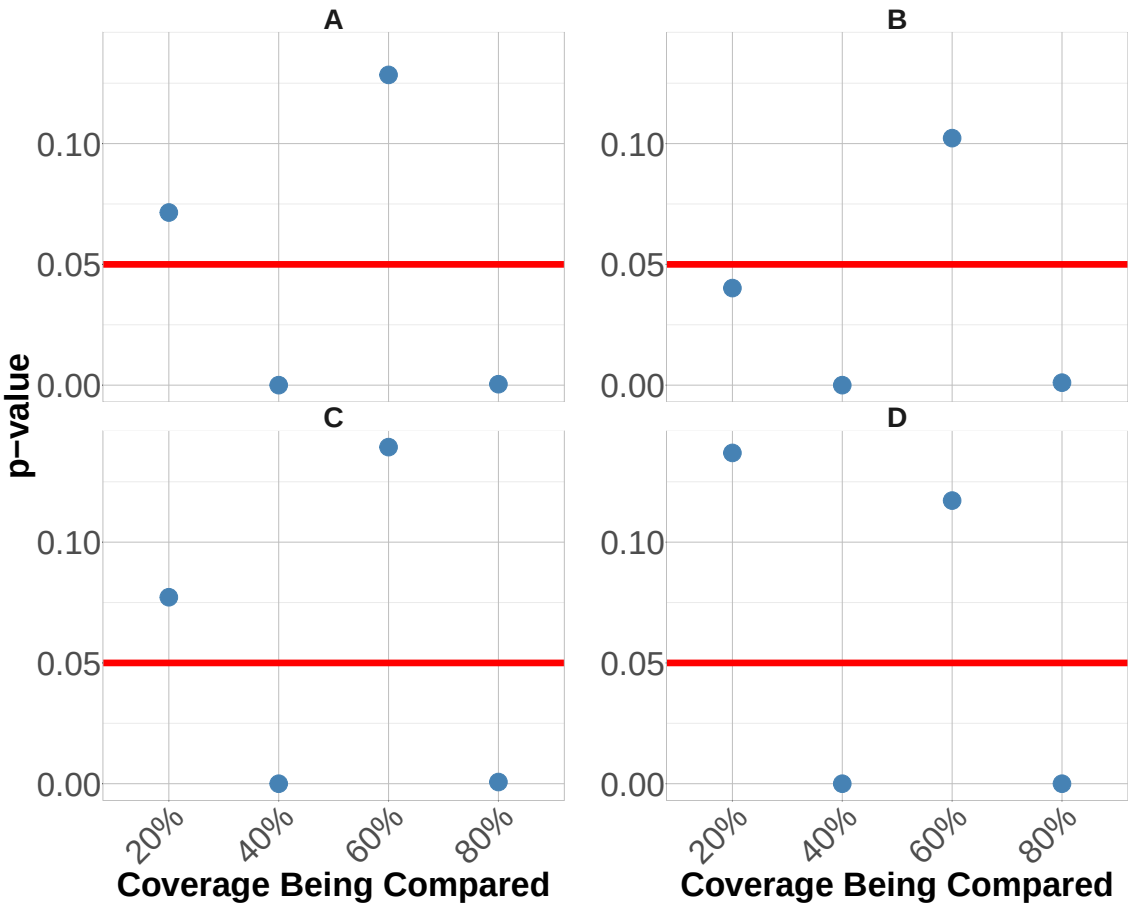

Figure 5.17: P-values from Welch's t-test comparing 1-day and 2-day delays between notification and testing for scenarios with one test per notification across different application coverage levels. Subplot (A) represents the total population, (B) corresponds to individuals under 18 years of age, (C) represents individuals aged 18–65, and (D) corresponds to individuals aged 66 years or older.

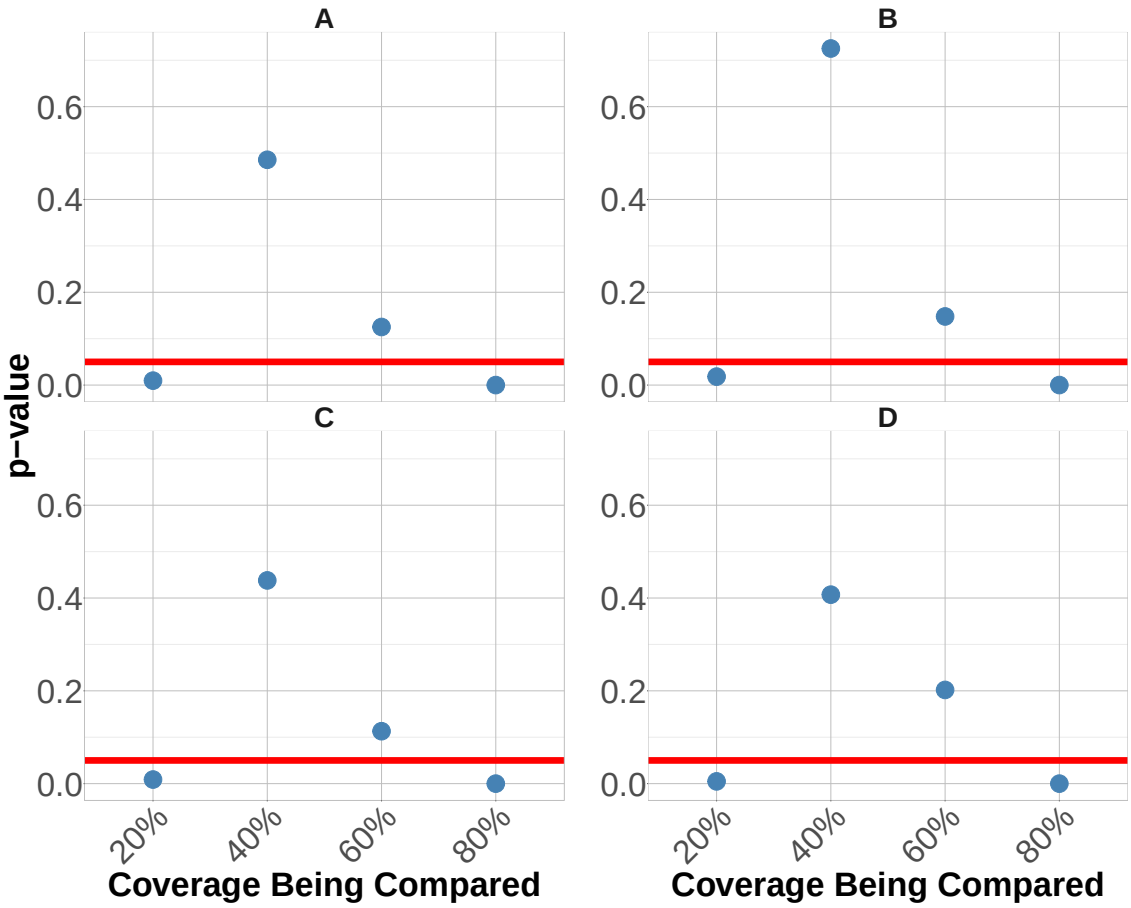

Figure 5.18: P-values from Welch's t-test comparing 1-day and 2-day delays between notification and testing for scenarios allowing up to two tests per notification across different application coverage levels. Subplot (A) represents the total population, (B) corresponds to individuals under 18 years of age, (C) represents individuals aged 18–65, and (D) corresponds to individuals aged 66 years or older.

Chapter 6

Discussion and Conclusion

Digital contact tracing (DCT) has emerged as a promising strategy for managing infectious disease outbreaks. Its largely automated nature addresses several limitations of manual contact tracing, including delays, labor intensity, and susceptibility to human error [5, 9]. However, its effectiveness is strongly dependent on external factors, particularly user adoption and compliance, which have limited its impact in real-world settings [23]. The objective of this study was to evaluate the effectiveness of DCT when integrated with self-testing and symptom-based isolation, and to identify the conditions under which it provides meaningful epidemiological benefit.

We first examined a strategy in which DCT and self-testing were the only interventions. In this setting, application coverage emerged as the primary determinant of epidemic outcomes. Increasing adoption from 0% to 80% produced a consistent reduction in attack rates, indicating a monotonic relationship between coverage and mitigation. This finding is consistent with prior studies [97, 98], which demonstrate that even moderate levels of uptake can substantially reduce transmission, with effectiveness increasing as adoption expands. Mechanistically, this reflects the growing proportion of infectious contacts that are identified and isolated as coverage increases, thereby interrupting transmission chains more efficiently.

We also evaluated the impact of delays between exposure notification and testing,

comparing 1-day and 2-day intervals. Despite the intuitive expectation that delaying testing may improve detection by allowing viral loads to increase, our results indicate that this factor has a limited effect on epidemic dynamics. In most scenarios, no statistically significant difference in attack rates was observed between the two delays. This suggests that, within the time scales considered, the infectious period overlaps sufficiently with both testing windows such that the marginal benefit of delaying testing is minimal.

The final parameter considered was the maximum number of tests performed following a notification. Allowing a second test improved outcomes at higher levels of application coverage (60% and 80%), but had negligible or inconsistent effects at lower coverage levels. This result highlights an important interaction between intervention intensity and population participation: repeated testing is most effective when a sufficiently large fraction of the population is engaged in the tracing system. At lower adoption levels, the limited reach of the system constrains the benefit of additional testing, as fewer infectious individuals are identified in the first place. These findings are consistent with prior recommendations for confirmatory testing to reduce false negatives [99–101], but emphasize that its effectiveness is contingent on broader system uptake.

We then extended the analysis to a second strategy incorporating mandatory symptom-based isolation. The introduction of this measure substantially altered the epidemic dynamics. Even in the absence of DCT, symptom-based isolation alone reduced the attack rate by approximately 39%, demonstrating its strong standalone effectiveness. As a result, the additional impact of DCT was diminished, and the previously observed monotonic relationship between application coverage and attack rate was no longer consistently present.

Under this combined strategy, the effects of increasing coverage became less predictable, with several instances in which lower coverage levels produced comparable reductions in attack rates to higher levels. This increased overlap across scenarios was confirmed by statistical analysis, which showed that many differences in mean attack rates were no longer statistically significant. These findings suggest that when a highly effective

intervention such as symptom-based isolation is already in place, the marginal benefit of DCT is reduced.

A similar pattern was observed when comparing the overall magnitude of intervention effects. The maximum relative reduction achieved under the DCT-only strategy exceeded that observed when symptom-based isolation was included, indicating that the latter absorbs a substantial portion of the achievable mitigation. Consequently, the addition of DCT yields diminishing returns, particularly when isolation is already triggered independently of the tracing system.

The impact of testing delay remained limited under this second strategy, with only half of the comparisons showing statistically significant differences. This further supports the conclusion that short delays in testing have a relatively minor influence on outbreak dynamics compared to other factors such as coverage and isolation behaviour. In contrast, the role of repeated testing became more nuanced. While statistically significant differences were observed across all scenarios, the direction of the effect varied. At lower coverage levels (20% and 40%), allowing a second test did not consistently improve outcomes and, in some cases, resulted in higher attack rates. At higher coverage levels, however, repeated testing continued to provide benefits. This reinforces the conclusion that the effectiveness of testing strategies strongly depends on the level of participation in the DCT system.

A key explanation for these observations lies in the dominant role of symptom-based isolation. In our model, symptomatic infection is the most common disease pathway, implying that a large proportion of infected individuals will isolate regardless of testing or notification. As a result, the additional contribution of DCT is reduced, and its effectiveness becomes secondary to the isolation mechanism. This also explains the disruption of the relationship between coverage and containment observed in the DCT-only scenario, where isolation was entirely dependent on testing and therefore strongly tied to application use.

This interaction between interventions is consistent with findings from previous work [102], which demonstrated that the combined implementation of multiple control measures can lead to interference effects. Specifically, highly effective interventions tend to

dominate epidemic outcomes, reducing the observable impact of additional measures. In this context, symptom-based isolation acts as the primary driver of transmission reduction, while DCT provides supplementary benefits that are most pronounced when participation is high.

6.1 Age-Dependent Summary

As discussed in earlier chapters, most trends observed at the population level, particularly those related to application coverage, testing delay, and the number of tests per notification, were consistently reflected across the three age groups. However, age-specific characteristics, including population size, contact patterns, and behavioral differences, contributed to distinct epidemiological outcomes within each subgroup [103].

Across baseline scenarios, the 18–65 age group experienced the highest cumulative incidence under the first and second strategies. In contrast, individuals aged 66 years or older consistently exhibited the lowest cumulative incidence, while the under 18 group occupied an intermediate position, with values closer to those of the middle age group. These patterns were also reflected in attack rates and relative reductions. The 18–65 group remained the most affected across all scenarios, which can be attributed to both its larger population share and higher levels of social interaction. This is consistent with empirical findings indicating that individuals aged 20–49 are key contributors to transmission dynamics [104], and that younger adults exhibit higher infection rates [105].

The under 18 group displayed similar trends to the 18–65 population, with only marginal differences in attack rates and relative reductions. In contrast, individuals aged 66 years or older consistently experienced lower attack rates, slower epidemic growth, and greater relative reductions across scenarios. This distinction is notable given that both the youngest and oldest groups were excluded from application use in the model. A plausible explanation lies in differences in contact patterns and behavioural responses. Older individuals generally have fewer social interactions and are more likely to adhere to non-pharmaceutical

interventions, such as social distancing and hygiene practices [103]. Additionally, reduced transmission within the 18–65 group, driven by application use, indirectly protects older individuals by limiting exposure pathways. This indirect protection effect is consistent with previous studies demonstrating that reductions in transmission among highly connected groups can disproportionately benefit more vulnerable populations [106].

Overall, these findings highlight the importance of age-structured dynamics in shaping epidemic outcomes and suggest that interventions targeting highly interactive age groups can yield broader population-level benefits.

6.2 Limitations

Despite the contributions of this thesis, several limitations should be acknowledged when interpreting the results. First, DCT remains a relatively recent intervention, and empirical data on its large-scale effectiveness are limited [107]. This is partly driven by low adoption rates in real-world settings, which are influenced by concerns regarding data privacy, trust in government, and willingness to comply with public health measures [21, 22]. Additional barriers include technological constraints, such as device incompatibility, and reduced familiarity with mobile applications among certain populations, particularly older individuals [23, 106]. As a result, the evidence base used to inform model assumptions is necessarily limited, and some parameters were derived from indirect or context-specific studies.

Second, the model relies on several simplifying assumptions that may not fully reflect real-world dynamics. For example, we assume full compliance with application usage, testing, and isolation protocols among participating individuals. In practice, adherence to such measures is often incomplete and may vary across demographic groups. Additionally, the model assumes that testing is widely available and does not produce false-positive results, while incorporating only limited representation of false negatives. These assumptions may lead to an overestimation of the effectiveness of testing-based interventions.

Third, behavioural heterogeneity is not explicitly incorporated beyond age stratification and a contact matrix. Factors such as socioeconomic status, occupation, mobility patterns, and individual risk perception can significantly influence contact rates, testing behaviour, and compliance with isolation. The absence of these dimensions limits the model's ability to capture more complex and realistic transmission dynamics.

Fourth, the model does not account for demographic processes such as births, natural deaths, or migration, nor does it incorporate additional epidemiological features such as waning immunity, reinfection, or vaccination. While these simplifications are appropriate for the time horizon considered, they restrict the generalizability of the results to longer-term or evolving epidemic scenarios.

Fifth, the stochastic nature of the model introduces variability in outcomes. Randomness is embedded in multiple components, including contact patterns, transmission events, disease progression, and testing outcomes. Although Monte Carlo simulations and bootstrap methods were employed to account for this variability and provide estimates, stochastic effects may still produce variability across scenarios that can complicate interpretation.

Finally, the structure of the contact network is based on the predefined contact matrix and does not capture dynamic changes in behaviour over time, such as adaptive responses to rising case counts or policy changes. In reality, individuals may alter their contact patterns in response to perceived risk, which could significantly influence transmission dynamics. These limitations highlight the need for cautious interpretation of the results and suggest that future work should focus on incorporating behavioural heterogeneity, partial compliance, and more detailed empirical data to enhance the realism and applicability of the model.

6.3 Future Work

This study opens several avenues for future research aimed at improving the realism and applicability of DCT models and better understanding its role in epidemic control. A

primary extension involves incorporating partial and dynamic compliance. In the present model, application users are assumed to fully adhere to testing, reporting, and isolation protocols, and symptomatic individuals are assumed to isolate immediately when required. In practice, adherence is often imperfect and may vary across individuals and over time [3]. Future work could introduce individual-specific compliance probabilities, potentially modulated by factors such as perceived risk, prior exposure to interventions, or behavioural fatigue. Incorporating time-dependent or state-dependent compliance would allow the model to capture more realistic behavioural responses and assess the robustness of DCT under imperfect adherence.

Another important direction is the inclusion of additional epidemiological states and health system dynamics. For example, extending the model to incorporate hospitalization and severe disease outcomes would enable the assessment of healthcare burden and system capacity constraints [108]. This extension could also facilitate the study of more complex disease processes, including reinfection, waning immunity, and the circulation of multiple strains [109, 110], thereby improving the model's relevance to long-term epidemic scenarios.

Future research could also explore the interaction between DCT and a broader set of interventions. While this study focused on self-testing and symptom-based isolation, integrating additional measures such as vaccination, mask use, and intermittent mobility restrictions would allow for the evaluation of combined intervention strategies [3, 111]. In particular, understanding how DCT complements or is diminished by highly effective interventions, such as vaccination or strict isolation policies, would provide valuable insights for designing optimal public health responses.

Another promising avenue is the incorporation of adaptive behaviour and dynamic contact patterns. In reality, individuals adjust their behaviour in response to perceived risk, public health messaging, and epidemic progression [112]. Embedding feedback mechanisms that modify contact rates or compliance based on epidemic indicators could significantly enhance the realism of the model and improve its predictive capacity.

Finally, future work should aim to calibrate and validate the model using empirical data from real-world implementations of digital contact tracing. As more data become available, parameter estimation and model validation will be critical for improving confidence in predictions and ensuring that the framework can support evidence-based policy decisions. These extensions would strengthen the capacity of the model to capture the complex interplay between behaviour, technology usage, and epidemiological dynamics, and enhance its utility for informing disease control strategies.

Bibliography

[1] Nishant Renu. “Technological advancement in the era of COVID-19”. In: *SAGE Open Medicine* 9 (2021), p. 20503121211000912.

[2] Kunming Cheng et al. “WHO declares the end of the COVID-19 global health emergency: lessons and recommendations from the perspective of ChatGPT/GPT-4”. In: *International Journal of Surgery* 109.9 (2023), pp. 2859–2862.

[3] Iain R Moyles, Jane M Heffernan, and Jude D Kong. “Cost and social distancing dynamics in a mathematical model of COVID-19 with application to Ontario, Canada”. In: *Royal Society open science* 8.2 (2021).

[4] Jay A Pandit et al. “Smartphone apps in the COVID-19 pandemic”. In: *Nature Biotechnology* 40.7 (2022), pp. 1013–1022.

[5] Alain Barrat et al. “Effect of manual and digital contact tracing on COVID-19 outbreaks: a study on empirical contact data”. In: *Journal of the Royal Society Interface* 18.178 (2021).

[6] Cochrane Public Health Group et al. “Digital contact tracing technologies in epidemics: a rapid review”. In: *Cochrane Database of Systematic Reviews* 2020.8 (1996).

[7] Igho J Onakpoya et al. “SARS-CoV-2 and the role of close contact in transmission: a systematic review”. In: *F1000Research* 10 (2022), p. 280.

[8] D COV. “Scientific Brief: SARS-CoV-2 Transmission”. In: (2021).

[9] Giulia Cencetti et al. “Digital proximity tracing on empirical contact networks for pandemic control”. In: *Nature communications* 12.1 (2021), p. 1655.

[10] Simay Ikier et al. “When is memory more reliable? Scientific findings, theories, and myths”. In: *Applied Neuropsychology: Adult* 31.1 (2024), pp. 77–94.

[11] Rossana Mastrandrea, Julie Fournet, and Alain Barrat. “Contact patterns in a high school: a comparison between data collected using wearable sensors, contact diaries and friendship surveys”. In: *PloS one* 10.9 (2015), e0136497.

[12] Leonardo Tonetto et al. “Contact duration: intricacies of human mobility”. In: *Online Social Networks and Media* 28 (2022), p. 100196.

[13] Florian Vogt et al. “Effectiveness evaluation of digital contact tracing for COVID-19 in New South Wales, Australia”. In: *The Lancet Public Health* 7.3 (2022), e250–e258.

[14] Muhammad Shahroz et al. “COVID-19 digital contact tracing applications and techniques: A review post initial deployments”. In: *Transportation Engineering* 5 (2021), p. 100072.

[15] Michael Spratt and TJ McIntyre. “Assessing data protection impact assessments: Lessons from COVID-19 contact tracing apps”. In: *Computer Law & Security Review* 60 (2026), p. 106233.

[16] Dennis Senn and Christina Loosli. “COVID-19 contact tracing apps”. In: *International Conference on Society 5.0*. Springer. 2021, pp. 77–92.

[17] Lucie White and Philippe van Basshuysen. “Privacy versus public health? A reassessment of centralised and decentralised digital contact tracing”. In: *Science and Engineering Ethics* 27.2 (2021), p. 23.

[18] Kiemute Oyibo and Plinio Pelegrini Morita. “COVID alert: factors influencing the adoption of exposure notification apps among Canadian residents”. In: *Frontiers in Digital Health* 4 (2022), p. 842661.

[19] Mohamad Fawaz Enaya et al. “A case study on the development of the German Corona-Warn-App”. In: *Journal of Systems and Software* 213 (2024), p. 112020.

[20] Paola Daniore et al. “Performance of the Swiss digital contact-tracing app over various SARS-CoV-2 pandemic waves: Repeated cross-sectional analyses”. In: *JMIR Public Health and Surveillance* 8.11 (2022), e41004.

[21] Siti Aqilah Jahari et al. “Navigating privacy concerns through societal benefits: A case of digital contact tracing applications”. In: *Journal of Consumer Behaviour* 21.3 (2022), pp. 625–638.

[22] Eugene Y Chan and Najam U Saqib. “Privacy concerns can explain unwillingness to download and use contact tracing apps when COVID-19 concerns are high”. In: *Computers in Human Behavior* 119 (2021), p. 106718.

[23] Rae Thomas et al. “Concerns and misconceptions about the Australian government’s COVIDsafe app: Cross-sectional survey study”. In: *JMIR public health and surveillance* 6.4 (2020), e23081.

[24] Haridimos Kondylakis et al. “COVID-19 mobile apps: a systematic review of the literature”. In: *Journal of medical Internet research* 22.12 (2020), e23170.

[25] J. R. Chasnov. *Mathematical Biology*. Creative Commons, 2023.

[26] Mark B Shapiro et al. “adaptive susceptible-infectious-removed model for continuous estimation of the COVID-19 infection rate and reproduction number in the United States: Modeling study”. In: *Journal of Medical Internet Research* 23.4 (2021), e24389.

[27] Seyed M Moghadas et al. “Projecting hospital utilization during the COVID-19 outbreaks in the United States”. In: *Proceedings of the National Academy of Sciences* 117.16 (2020), pp. 9122–9126.

[28] Seyed M Moghadas et al. “The implications of silent transmission for the control of COVID-19 outbreaks”. In: *Proceedings of the national academy of sciences* 117.30 (2020), pp. 17513–17515.

[29] Apoorva Anand et al. “Self-tests for COVID-19: what is the evidence? A living systematic review and meta-analysis (2020–2023)”. In: *PLOS Global Public Health* 4.2 (2024), e0002336.

[30] Andrew S Hoffman et al. “Towards a seamful ethics of Covid-19 contact tracing apps?” In: *Ethics and Information Technology* 23.Suppl 1 (2021), pp. 105–115.

[31] Tzung-Jeng Hwang et al. “Loneliness and social isolation during the COVID-19 pandemic”. In: *International psychogeriatrics* 32.10 (2020), pp. 1217–1220.

[32] Zhiru Gao et al. “A systematic review of asymptomatic infections with COVID-19”. In: *Journal of Microbiology, Immunology and Infection* 54.1 (2021), pp. 12–16.

[33] Rongrong Yang, Xien Gui, and Yong Xiong. “Comparison of clinical characteristics of patients with asymptomatic vs symptomatic coronavirus disease 2019 in Wuhan, China”. In: *JAMA network open* 3.5 (2020), e2010182.

[34] Fredrik Methi and Elisabeth Henie Madslien. “Lower transmissibility of SARS-CoV-2 among asymptomatic cases: evidence from contact tracing data in Oslo, Norway”. In: *BMC medicine* 20.1 (2022), p. 427.

[35] Mingwang Shen et al. “Mass testing—An underexplored strategy for COVID-19 control”. In: *The Innovation* 2.2 (2021).

[36] Cecile Philippe et al. “Mass testing to end the COVID-19 public health threat”. In: *The Lancet Regional Health–Europe* 25 (2023).

[37] Beena Bhamani et al. “Mass testing and treatment to accelerate malaria elimination: a systematic review and meta-analysis”. In: *The American Journal of Tropical Medicine and Hygiene* 110.4 Suppl (2024), p. 44.

[38] Moira A Mugglestone et al. “Presymptomatic, asymptomatic and post-symptomatic transmission of SARS-CoV-2: Joint British infection association (BIA), health-care infection society (HIS), infection prevention society (IPS) and royal College of pathologists (RCPath) guidance”. In: *BMC Infectious Diseases* 22.1 (2022), p. 453.

[39] Farida Al-Hosani et al. “A review of COVID-19 mass testing in the United Arab Emirates”. In: *Frontiers in Public Health* 9 (2021), p. 661134.

[40] Chad R Wells et al. “Comparative analyses of eighteen rapid antigen tests and RT-PCR for COVID-19 quarantine and surveillance-based isolation”. In: *Communications medicine* 2.1 (2022), p. 84.

[41] Hiroshi Nishiura and Gerardo Chowell. “The effective reproduction number as a prelude to statistical estimation of time-dependent epidemic trends”. In: *Mathematical and statistical estimation approaches in epidemiology*. Springer, 2009, pp. 103–121.

[42] Razvan G Romanescu et al. “The effective reproductive number: Modeling and prediction with application to the multi-wave Covid-19 pandemic”. In: *Epidemics* 44 (2023), p. 100708.

[43] Sera Whitelaw et al. “Applications of digital technology in COVID-19 pandemic planning and response”. In: *The Lancet Digital Health* 2.8 (2020), e435–e440.

[44] Ting Lei et al. “Using Health QR Code to Fight Against COVID-19: Chinese Government’s New Way of Collaborative Governance with Enterprises”. In: *2020 International Conference on Management, Economy and Law (ICMEL 2020)*. Atlantis Press. 2020, pp. 194–198.

[45] Qing Ye, Jin Zhou, and Hong Wu. “Using information technology to manage the COVID-19 pandemic: development of a technical framework based on practical experience in China”. In: *JMIR medical informatics* 8.6 (2020), e19515.

[46] Bara'Abdallah AlShurman et al. "Understanding the COVID-19 vaccine policy terrain in Ontario Canada: a policy analysis of the actors, content, processes, and context". In: *Vaccines* 11.4 (2023), p. 782.

[47] Franziska Herbert et al. "{"Fast}, Easy,{Convenient."} Studying Adoption and Perception of Digital Covid Certificates". In: *Eighteenth Symposium on Usable Privacy and Security (SOUPS 2022)*. 2022, pp. 463–482.

[48] Jaap-Henk Hoepman. "A critique of the google apple exposure notification (GAEN) framework". In: *Privacy Symposium: Data Protection Law International Convergence and Compliance with Innovative Technologies*. Springer. 2022, pp. 41–58.

[49] Bryan WK Chow et al. "Use of a digital contact tracing system in Singapore to mitigate COVID-19 spread". In: *BMC Public Health* 23.1 (2023), p. 2253.

[50] Antonis A Kousoulis et al. "Revisiting the ebola epidemic in west africa: the role of emotional determinants in public responses". In: *African Journal of Infectious Diseases* 17.2 (2023), pp. 14–22.

[51] Lisa O Danquah et al. "Use of a mobile application for Ebola contact tracing and monitoring in northern Sierra Leone: a proof-of-concept study". In: *BMC infectious diseases* 19.1 (2019), p. 810.

[52] Laura Di Domenico et al. "Impact of lockdown on COVID-19 epidemic in Île-de-France and possible exit strategies". In: *BMC medicine* 18.1 (2020), p. 240.

[53] Piotr Sapiezynski et al. "Interaction data from the copenhagen networks study". In: *Scientific Data* 6.1 (2019), p. 315.

[54] Melissa Tracy, Magdalena Cerdá, and Katherine M Keyes. "Agent-based modeling in public health: current applications and future directions". In: *Annual review of public health* 39 (2018), pp. 77–94.

[55] Affan Shoukat and Seyed M Moghadas. “Agent-based modelling: an overview with application to disease dynamics”. In: *arXiv preprint arXiv:2007.04192* (2020).

[56] José Manuel Galán et al. “Errors and artefacts in agent-based modelling”. In: *Journal of Artificial Societies and Social Simulation* 12.1 (2009), pp. 1–1.

[57] Seyed M Moghadas and Majid Jaberi-Douraki. *Mathematical modelling: a graduate textbook*. John Wiley & Sons, 2018.

[58] Zhihua Liu et al. “A COVID-19 epidemic model with latency period”. In: *Infectious Disease Modelling* 5 (2020), pp. 323–337.

[59] AB Pant. *Dictionary of toxicology*. Springer, 2024.

[60] Yutong Wang et al. “Asymptomatic and pre-symptomatic infection in Coronavirus Disease 2019 pandemic”. In: *Medical Review* 2.1 (2022), pp. 66–88.

[61] Nabila Shaikh, Pooja Swali, and Rein MGJ Houben. “Asymptomatic but infectious–The silent driver of pathogen transmission. A pragmatic review”. In: *Epidemics* 44 (2023), p. 100704.

[62] Robin N Thompson, Christopher A Gilligan, and Nik J Cunniffe. “Detecting presymptomatic infection is necessary to forecast major epidemics in the earliest stages of infectious disease outbreaks”. In: *PLoS computational biology* 12.4 (2016), e1004836.

[63] Hongyang Liu and Sharon Joines. “Older adults’ experience with and barriers to learning new technology: A focus group study.” In: *Gerontechnology* 20.1 (2020).

[64] Christopher Steven Marcum. “Age differences in daily social activities”. In: *Research on aging* 35.5 (2013), pp. 612–640.

[65] Thomas N Vilches et al. “Economic evaluation of COVID-19 rapid antigen screening programs in the workplace”. In: *BMC medicine* 20.1 (2022), p. 452.

[66] Hui Xiang et al. “Non-pharmaceutical interventions (NPIs) to control influenza spread among children in primary school and kindergarten: class-suspension or symptom-based isolation?” In: *BMC Infectious Diseases* 25.1 (2025), p. 324.

[67] J Jung et al. “Risk of transmission of COVID-19 from healthcare workers returning to work after a 5-day isolation, and kinetics of shedding of viable SARS-CoV-2 variant B. 1.1. 529 (Omicron)”. In: *Journal of Hospital Infection* 131 (2023), pp. 228–233.

[68] Kazuyuki Chibana et al. “Quantitative Antigen Test-Based Return-to-Work Strategy for COVID-19-Positive Healthcare Workers: A Single-Center Study from Nikko Medical Center”. In: *Dokkyo Medical Journal* 4.6 (2025), pp. 447–453.

[69] Joel Hellewell et al. “Feasibility of controlling COVID-19 outbreaks by isolation of cases and contacts”. In: *The Lancet Global Health* 8.4 (2020), e488–e496.

[70] Pratha Sah et al. “Accelerated vaccine rollout is imperative to mitigate highly transmissible COVID-19 variants”. In: *EClinicalMedicine* 35 (2021).

[71] Luca Ferretti et al. “Quantifying SARS-CoV-2 transmission suggests epidemic control with digital contact tracing”. In: *science* 368.6491 (2020), eabb6936.

[72] Andrew A Sayampanathan et al. “Infectivity of asymptomatic versus symptomatic COVID-19”. In: *Lancet (London, England)* 397.10269 (2020), p. 93.

[73] Thomas N Vilches et al. “Multifaceted strategies for the control of COVID-19 outbreaks in long-term care facilities in Ontario, Canada”. In: *Preventive medicine* 148 (2021), p. 106564.

[74] Qun Li et al. “Early transmission dynamics in Wuhan, China, of novel coronavirus–infected pneumonia”. In: *New England journal of medicine* 382.13 (2020), pp. 1199–1207.

[75] Affan Shoukat et al. “Lives saved and hospitalizations averted by COVID-19 vaccination in New York City: a modeling study”. In: *The Lancet Regional Health–Americas* 5 (2022).

[76] Joël Mossong et al. “Social contacts and mixing patterns relevant to the spread of infectious diseases”. In: *PLoS medicine* 5.3 (2008), e74.

[77] Christopher I Jarvis et al. “Quantifying the impact of physical distance measures on the transmission of COVID-19 in the UK”. In: *BMC medicine* 18.1 (2020), p. 124.

[78] Seyed M Moghadas et al. “The impact of vaccination on coronavirus disease 2019 (COVID-19) outbreaks in the United States”. In: *Clinical Infectious Diseases* 73.12 (2021), pp. 2257–2264.

[79] Kenji Mizumoto et al. “Estimating the asymptomatic proportion of coronavirus disease 2019 (COVID-19) cases on board the Diamond Princess cruise ship, Yokohama, Japan, 2020”. In: *Eurosurveillance* 25.10 (2020), p. 2000180.

[80] Hiroshi Nishiura et al. “Estimation of the asymptomatic ratio of novel coronavirus infections (COVID-19)”. In: *International journal of infectious diseases* 94 (2020), pp. 154–155.

[81] Anne Kimball. “Asymptomatic and presymptomatic SARS-CoV-2 infections in residents of a long-term care skilled nursing facility—King County, Washington, March 2020”. In: *MMWR. Morbidity and mortality weekly report* 69 (2020).

[82] Affan Shoukat et al. “Projecting demand for critical care beds during COVID-19 outbreaks in Canada”. In: *Cmaj* 192.19 (2020), E489–E496.

[83] Klaus Dietz. “The estimation of the basic reproduction number for infectious diseases”. In: *Statistical methods in medical research* 2.1 (1993), pp. 23–41.

[84] Kevin Zhang et al. “The impact of mask-wearing and shelter-in-place on COVID-19 outbreaks in the United States”. In: *International Journal of Infectious Diseases* 101 (2020), pp. 334–341.

[85] Weimo Zhu. “Making bootstrap statistical inferences: A tutorial”. In: *Research quarterly for exercise and sport* 68.1 (1997), pp. 44–55.

[86] Guy Katriel and Lewi Stone. “Attack rates of seasonal epidemics”. In: *Mathematical biosciences* 235.1 (2012), pp. 56–65.

[87] Marlies Noordzij et al. “Measures of disease frequency: prevalence and incidence”. In: *Nephron Clinical Practice* 115.1 (2010), pp. c17–c20.

[88] David L Streiner. “Let me count the ways: measuring incidence, prevalence, and impact in epidemiological studies”. In: *The Canadian Journal of Psychiatry* 43.2 (1998), pp. 173–179.

[89] Khaled Kasim. *Basic concepts of modern epidemiology: Epidemiology and research*. LAP LAMBERT Academic Publishing, 2012.

[90] Prabhaker Mishra et al. “Descriptive statistics and normality tests for statistical data”. In: *Annals of cardiac anaesthesia* 22.1 (2019), pp. 67–72.

[91] Aynur Yonar et al. “A comparative analysis for homogeneity of variance tests”. In: *Journal of Science and Arts* 24.2 (2024), pp. 305–328.

[92] RW McGee. “Welch’s T-test: the robust default for comparing two groups in psychological research”. In: *Sociology & Social Policy* 2.2 (2025), pp. 14–20.

[93] Ben Derrick, Deirdre Toher, and Paul White. “Why Welch’s test is Type I error robust”. In: *The Quantitative Methods in Psychology* 12.1 (2016).

[94] Tae Kyun Kim. “Understanding one-way ANOVA using conceptual figures”. In: *Korean journal of anesthesiology* 70.1 (2017), p. 22.

[95] Hervé Abdi, Lynne J Williams, et al. “Tukey’s honestly significant difference (HSD) test”. In: *Encyclopedia of research design* 3.1 (2010), pp. 1–5.

[96] Anita Nanda et al. “Multiple comparison test by Tukey’s honestly significant difference (HSD): Do the confident level control type I error”. In: *International Journal of Statistics and Applied Mathematics* 6.1 (2021), pp. 59–65.

[97] Ahmed Elmokashfi et al. “Nationwide rollout reveals efficacy of epidemic control through digital contact tracing”. In: *Nature communications* 12.1 (2021), p. 5918.

[98] Tyler M Yasaka, Brandon M Lehrich, and Ronald Sahyouni. “Peer-to-peer contact tracing: development of a privacy-preserving smartphone app”. In: *JMIR mHealth and uHealth* 8.4 (2020), e18936.

[99] Kamalini Ramdas, Ara Darzi, and Sanjay Jain. “‘Test, re-test, re-test’: using inaccurate tests to greatly increase the accuracy of COVID-19 testing”. In: *Nature medicine* 26.6 (2020), pp. 810–811.

[100] Apurv Soni et al. “Performance of rapid antigen tests to detect symptomatic and asymptomatic SARS-CoV-2 infection: a prospective cohort study”. In: *Annals of internal medicine* 176.7 (2023), pp. 975–982.

[101] Eric Lai. “Prior Knowledge of Diagnostic Results Does Not Bias A Subject’s Interpretation of At-Home COVID-19 Antigen Tests”. In: *COVID* 3.4 (2023), pp. 637–642.

[102] Michael A Andrews and Chris T Bauch. “Disease interventions can interfere with one another through disease-behaviour interactions”. In: *PLoS computational biology* 11.6 (2015), e1004291.

[103] Jung Ki Kim and Eileen M Crimmins. “How does age affect personal and social reactions to COVID-19: Results from the national Understanding America Study”. In: *PloS one* 15.11 (2020), e0241950.

[104] Mélodie Monod et al. “Age groups that sustain resurging COVID-19 epidemics in the United States”. In: *Science* 371.6536 (2021), eabe8372.

[105] Edward Goldstein, Marc Lipsitch, and Muge Cevik. “On the effect of age on the transmission of SARS-CoV-2 in households, schools, and the community”. In: *The Journal of infectious diseases* 223.3 (2021), pp. 362–369.

[106] Jesús A Moreno López et al. “Anatomy of digital contact tracing: Role of age, transmission setting, adoption, and case detection”. In: *Science advances* 7.15 (2021), eabd8750.

[107] Robert A Kleinman and Colin Merkel. “Digital contact tracing for COVID-19”. In: *Cmaj* 192.24 (2020), E653–E656.

[108] Janice Moore and Meir Shillor. “A modified SIR model with dependent infection and hospitalization rates”. In: *Biomath* 13.2 (2024), pp. 2411146–2411146.

[109] Lixin Lin et al. “The disease severity and clinical outcomes of the SARS-CoV-2 variants of concern”. In: *Frontiers in public health* 9 (2021), p. 775224.

[110] Nhu Ngoc Nguyen et al. “High rate of reinfection with the SARS-CoV-2 Omicron variant”. In: *The Journal of infection* 85.2 (2022), p. 174.

[111] Hamid Bohloli et al. “Combining government, non-pharmaceutical interventions and vaccination in optimal control COVID-19”. In: *International Journal of Healthcare Management* 16.1 (2023), pp. 61–69.

[112] Bryce Morsky et al. “The impact of threshold decision mechanisms of collective behavior on disease spread”. In: *Proceedings of the National Academy of Sciences* 120.19 (2023), e2221479120.